

NPS ARCHIVE
1968
WILLIAMS, D.

DETERMINATION OF PERFORMANCE PARAMETERS
OF A DUAL DISCHARGE RADIAL TURBINE

by

David Daniel Williams

DUDLEY KNOX LIBRARY
ROYAL POSTGRADUATE SCHOOL
BERKELEY CA 93943-5101

UNITED STATES NAVAL POSTGRADUATE SCHOOL



THESIS

DETERMINATION OF PERFORMANCE PARAMETERS

OF A

DUAL DISCHARGE RADIAL TURBINE

by

David Daniel Williams

December 1968

This document has been approved for public release and sale; its distribution is unlimited.

LIBRARY
NAVAL POSTGRADUATE SCHOOL
MONTEREY, CALIF. 93940

DETERMINATION OF PERFORMANCE PARAMETERS
OF A

DUAL DISCHARGE RADIAL TURBINE

by

David Daniel Williams
Lieutenant, United States Navy
B. S., Naval Academy, 1962

Submitted in partial fulfillment of the
requirements for the degree of

MASTER OF SCIENCE IN AERONAUTICAL ENGINEERING

from the

NAVAL POSTGRADUATE SCHOOL
December 1968

ABSTRACT

This study was conducted to establish the performance parameters of a radial inflow, dual discharge turbine and to determine the effect of variations in axial clearance on these parameters. The representative stream surface is taken at the outer discharge radius instead of at a computed mass-average discharge radius, as was done previously. This technique results in considerably simplified computations and in better correlation of the rotor loss parameters.

Tests were conducted at axial clearances from 0.015 to 0.081 inches and at total-to-static pressure ratios from 1.2 to 1.7 for each clearance. The test installation is located at the Turbo-Propulsion Laboratory of the Naval Postgraduate School, Monterey, California.

TABLE OF CONTENTS

SECTION	PAGE
1. INTRODUCTION	17
2. THE ICP RADIAL TURBINE	19
2.1 Description of Turbine Assembly	19
2.2 Modifications to Turbine Assembly	21
3. ANALYSIS OF SCROLL AND GUIDE VANE PERFORMANCE	23
3.1 Instrumentation and Test Procedures	24
3.2 Theoretical Analysis	28
3.3 Data Reduction: Program SCROLL	31
3.4 Discussion of Results	31
4. ANALYSIS OF OVERALL TURBINE PERFORMANCE	36
4.1 Instrumentation	36
4.2 Test Procedures	39
4.3 Theoretical Analysis	43
4.4 Data Reduction: Programs RADIAL and NOSPD	52
4.5 Discussion of Results	52
5. CONCLUSIONS	61
ILLUSTRATIONS	63
REFERENCES	101
APPENDIX A: Program SCROLL	102
A1. Main Program	102
A2. Subroutine TEMP	103
A3. Subroutine FLOW	103
A4. Subroutine PRESS	105
A5. Method of Assembly of Input Data	105

APPENDIX B:	Program PHIAL	119
	B1. Subroutines TEMP and FLOW	120
	B2. Subroutine PRESS	120
	B3. Subroutine EDC	121
	B4. Subroutines TORQ and DYNA	122
	B5. Subroutine TURB	123
	B6. Subroutine PHIAL	123
	B7. Subroutine REFER	124
	B8. Method of Assembly of Input Data	124
APPENDIX C:	Program NOSP	148

LIST OF TABLES

TABLE		PAGE
A1	Listing of Program SCROLL	107
A2	Results from Program SCROLL Clearance 0.081 In.	111
A3	Results from Program SCROLL Clearance 0.072 In.	112
A4	Results from Program SCROLL Clearance 0.061 In.	113
A5	Results from Program SCROLL Clearance 0.050 In.	114
A6	Results from Program SCROLL Clearance 0.041 In.	115
A7	Results from Program SCROLL Clearance 0.030 In.	116
A8	Results from Program SCROLL Clearance 0.024 In.	117
A9	Results from Program SCROLL Clearance 0.015 In.	118
B1	Listing of Program RADIAL	126
B2	Additional Control Cards Required for Program RADIAL	136
B3	Torque Calibration Data	137
B4	Program RADIAL Input Data Clearance 0.081 In.	138
B5	Results from Program RADIAL Clearance 0.081 In.	139
B6	Program RADIAL Input Data Clearance 0.061 In.	140
B7	Results from Program RADIAL Clearance 0.061 In.	141
B8	Program RADIAL Input Data Clearance 0.041 In.	142
B9	Results from Program RADIAL Clearance 0.041 In.	143

TABLE		PAGE
B10	Program RADIAL Input Data Clearance 0.024 In.	144
B11	Results from Program RADIAL Clearance 0.024 In.	145
B12	Program RADIAL Input Data Clearance 0.015 In.	146
B13	Results from Program RADIAL Clearance 0.015 In.	147
C1	Listing of Program NOSPД	149
C2	Results from Program NOSPД	154

LIST OF ILLUSTRATIONS

FIGURE		PAGE
1.	Active Rotor Test Installation	63
2.	Dummy Rotor Test Installation	64
3.	Wooden Scroll Insert	65
4.	Turbine Scroll and Guide Vane Assembly	66
5.	Cross-Section of Turbine	67
6.	Dummy Rotor and Flow Straighteners	68
7.	Active Rotor	69
8.	Left Turbine Discharge	70
9.	Turbine Inlet Piping, Flow Control Valves, and Flow Measuring Orifice	71
10.	Remote Control for Flow Regulation, Vortec Remote Throttle Control, and Daytronic Strain Gage Digital Indicator	72
11.	Schematic of Radial Turbine Instrumentation	73
12.	Meriam Mercury Micromanometers	74
13.	Brown Potentiometer	75
14.	Temperature-Entropy Diagram for Radial Turbine	76
15.	Velocity Diagrams for Radial Turbine	77
16.	Velocity Coefficient vs. Mach Number	78
17.	Absolute Rotor Inlet Flow Angle vs. Mach Number	79
18.	Velocity Coefficient vs. Mach Number from Derived Equation	80
19.	Absolute Rotor Inlet Flow Angle vs. Mach Number from Derived Equation	81
20.	Dummy Alignment Shaft	82
21.	Flux Cutter, Quill Shaft, and Dynamometer Torque Capsule	83

FIGURE		PAGE
22.	Electronic Speed Counter and Vibration Analyzer	84
23.	Five Inch Inlet Pipe and Bearing Lubrication Unit	85
24.	Schematic of Turbine Lubrication System	86
25.	Automatic Data Acquisition System	87
26.	Torque Capsule Calibration Apparatus	88
27.	Degree of Reaction vs. Head Coefficient	89
28.	Overall Efficiency (No Bearing Losses) vs. Referred Speed	90
29.	Overall Efficiency (No Bearing Losses) vs. Head Coefficient	91
30.	Overall Efficiency (with Bearing Losses) vs. Referred Speed	92
31.	Overall Efficiency (with Bearing Losses) vs. Head Coefficient	93
32.	Rotor Velocity Coefficient (No Bearing Losses) vs. Head Coefficient	94
33.	Rotor Velocity Coefficient (with Bearing Losses) vs. Head Coefficient, Clearance 0.081 In.	95
34.	Rotor Velocity Coefficient (with Bearing Losses) vs. Head Coefficient, Clearance 0.061 In.	96
35.	Rotor Velocity Coefficient (with Bearing Losses) vs. Head Coefficient, Clearance 0.041 In.	97
36.	Rotor Velocity Coefficient (with Bearing Losses) vs. Head Coefficient, Clearance 0.024 In.	98
37.	Rotor Velocity Coefficient (with Bearing Losses) vs. Head Coefficient, Clearance 0.015 In.	99
38.	Referred Moment (with Bearing Losses) vs. Referred Speed	100

TABLE OF SYMBOLS

Symbol	FORTTRAN	Definition	Units
A_1	- - - -	Meridional cross-sectional area of rotor inlet	ft^2
A_5	- - - -	Cross-sectional area of five inch inlet pipe	ft^2
B_1	B1	Perpendicular distance between shroud inner extremities	in
C	- - - -	Flow measurement factor dependent on units, orifice diameter, and type of pressure taps	- - -
C_{f1}	CF1	Pressure conversion factor	$\text{lb}/\text{ft}^2/\text{in Hg}$
$Clnc$	CLNC	Rotor axial tip clearance, on one side of blade only	in
C_0	C0	Velocity corresponding to the isentropic enthalpy drop through the turbine	ft/sec
C_p	CP5	Constant pressure specific heat, based on total inlet temperature	$\text{BTU}/\text{lb}_m \text{ } ^\circ\text{F}$
$C_p \text{ (avg)}$	CP	Constant pressure specific heat, based on average temperature t	$\text{BTU}/\text{lb}_m \text{ } ^\circ\text{F}$
D_1	D1	Rotor diameter at inlet, 9.40 in.	in
D_{20}	- - - -	Rotor outer discharge diameter, 5.88 in.	in
F	SR	Scale reading	lb
Fr	- - - -	Reynolds number correction factor	- - - -
G_{Hg}	GHG	Specific gravity of mercury at t_{rm}	- - - -
G_{H2O}	GWR	Specific gravity of water at t_{rm}	- - - -
g	32.174	Unit Conversion Factor	$\text{ft-lb}_m/\text{lb-sec}^2$
H_E	- - - -	Total enthalpy at equivalent state point E	BTU/lb_m

<u>Symbol</u>	<u>FORTTRAN</u>	<u>Definition</u>	<u>Units</u>
HP_f	HPF	Power required to overcome bearing friction	hp
H_R	- - - -	Relative total enthalpy at rotor inlet	BTU/lb _m
H_{refl}	HREF1	Measured reference pressure applied to water manometer board	in Hg gage
h_1	- - - -	Static enthalpy at rotor inlet	BTU/lb _m
h_2	- - - -	Static enthalpy at rotor discharge	BTU/lb _m
$h_1(\text{avg})$	H1	Average static pressure ahead of rotor	in H ₂ O gage
ΔH_{is}	DHIS	Isentropic total enthalpy drop across turbine	BTU/lb _m
ΔH_w	- - - -	Enthalpy drop representing work output of turbine	BTU/lb _m
Δh_{lvc}	DPVC	Measured pressure differential across flow orifice, from vena contracta taps	in Hg
J	778.16	Joule's constant	ft-lb/BTU
k_{is}	HEAD	Isentropic head coefficient	- - - -
M	TNET	Net torque output of turbine	ft-lb
M_f	BFM	Bearing friction moment	ft-lb
M_{ref}	TNETR	Referred net torque output of turbine	ft-lb
M_1	ACH1	Mach number at rotor inlet	- - - -
N	RPM	Measured turbine speed	rpm
N_{ref}	RPMR	Referred turbine speed	rpm
P_{atm}	PATM	Barometric pressure	in Hg
P_{t0}	PTO	Absolute total pressure ahead of turbine	in Hg abs

Symbol	FORTTRAN	Definition	Units
P_{t0}/p_1	PR1	Pressure ratio across scroll and guide vanes	- - - -
P_{t0}/p_2	PR2	Pressure ratio across turbine	- - - -
P_E	- - - -	Equivalent rotor inlet static pressure	in Hg abs
p_0	PS5	Absolute static pressure at turbine inlet	in Hg abs
p_1	P1	Average absolute static pressure at rotor inlet	in Hg abs
p_{1VC}'	PUVC	Measured pressure upstream of flow orifice, from vena contracta tap	in Hg gage
p_{1VC}	PVC	Absolute pressure upstream of flow orifice from vena contracta taps	in Hg abs
p_2	P2	Static discharge pressure	in Hg abs
p_5'	P5P	Measured static pressure at turbine inlet	in Hg gage
R_g	53.3448	Gas constant for air	ft-lb/lb _m -°R
R_1	R1	Rotor inlet radius, 4.70 in.	in
R_{20}	R20	Rotor outer discharge radius, 2.94 in	in
r	DR	Isentropic degree of reaction	- - - -
T	T	Torque measured by dynamometer	ft-lb
TCD	TCD	Torque calibration data	counts
TQ	TQ	Torque indicator reading	counts
T_E	- - - -	Equivalent rotor inlet temperature	°R
T_{ref}	TR	Referred torque output for no-loss case	ft-lb
T_{to}	T5	Total temperature ahead of turbine	°R
T_0	T0	Static temperature ahead of turbine	°R

<u>Symbol</u>	<u>FORTTRAN</u>	<u>Definition</u>	<u>Units</u>
T_1	T1	Static temperature ahead of rotor	$^{\circ}\text{R}$
T_1'	- - - -	Static temperature at rotor inlet for isentropic expansion from P_{t0} to p_1	$^{\circ}\text{R}$
T_1^*	- - - -	Static temperature at rotor inlet resulting from rotor incidence losses	$^{\circ}\text{R}$
T_2'	- - - -	Static discharge temperature resulting from isentropic expansion from p_E to p_2	$^{\circ}\text{R}$
T_2''	- - - -	Static temperature at discharge resulting from isentropic expansion from P_{t0} to p_2	$^{\circ}\text{R}$
T_4	T4	Total temperature ahead of flow orifice	$^{\circ}\text{R}$
T_{20}	T20	Lubricating oil inlet temperature	$^{\circ}\text{F}$
T_{21}	T21	Lubricating oil temperature at discharge from right bearing	$^{\circ}\text{F}$
T_{22}	T22	Lubricating oil temperature at discharge from left bearing	$^{\circ}\text{F}$
ΔT_{is}	DTIS	Isentropic temperature drop from P_{t0} to p_2	$^{\circ}\text{R}$
ΔT_W	DTW	Temperature drop corresponding to actual work output of turbine	$^{\circ}\text{R}$
t	A	Average temperature through turbine	$^{\circ}\text{F}$
tare	STARE	Tare of precision scales	lb
t_{cj}	TCJ	Thermocouple reference cold junction temperature	$^{\circ}\text{F}$
t_{rm}	TRM	Control room temperature	$^{\circ}\text{F}$
U_1	U1	Peripheral speed of rotor at inlet	ft/sec
U_{20}	U20	Peripheral speed of rotor at outer discharge radius	ft/sec

Symbol	FORTTRAN	Definition	Units
V	- - - -	Thermocouple reading	mv
V ₀	VO	Velocity at turbine inlet	ft/sec
V ₁	V1	Absolute flow velocity at rotor inlet	ft/sec
V _{u1}	VUL	Peripheral component of V ₁	ft/sec
V _{m1}	VM1	Meridional component of V ₁	ft/sec
V _{ith}	VITH	Theoretical absolute rotor inlet velocity for no losses	ft/sec
V ₂₀	V20	Absolute discharge flow velocity at outer radius of rotor	ft/sec
V _{u20}	VU20	Peripheral component of V ₂₀	ft/sec
V _{m20}	VM20	Meridional component of V ₂₀	ft/sec
V ₄	V4	Thermocouple reading ahead of flow orifice	mv
V ₅	V5	Thermocouple reading at turbine inlet	mv
V ₂₀	V20	Thermocouple reading at lube oil inlet	mv
V ₂₁	V21	Thermocouple reading at lube oil discharge from right bearing	mv
V ₂₂	V22	Thermocouple reading at lube oil discharge from left bearing	mv
W ₁	W1	Relative flow velocity at rotor inlet	ft/sec
W _{u1}	WU1	Peripheral component of W ₁	ft/sec
W ₂₀	W20	Relative flow velocity at rotor discharge outer radius	ft/sec
W _{u20}	WU20	Peripheral component of W ₂₀	ft/sec
W _{20th}	W20TH	Theoretical relative flow velocity at outer discharge radius, for isentropic expansion from p _E to p ₂	ft/sec

<u>Symbol</u>	<u>FORTTRAN</u>	<u>Definition</u>	<u>Units</u>
\dot{W}	WVC	Mass flow rate, for vena contracta taps	lb_m/sec
\dot{W}_{ref}	WVCR	Referred mass flow rate	lb_m/sec
\dot{W}_{oil}	- - - -	Mass flow rate of lubricating oil	lb_m/sec
Y_1	Y	Factor accounting for compressibility effects in flow measuring orifice	- - - -

Symbol	FORTTRAN	Definition	Units
<u>GREEK SYMBOLS</u>			
α	A	Area multiplier accounting for thermal expansion of flow orifice	- - - -
α_1	ALPH1	Absolute rotor inlet flow angle	degrees
α_{20}	ALF2	Absolute rotor discharge flow angle at outer radius, for no bearing loss case	degrees
α_{20L}	ALF2L	Absolute rotor discharge flow angle at outer radius, bearing losses considered	degrees
β_1	BETA1	Relative rotor inlet flow angle	degrees
β_{20}	BET20	Relative rotor discharge flow angle at outer radius	degrees
γ	GAMMA	Ratio of specific heats based on T_{t0}	- - - -
$\gamma_{(avg)}$	GAM	Ratio of specific heats based on t	- - - -
$(\gamma - 1) / \gamma$	EXP	Exponent	- - - -
δ	DEL	Referred pressure ratio, $P_{t0} / 14.7$	- - - -
ϵ	EPS	Factor which corrects flow rate through the turbine for varying values of γ	- - - -
η	ETA	Total-to-static turbine efficiency, bearing losses not considered	per cent
η_L	ETAL	Total-to-static turbine efficiency, including bearing losses	per cent
ϕ	PHI	velocity coefficient for scroll and guide vanes	- - - -
ψ	PSI	Velocity coefficient for rotor, based on ratio of actual to theoretical relative discharge velocities, bearing losses not considered	- - - -

<u>Symbol</u>	<u>FORTTRAN</u>	<u>Definition</u>	<u>Units</u>
Ψ_L	PSIL	Velocity coefficient for rotor, bearing losses included	- - - -
ρ_0	RHO	Density at turbine inlet	lb _m /ft ³
ρ_1	RHO	Density at rotor inlet	lb _m /ft ³
Θ	THETA	Referred temperature ratio, $T_{to}/518.7$	- - - -
ω	ROSP	Rotational speed of rotor	radians/sec
ζ_N	ZETAN	Loss coefficient for scroll and guide vanes	- - - -
ζ_R	ZETR	Rotor loss coefficient, bearing losses not considered	- - - -
ζ_{RL}	ZETRL	Rotor loss coefficient, with bearing losses	- - - -

SECTION I

INTRODUCTION

As requirements for smaller more powerful turbines increase, to keep pace with the needs of the rapidly expanding aerospace industry, more and more attention is given to radial turbines. Since the radial turbine can extract more energy per stage than an axial turbine, it is more useful in applications where space limitations preclude the use of a staged axial turbine. Currently, it is therefore used extensively for aircraft electric power generation, in aircraft cockpit and equipment cooling systems, in cryogenic systems, and in missile auxiliary power systems.

As a consequence of the increasingly widespread use of the radial turbine, the establishment of performance parameters as an aid to the design of these turbines is of fundamental importance. It is the objective of this report to establish some of the performance parameters for a particular radial inflow, dual discharge turbine using air as an operating fluid and relating these parameters in such a way that they may be applied to geometrically similar turbines operating with different fluids and in different environments.

Although similar studies have previously been conducted on this machine, this investigation differs in two important aspects. First, several significant and necessary changes in the internal dimensions of the turbine were made, thus resulting in a somewhat different machine than that previously tested. Also, the method of analysis used is a considerably simplified one, which yields more significant results with less computational effort than those methods previously employed by referring all losses to the outer discharge radius rather than a computed average radius.

Additionally, this project had as an objective a significant expansion of the operating ranges examined beyond those previously considered.

Because the evaluation of turbine performance parameters involves a formidable computation requirement, the data obtained in the experiments were reduced by means of the computer programs described herein, which are written in FORTRAN IV language for the IBM 360 computer system used at the Naval Postgraduate School.

The author gratefully acknowledges the guidance and counsel of Professor Robert D. Zucker, of the Department of Aeronautics, Naval Postgraduate School, and of Professor Michael H. Vavra of the same department. Thanks are due also to Mr. James E. Hammer and his coworkers on the technical staff of the Turbopropulsion Laboratory for their many hours of hard work in modifying, repairing, and operating the turbine test rig.

SECTION 2

THE I.C.P. RADIAL TURBINE

The turbine used in this investigation is a dual discharge, radial inflow turbine installed at the Turbopropulsion Laboratory of the Department of Aeronautics, Naval Postgraduate School. It was originally designed and built by the Aerojet General Corporation, for application as the power supply for a missile propulsion combustion cycle. The original performance evaluation was conducted by Vavra (1), with subsequent investigations by Finn (2), Riley (3), and Boshoven (4).

2.1 Description of Turbine Assembly

The basic turbine test installations used are shown in Figures 1 and 2. The turbine assembly consists of: the wooden inlet casing, with its inner contour in the shape of a varying diameter torus, or scroll; a circular stainless steel guide vane assembly consisting of seven circular-arc blades and the rings themselves; the rotor assembly; and two plexi-glass shrouds.

The inner contour of the inlet casing was formed by casing plaster of paris around a wooden insert of the desired scroll dimensions. The inner surface of the scroll was varnished to prevent erosion. The wooden insert used in this process is shown in Figure 3, and Figure 4 presents a cross-section of the wooden casing, showing the shape of the scroll and the locations of the various scroll pressure taps. It is worthy of note that the flow entry is not tangential, as is customarily the case in radial turbine installations. This characteristic is a result of design requirements in the originally proposed missile installation.

A cross-section of the turbine is shown in Figure 5. In this view are indicated the turbine dimensions and minimum clearance as they existed for the test runs. The clearance, or axial distance between the rotor and the shrouds, was increased during the tests by means of circular metal shims inserted between the shroud flanges and the aluminum rings on which they rest.

The series of tests conducted utilized two different rotors. The "dummy" rotor, so called because it does not rotate, is a special device designed to permit measurement of the torque generated by the incoming flow and thus provides a measure of scroll and guide vane performance. This rotor is shown in Figure 6. It has a diameter of 9.50 inches, an axial length of 8.50 inches, and 36 meridional blades. This diameter places the blade leading edges at the radius which corresponds to that of the annulus containing the static pressure taps ahead of the rotor, and the axial length extends the blade trailing edges beyond the shrouds.

The "active" rotor, or the power-producing rotating element, is shown in Figure 7. It is 9.40 inches in diameter and has an axial length of 5.00 inches. The rotor discharge radius is 1.76 inches at the hub and 2.94 inches at the tip. The fifteen blades have a spacing at the discharge varying from 0.737 to 1.232 inches, hub to tip respectively. The actual rotor discharge area on one side of the rotor is 6.43 square inches, including an effective flow area through the radial gap between the blades and the shroud taken at the discharge plane (1). A view of the left rotor discharge, showing the plexiglass shroud and several of the eight shroud pressure taps which measure static pressure at the rotor inlet, is given in Figure 8.

2.2 Modifications to Turbine Assembly

When the turbine assembly was dismantled in preparation for this series of tests, it was discovered that one of the plexiglass shrouds was deeply gouged. Since removal of enough material to eliminate this fault would have destroyed the contour of the shroud, it was decided to cut the contours of both shrouds so that they would exactly fit the rotor contour. Additionally, it was decided to correct several dimensional discrepancies noted in earlier reports.

Riley (3) indicates a distance of 0.943 inch between the inner extremities of the shrouds. Since the axial width of the blade tips is 0.894 inch, this indicates a basic (unshimmed) axial tip clearance of 0.025 inch on each side of the blade. Boshoven (4), however, determined the distance between shrouds to be 0.966 inch, with a resulting unshimmed clearance of 0.036 inch. Additionally, Boshoven discovered that the inside extremity of the left shroud (as viewed from the turbine inlet) was offset 0.016 inch more from the guide vane ring than the right shroud.

In order to correct these discrepancies, an extensive series of measurements was undertaken. The guide vane rings, which were found to be warped, were lapped until they were flat, and all rough edges, burrs, and high spots on the inner surfaces of the casing halves were carefully removed. This resulted in a consistency to within 0.0025 inch in the dimension between the shroud support rings, at all points around the periphery. Initial measurements showed a maximum variation of 0.01 inch in this dimension.

Measurements with the reworked shrouds installed then showed a minimum clearance of 0.0477 inch, with the left shroud offset axially outward 0.0056 inch more than the right. The shroud flange thicknesses were then reduced so as to compensate for this dissymmetry and to yield

a final unshimmed clearance of 0.015 inch. Subsequent measurement of the axial travel of the active rotor, from contact at one shroud face to contact at the other, verified that all calculated clearances used in these tests were correct to within ± 0.002 inch.

Additional modifications were made to the dummy rotor in order to correct the axial stagger and unequal widths of the blades and to correct as much as possible the large gaps which were found to exist between the rotor blade contours and the shroud contours. By careful machining, the blade contours were made uniform, and a much closer fit was made to the shroud contours, even though it was not possible to completely correct this condition and still maintain the blade width.

It is thus apparent that the results obtained from the turbine after this series of modifications could differ to a marked degree from those previously obtained under identical operating conditions. It also seems to this author that both Riley (3) and Boshoven (4) were operating at clearances somewhat greater than stated in their respective studies. Based only on these modifications, the distance between the shroud inner extremities for their tests would have been approximately 0.989 inch, yielding a minimum clearance of 0.048 inch. This may be compared with the minimum clearance of 0.0245 inch reported by Riley and 0.036 inch reported by Boshoven.

Other modifications to the components of the test rig were made and are covered in the sections to which they apply. In this section only those modifications basic to the radial turbine itself are discussed.

SECTION 3

ANALYSIS OF SCROLL AND GUIDE VANE PERFORMANCE

In order to evaluate the performance parameters of a turbine, it is necessary to divide the losses into those which occur in the inlet guide vanes and those which occur in the rotor itself. Riley (3) and Boshoven (4) have used the special dummy rotor installation previously described (Figure 2) to determine the losses in the stator, or scroll and guide vane assembly. The installation determines the average conditions at the rotor inlet and thus provides an indication of scroll and guide vane efficiency as well as the absolute velocity (in both magnitude and direction) at the rotor inlet.

Riley (3) concluded that the velocity coefficient, which is a measure of the losses occurring in the inlet manifold and guide vanes, as well as the absolute inlet flow angle, was essentially constant in the range of turbine pressure ratios and axial clearances examined. The results obtained by Boshoven (4) indicate that this assumption is invalid; in fact, the velocity coefficients were found to increase with pressure ratio for a given clearance, and the absolute rotor inlet flow angles were found to decrease linearly with pressure ratio. Specific results of these earlier tests are discussed in detail in Section 3.3.

It was originally intended to utilize the dummy rotor test data of Boshoven (4) in this experiment. However, because of the extensive modifications previously discussed, it was necessary to repeat these tests. This repetition yielded the additional advantage of permitting testing over a wider range of clearances.

3.1 Instrumentation and Test Procedures

The dummy rotor shown in Figure 6 is mounted on self-aligning ball bearings and replaces the turbine rotor. Its purpose is to turn the flow from the guide vanes into the axial direction and to discharge it with no peripheral velocity component. If this condition is met, the losses in the scroll and guide vanes may be determined by measuring the torque exerted on the static dummy rotor, the flow rate, the conditions at the manifold inlet, and the static pressure at the dummy rotor inlet.

As was previously mentioned, the dummy rotor has an axial length of 8.50 inches, which extends the blade trailing edges beyond the shrouds. To insure that the discharge flow had no whirl components, flow straighteners, also shown in Figure 6, were used. These devices consist of aluminum caps containing a 1.00 inch depth of 0.125 by 0.0015 inch honeycomb material. The caps slide over the rotor shaft and cover the rotor blade trailing edges. The entire dummy rotor assembly is supported by brackets attached to the manifold casing, as shown by Figure 2.

Air for turbine operation was supplied by an Allis-Chalmers 12-stage axial compressor. Air from the main supply line passes through a four-inch pipe, a settling tank, a five-inch pipe, and then into the turbine. The flow rate was regulated by remotely controlled butterfly valves in the inlet line to the turbine and in the outside discharge line of the Allis-Chalmers compressor. (See Figure 9.) The controls for operating these valves are located in the control room (Figure 10).

The flow rate of the incoming air was measured with a sharp-edged orifice located in the four-inch inlet pipe. This orifice is also shown in Figure 9. The pressure ahead of the orifice and the pressure differential across the orifice were measured with standard vena contracta taps. The total temperature ahead of the orifice was measured with an

iron-constantan thermocouple installed in a Kiel temperature probe. The orifice installation conforms to standards set forth by Stearns, et al. (5).

The total inlet conditions in the five-inch pipe just upstream of the turbine were measured with a Kiel probe, also incorporating an iron-constantan thermocouple. The static pressure at the same location was measured by two static pressure taps in the line. The static pressure at the rotor inlet was measured by pressure taps located at eight peripheral stations in each shroud. The axial location of these taps is depicted in Figure 5, and their peripheral locations are shown in Figure 4. These taps were moved to the positions shown from their original locations near the shroud inner extremities by Boshoven (4) in order to reduce the effects of local pressure perturbations experienced in previous tests.

The torque exerted on the dummy rotor by the flow was measured on a 25-pound capacity Toledo precision scale, shown in Figure 2. A twelve-inch lever arm was attached to the rotor shaft and incorporated a simple provision for leveling, so that the force was exerted on the scale through an exactly vertical link. This was done to preserve the direct relationship between scale reading and moment. A counter balance was added to the lever arm in order to extend the capacity of the scales to accommodate higher mass flow rates.

A general schematic of the instrumentation used in this and the subsequent active rotor tests is shown in Figure 11. From this schematic it may be seen that the pressure upstream of the flow measuring orifice, the total and static pressures at the turbine inlet, and the reference pressures 1 and 2 were read from an eleven column, 40-inch mercury manometer board located in the control room. This board was referenced to

atmospheric pressure. Additionally, one arbitrarily selected scroll pressure tap was connected to the mercury board, and this pressure, together with the total inlet pressure, was used to set the pressure ratio across the scroll and guide vanes. The total inlet pressure displayed on the mercury board was used only for setting this pressure ratio since a more representative total pressure was computed in the data reduction.

The sixteen shroud pressure taps that measure the static pressure at the rotor inlet were read on a fifty-column, 96-inch water manometer board. Also displayed on this board were the pressures at various stations in the scroll itself, although these pressures were not used in the tests. These pressures were measured against atmospheric pressure for the entire series of dummy rotor runs. However, additional, controlled, pressures could have been imposed on the water board reservoirs by means of regulated house air if this had become necessary in order to avoid exceeding the limits of the manometer board. These pressures (the reference pressures 1 and 2 mentioned above) were displayed on the mercury manometer board. The first of these pressures, displayed on column 10 of the mercury board, was recorded as a test datum since it applied to the sixteen columns which indicated the rotor inlet pressures. The value of this pressure was thus zero for all dummy rotor runs.

The pressure differential across the flow orifice was measured on a 20-inch Meriam model 34FB2 mercury micro-manometer, which has a measuring accuracy of ± 0.001 inch. A pair of these instruments is shown in Figure 12.

The potentials generated by the iron-constantan thermocouples were measured on a 48-channel Brown potentiometer, manufactured by Minneapolis-Honeywell. This potentiometer, shown in Figure 13, was located in the control room and used an ice bath in the test cell as a cold junction reference.

A series of eighteen test runs were made on the dummy rotor installation, of which eight are documented in this report. These eight runs represent clearances of 0.015, 0.024, 0.030, 0.041, 0.051, 0.061, 0.072, and 0.081 inches, respectively. For each clearance ten pressure ratios were sampled, ranging in value from 1.05 to 1.65. These pressure ratios represent the ratio of total turbine inlet pressure to the static pressure at the rotor inlet.

This large number of runs was necessitated by several factors. Data from the initial runs possessed an unacceptable degree of scatter. This was attributed to an unstable supply of source air from the Allis-Chalmers compressor. When this unsatisfactory trend was discovered, the speed control system was overhauled, and the subsequent test results were significantly improved.

Additionally, the stability of the system was improved by judicious use of the aforementioned butterfly control valve. Experimentation showed that if less of the excess air from the compressor were discharged to the outside, the compressor would be operating at a higher pressure ratio, (with a greater pressure drop across the valve feeding the turbine), and the pressurized air in the house plumbing would act as an additional plenum. The system fluctuations would then be substantially reduced. These improvements in equipment and operating technique, as well as the inevitable improvement in data taking technique, led to such improved results that many runs were repeated in order to obtain the best possible test data.

As first observed by Boshoven (4), it was noted that the pressure distribution around the shroud was very sensitive to the relative positions of the rotor blade leading edges. To eliminate this factor as a possible variable, it was arranged to permit the return of the rotor to

the same location each time a new pressure ratio was set. This was accomplished by means of a wing nut on the end of the rod connecting the moment arm to the scale.

It was also observed that the pressures seemed to be higher by about 4 to 5 inches of water at the right side of the rotor inlet than at the left. This condition could be eliminated by moving the rotor approximately 0.001 inch axially to the left; but since the condition was also present in the scroll itself, it was attributed to scroll pressure distribution rather than to misalignment. The rotor was centered for all runs.

3.2 Theoretical Analysis

From the law of moment of momentum (6), the moment M exerted on the dummy rotor by the flow is given by

$$M = (\dot{W}/g) R_1 V_{u1} \quad (1)$$

where \dot{W} is the mass flow rate, R_1 is the inlet radius of the dummy rotor, and V_{u1} is the peripheral velocity component at R_1 . Equation (1) is valid for the case of steady flow in the dummy rotor because the pressures acting over the inlet and discharge areas cannot produce a moment about the axis, and because the flow straighteners insure an axial discharge velocity.

A measure of the performance of the scroll and guide vanes is given in the form of the velocity coefficient, ϕ , which is defined by

$$\phi \equiv V_1 / V_{1th} \quad (2)$$

where V_1 is the average velocity at the dummy rotor inlet and V_{1th} is the theoretical velocity at the dummy rotor inlet which would result from an isentropic expansion from the manifold inlet total conditions P_{t0} , T_{t0} ,

to the static pressure p_1 at the dummy rotor inlet. This process is shown on the T-s diagram of Figure 14. The component velocities may be seen on Figure 15.

From the energy equation for an adiabatic, no work process, the velocity V_1 at the dummy rotor inlet is

$$V_1 = \sqrt{2gJc_p(T_{t0} - T_1)} \quad (3)$$

If use is made of the isentropic pressure-temperature relation for a perfect gas and of Equation (2), V_1 may be alternately expressed as

$$V_1 = \phi \sqrt{2gJc_p T_{t0} \left[1 - (P_1/P_{t0})^{\frac{\gamma-1}{\gamma}} \right]} \quad (4)$$

Application of the equation of continuity at the dummy rotor inlet yields the following expression for the average meridional velocity component:

$$V_{m1} = \dot{W} / \rho_1 A_1 \quad (5)$$

where ρ_1 is the density at the dummy rotor inlet, and A_1 is the cross-sectional area normal to the flow (meridional cross-section). The area A_1 is given by

$$A_1 = 2\pi R_1 B_1 \quad (6)$$

where B_1 is the distance between the shrouds at the rotor inlet. Using the equation of state for a perfect gas, ρ_1 may be expressed as

$$\rho_1 = P_1 / R_g T_1 \quad (7)$$

Substitution of this relation and Equation (6) into Equation (5) yields the resultant expression for V_{m1} :

$$V_{m1} = \frac{\dot{W} R_g T_1}{2\pi R_1 B_1 P_1} \quad (8)$$

From Equation (1), the peripheral velocity may be expressed as

$$V_{u1} = \frac{M g}{R_1 \dot{W}} \quad (9)$$

and V_1 may additionally be given by

$$V_1 = \sqrt{V_{u1}^2 + V_{m1}^2} \quad (10)$$

Thus, three equations expressing the velocity V_1 are established, these being Equations (3), (4), and (10). Upon substitution of Equations (8) and (9) into Equation (10), it may be seen that this set of three equations contains three unknowns. The unknown quantities to be determined are the velocity V_1 , the velocity coefficient ϕ , and the temperature T_1 , all other quantities being either constants or determined directly from measured data. Solution of this system of equations establishes the velocity components, which may then be used to calculate the absolute flow angle at the dummy rotor inlet, according to the relation

$$\alpha_1 = \tan^{-1} (V_{u1} / V_{m1}) \quad (11)$$

A nozzle loss coefficient, ζ_N , may be obtained from the relation

$$\zeta_N = 1 - \phi^2 = 1 - \eta \quad (12)$$

where η is an efficiency based on the ratio of the actual-to-isentropic temperature drop across the scroll and guide vanes. It is introduced here only to illustrate the significance of ζ_N and ϕ .

3.3 Reduction of Data: Program SCROLL

The computer program SCROLL, listed in Appendix A, determines the unknown quantities, V_1 , ϕ , and T_1 , and the absolute inlet angle, α_1 , from the test data using an iterative procedure. The program makes temperature corrections to the physical properties of air and to the specific gravities of the water and mercury used as manometer fluids. It converts the manometer readings and thermocouple voltages into pressures and temperatures, as required, and then establishes the mass flow rate. The average conditions at the dummy rotor inlet are then calculated from the measured torque in accordance with the previously given relations.

Program SCROLL has been described in detail by Riley (3) and Boshoven (4). Except for conversion to the FORTRAN IV language, the program used in this experiment remains essentially the same; therefore, the details of the computational processes will not be repeated. However, certain minor changes were incorporated in the temperature corrections applied to the manometer fluids, in the thermocouple equations used, and in the pressure and flow rate solutions. These changes are briefly described in Appendix A, although they become evident if the program used in this report is compared with either of the two above-listed references.

3.4 Discussion of Results

The results of program SCROLL consist primarily of values of the velocity coefficient, ϕ , and the absolute flow angle at the rotor inlet, α_1 . These values are plotted versus M_1 , the Mach number at the rotor inlet, as opposed to the pressure ratio, P_{t0}/P_1 , because the Mach number is a more significant parameter in the application of test results to geometrically similar machines. Figure 16 shows ϕ as a function of

M_1 for each of the eight clearances tested, and Figure 17 is a similar plot for α_1 as a function of M_1 . Each of the curves was fitted to the data obtained for that run by the least squares method. The tabulated results for each of the eight runs are given in Appendix A.

It may be seen from Figure 16 that the velocity coefficient increases with Mach number, the average increase being approximately 4.75 per cent over a Mach number range of 0.2 to about 0.8. This percentage increase is practically the same regardless of clearance. This increase is due, at least in part, to the decreasing coefficient of friction in the scroll and guide vanes, which results from the increasing Reynolds number.

The coefficient ϕ generally increases with decreasing clearance for a given pressure ratio with the maximum values of ϕ occurring at the minimum clearance of 0.015 inches. As clearance is increased beyond a value of about 0.070 inches, the incremental drop in ϕ per increment of clearance increase appears to become much larger. An explanation for this occurrence is that as clearance is increased, an increasing amount of flow escapes around the blade tips. This flow loses angular momentum by wall friction and subsequently strikes the dummy rotor blades at some lesser radius, thus imparting a reduced amount of torque to the rotor. The cumulative effect of this energy loss would logically become more pronounced at increased clearances. The overlapping of certain of the curves in Figure 16 at the lower Mach numbers occurred because of the relative insensitivity of the instrumentation at low pressures.

Figure 17 shows that the absolute rotor inlet flow angle, α_1 , increases with increasing Mach number up to a Mach number of approximately 0.4. Beyond that point, α_1 decreases with increasing Mach number. These changes are small, although they appear to be significant because of the

highly expanded scale of Figure 17. In fact, the average maximum change in α_1 over the range of Mach numbers is approximately 0.52 degrees. In general, increasing the mass flow rate will increase V_1 and, of course, the components V_{u1} and V_{m1} . The variations in the magnitudes of these two quantities as the Mach number is increased determine the variations of α_1 , as shown by Equation (11).

It is also shown on Figure 17 that the angle α_1 increases as clearance increases. This is primarily because V_{m1} is inversely proportional to the meridional cross section, which increases with clearance since it depends on the distance between the shrouds. By Equation (11), the smaller values of V_{m1} result in larger inlet flow angles.

It was concluded by Riley (3) that the velocity coefficient ϕ was essentially independent of the pressure ratio P_{t0}/P_1 , and that a constant representative value of 0.889 was sufficiently accurate. Although he determined that α_1 decreases with increasing pressure ratio, he also assumed a representative value of 80.0 degrees for α_1 .

Boshoven (4) subsequently investigated the scroll and guide vane performance in greater detail and obtained results that agree in a qualitative sense with those described above. Because of the many modifications made to the machine components, both in preparation for this experiment and during the course of Boshoven's, a more precise comparison is not warranted. It is worthy of note, however, that Boshoven did not obtain the continuous decrease in ϕ with increasing clearance which is apparent from Figure 16. Further, the increase in ϕ with Mach number found in the present tests is more pronounced than Boshoven's, his increase being on the order of 2 per cent for a given clearance, over the range of Mach numbers. It is felt that these changes have occurred because of the machining of the rotor so that it more closely fits the shroud contours,

thus minimizing flow loss around the blades and permitting closer minimum clearances.

An examination of the data points given in Figure 16 for \emptyset as a function of Mach number shows that some scatter exists. This scatter may be attributed to fluctuations in the air supply from the Allis-Chalmers compressor. The presence of this problem and methods undertaken to alleviate it have been discussed previously in Section 3.1. This scatter of data is also present in the curves of α_1 as a function of Mach number given in Figure 17, but to a lesser extent.

In order to use the results of the dummy rotor tests in later data reduction programs, it was necessary to obtain equations representing \emptyset and α_1 in the form

$$\alpha_1 = \text{Constant} [f_1 (\text{clearance})][f_2 (\text{Mach number})]$$

The function f_1 was obtained by first taking the ratio of α_1 to α_1 maximum at each Mach number, for each clearance. The values of this ratio were then plotted versus clearance. From this plot an average curve was obtained, and its equation was computed by the least squares technique. The resulting equation expressed $\alpha_1 / \alpha_{1\text{max}}$ as a dimensionless function of clearance.

The function f_2 was obtained by computing the ratio of α_1 to the value of α_1 at a Mach number of 0.5, and plotting this ratio versus Mach number for each clearance. Again, an average curve was determined, and its equation was computed. This equation, again dimensionless, expresses $\alpha_1 / \alpha_{1(M=.5)}$ as a function of Mach number.

The appropriate scaling factor was determined for each test point. An average of all of these factors, which did not differ greatly in value, was taken as the constant in the above expression. The equation for \emptyset was determined in the same manner.

The final equations resulting from this procedure were

$$\alpha_1 = (81.762) [.98267 + .26958 (Clnc) - .65080 (Clnc)^2] \quad (13)$$

$$[.99624 + .02223 (M_1) - .02940 (M_1)^2]$$

$$\phi = (.92473) [1.01433 - 1.24601 (Clnc) + 24.06839 (Clnc)^2 \quad (14)$$

$$- 180.36258 (Clnc)^3]$$

$$[.93149 + .18292 (M_1) - .09202 (M_1)^2]$$

Families of curves produced by these equations are given in Figures 18 and 19, for ϕ and α_1 respectively. These curves agree well with those of Figures 16 and 17 when consideration is given to the approximations introduced in the derivations of Equations (13) and (14). For the velocity coefficient, ϕ , the maximum difference which exists at any point between the curves of Figure 16 and those of Figure 18 is 0.0052. A similar comparison for α_1 yields a maximum difference of 0.06 degrees. Because of the manner in which Equations (13) and (14) were derived, the most significant discrepancies occur near the extremes of the Mach number range.

SECTION 4

ANALYSIS OF OVERALL TURBINE PERFORMANCE

The turbine overall performance tests, when combined with the results of the dummy rotor tests, provided data from which detailed performance parameters of the turbine could be evaluated. The specific parameters evaluated were: the total-to-static overall efficiency; velocity and loss coefficients for the rotor and guide vanes; rotor inlet and outlet flow angles; referred speed, moments, and flow rates; the head coefficient; and the degree of reaction. Calculations were made assuming no bearing losses and also for the case of "maximum" bearing losses. Bearing loss values were determined from equations given by Vavra (1), which were established from coast-down tests. The analysis was made using a "mean" streamline approach, which is defined as utilizing a representative streamline along which the measured flow conditions are assumed to exist. This streamline was taken as that at the outer discharge radius of the turbine for this analysis, and thus all losses are referred to that outer radius.

4.1 Instrumentation

The "active" rotor shown in Figure 7 was installed for this series of tests, and the rotor and wooden casing were placed in an aluminum test stand. Figure 1 shows the test installation. Alignment of the scroll with respect to the rotor was accomplished by the use of the dummy alignment shaft and dial micrometers shown in Figure 20. Precise alignment was found to be quite difficult because the massive wooden casing and scroll assembly had to be positioned relative to the rotor. Positioning was accomplished by means of four adjusting bolts located at the bottom

of the casing and by four angle-irons attached to the casing and resting on the bearing supports. In spite of the difficulty involved, alignment of the concentric aluminum rings which serve as supports for the shrouds was obtained to within ± 0.001 inch in the radial direction from the dummy alignment shaft. These rings were found to deviate from a plane perpendicular to the rotor axis by less than 0.002 inch at a radius of 4.7 inches.

The power developed by the turbine was absorbed by a Vortec Products Company air dynamometer, model 20.075, shown in Figure 1. Lubrication of the dynamometer was accomplished by an oil mist generated by air pressure. The torque output was measured with a torque capsule having a maximum rated capacity of 400 inch-pounds. This capsule utilized strain gages arranged on an internal flexure and was additionally instrumented with an iron-constantan thermocouple to provide a means of monitoring the capsule temperature. The signal generated by the strain gages was read on a Daytronic model 700 digital indicator located in the control room (Figure 10).

The dynamometer shroud was modified from the configuration used by Riley (3) so as to discharge the hot exhaust air radially outward, rather than back onto the torque capsule and housing, in order to minimize thermal effects on the torque capsule. The circular aluminum ring visible in Figure 1 was used to accomplish this modification. Additionally, a wooden baffle, not shown on Figure 1, was used to protect the capsule from the cold turbine discharge air, and to prevent any interference between the dynamometer discharge and the right rotor discharge.

Figure 21 shows the inner face of the torque capsule, the steel quill shaft used to connect the dynamometer to the turbine, and the magnetic pick-up and six-lobe flux cutter used to measure turbine speed. The turbine speed was read from a Hewlett-Packard electronic counter located in the

control room (Figure 22). Speed was regulated by means of a remotely controlled motor on the dynamometer itself, which changes the load capacity of the dynamometer. The remote control unit is shown in Figure 10, and the drive motor is shown in Figure 1.

Lubrication of the turbine bearings was provided by a dry-sump system utilizing a gear-driven oil pump and an upper and a lower oil mist injector for each bearing. The lubricating fluid used was 1010 jet engine oil. The cart containing the pump, oil reservoir, heat exchanger, and system pressure gages is shown in Figure 23, and the lubrication system is shown schematically in Figure 24. For these tests the previously existing system was changed to that shown in Figure 24 to permit measurement of the oil temperature into the bearings and at the point of discharge from both bearings. This was accomplished with iron-constantan thermocouples installed as shown on the schematic.

Figure 24 also shows the iron-constantan thermocouples used to measure the bearing outer race temperatures. Vibration signals from the bearings were detected by a piezo-quartz accelerometer mounted on the upper left bearing cap and monitored on a Panoramic vibration analyzer manufactured by the Singer Metrics Company. The accelerometer is visible in Figure 8, and the analyzer is shown in Figure 22.

The pressures and flow rates were measured in the same manner as for the dummy rotor test previously described. The signals from the thermocouples were initially read from the Brown potentiometer shown in Figure 13. During the latter part of the testing period, however, they were read from a new automatic data acquisition system manufactured by B & F Instruments, Inc. This system is shown in Figure 25.

4.2 Test Procedures

Test runs were conducted at five different axial clearances: 0.081, 0.061, 0.041, 0.024, and 0.015 inches. For each clearance, runs were made at total inlet to static discharge pressure ratios of 1.2, 1.3, 1.4, 1.5, 1.6, and 1.7. At each pressure ratio, turbine speed was varied from the minimum speed (maximum load condition) for that pressure, to the highest speed attainable, in increments of about 1,500 rpm. Maximum speed was restricted to 18,000 rpm for reasons of safety.

Measurement of the torque at zero speed was also made for each pressure ratio at each clearance. This was accomplished by engaging the dynamometer rotor lock and measuring the resulting torque.

As turbine speed was increased during the first run, a point was reached at which the bearings overheated and started to seize, causing a rapid drop in speed. The turbine was dismantled and carefully examined. No apparent damage had been incurred by the ball bearings. The oil system was flushed and refilled, and the unit was reassembled. This condition repeated itself in several subsequent runs, occurring whenever the bearing temperature reached approximately 135°F. Additionally, considerable amounts of oil were being lost from around the shaft and bearing caps at higher speeds. Apparently neither of these conditions had existed in previous tests.

Since the bearings themselves did not appear to be at fault, extensive tests were made to determine whether changing the amount of lubricating oil flow would alleviate these problems. It was found that varying the oil system pressure from 10 pounds per square inch to 50 pounds per square inch would reduce the bearing temperature a maximum of six degrees, but this variation did not significantly reduce leakage. A solution was ultimately found to both problems by carefully positioning

the oil injectors so that they discharged directly into the balls of the bearing and did not strike the race and by slightly enlarging the injector orifices so as to increase the mass flow rate of the oil. The bearing temperatures could then be kept below a maximum of about 125°F at 18,000 rpm, and oil leakage was negligible.

The fact that the bearings experienced a maximum temperature increase of about 50° over the range of speeds tested, whereas in previous tests the increase had been only about half as much (7), created a question as to the applicability of the bearing loss information obtained from the coast-down tests conducted by Vavra (1). It was therefore decided to attempt to evaluate the bearing losses by measuring the oil flow rate and the amount of heat absorbed by the oil as it flowed across the bearings. If the constant pressure specific heat, C_p , of the oil were known, the energy lost in the bearings could be obtained from the relation

$$\text{BFM} = \frac{\dot{W}_{\text{oil}} C_{p\text{oil}} \Delta T_{\text{bearings}}}{\omega} \quad (15)$$

where BFM is the bearing friction moment in foot-pounds and ω is the turbine rotational speed.

Numerous tests were made in order to calibrate the mass flow rate of the oil with the system pressure, and the lubrication system was modified to include the previously discussed thermocouples ahead of and after the bearings. Flow rate calibration was accomplished by weighing the amount of oil discharged by the injectors on each side in a given time interval.

In attempting to evaluate bearing losses by this technique, the results obtained from several test points indicated losses on the order of 20 per cent of the minimum losses predicted by Vavra (1). In fact, it was discovered that the exposure of the inlet lines, the bearing block itself, and the sumps to the cold discharge air sometimes produced cooler

temperatures on the discharge side of the bearings than existed ahead of the injectors. Since insulation of the oil lines and the bearing blocks to the extent necessary to overcome this deficit was not feasible, this attempt to determine the bearing losses was abandoned. The oil temperatures were recorded as data for future use, however, and appear in Appendix B.

The dynamometer torque capsule was calibrated both before and after each day's runs in order to permit consideration of any variations during the course of the runs. Calibration was accomplished by use of the device shown in Figure 26. An aluminum plug was fabricated to fit into the torque ring of the capsule. Torque was applied by loading the weight pans on the moment arm, which was attached to the plug. Riley (3) attached the moment arm directly to the inlet side of the dynamometer; thus, a moment was introduced due to the axial distance between the capsule and the point of application of the load. The apparatus used in these tests reduced this potential source of error almost entirely.

Loads of 0 to 400 inch-pounds were applied to the capsule in 100 inch-pound increments. The span of the digital readout was set at 0 to 1000 counts, the latter approximately corresponding to 400 inch-pounds. Calibration readings were taken for both increasing and decreasing loads in order to evaluate the amount of hysteresis present in the readout. As each load was applied, the capsule housing was tapped gently with a mallet to overcome any drag in the capsule itself and to eliminate errors caused by lag in the servomechanism of the digital counter. This procedure is valid, because a like amount of vibration was observed to exist under the dynamic load conditions of an actual test run. Using this technique, the amount of hysteresis present between the loading and unloading cycles was found to be negligible.

The torque readouts for calibrations performed both before and after the test runs were found to vary linearly with applied torque. However, the data obtained after the run were generally higher, by 2 to 3 counts at zero load, to 13 to 15 counts at 400 inch-pounds, than the original calibration. This was felt to be due to the thermal effects of the higher capsule temperatures which existed during the run. A thermocouple was installed in the capsule in an attempt to establish some correlation between this temperature rise and the torque count increase. Tests in which the capsule was heated from the outside with a strip heater were inconclusive, because similar increase in torque counts for given torque loadings could not be produced, even though the temperatures indicated by the thermocouple were considerably higher than those recorded during the actual test runs.

When the turbine is in operation, the capsule is heated from within by heat from the dynamometer bearings. This is modified by the dynamometer water cooling system and by the cold turbine discharge air. A method of reproducing the interaction of all of these conditions in static calibration tests was not found, and so the torque calibration data ultimately used represented an average of the data obtained before and after the test runs. This accounts for some increase due to thermal effects and is felt to be a reasonable representation. In some instances, the capsule temperature was observed to increase immediately following shut-down, while at other times the reverse effect occurred. It is felt that more representative temperature data could be obtained by relocating the thermocouple on the flexure closer to the strain gages.

The compressor which provides house air failed after two clearances, 0.081 and 0.061 inches, had been tested. This compressor provides air to the speed controls of the Allis-Chalmers compressor and also provides the

air which is used as a reference pressure for the water manometer board. The remaining three clearances were tested using a smaller auxiliary compressor, which introduced considerable fluctuations into the house air system.

4.3 Theoretical Analysis

The known quantities necessary for the turbine analysis as performed in this project are: mass flow rate; total inlet temperature and pressure; static inlet pressure; turbine speed and torque output; atmospheric pressure and temperature; and the absolute rotor inlet flow angle and velocity coefficient based on the results of the scroll and guide vane analysis.

The working fluid is assumed to undergo an adiabatic process, since the quantity of heat passing through the casing is negligible compared to the enthalpy change undergone by the fluid as it passes through the turbine. It is additionally assumed that the fluid behaves as a perfect gas.

The flow is assumed to have axisymmetric stream surfaces; thus, in effect, the analysis is one-dimensional, based on the determination of the flow properties along a particular streamline lying on a chosen surface of revolution. Vavra (8) states that the major portion of the rotor losses is due to secondary flow phenomena, tip leakage losses, and the loss that occurs because of the motion of the blade tips in the wall boundary layers. Thus it would appear that the majority of the losses occur near the shrouds, and the representative streamline was accordingly chosen as that existing at the outer radius of the rotor discharge. It was felt that this approach would yield a better correlation of results than that obtained from use of a calculated mass-averaged mean radius at the rotor discharge (7).

It is assumed that the relative flow angle β_{20} , calculated from the blade dimensions, is very nearly equal to the actual relative flow angle at the outer discharge radius (where β_{20} assumes its maximum value). This implies that the so-called slip factor may be neglected. Verification of the validity of this assumption is given by the flow surveys taken at the rotor discharge by Riley (3). Accordingly, β_{20} was calculated from Equation A2(4) of (1) and found to be equal to -69.85 degrees at the outer radius. This value was used in all calculations.

The thermodynamic process of a fluid passing through a turbine is given in Figure 14. The resulting flow velocities are shown in Figure 15. The derivations which follow are based on these two diagrams.

Referring to Figure 14, for a reversible, adiabatic process,

$$\frac{T_2''}{T_{t0}} = \left(\frac{P_2}{P_{t0}} \right)^{\frac{\gamma-1}{\gamma}} \quad (16)$$

where T_2'' represents the static temperature at the rotor discharge for an isentropic expansion through the turbine to P_2 . The isentropic temperature drop which would occur for such an expansion is

$$\Delta T_{is} \equiv T_{t0} - T_2'' \quad (17)$$

and may therefore be expressed as

$$\Delta T_{is} = T_{t0} \left[1 - \left(P_2 / P_{t0} \right)^{\frac{\gamma-1}{\gamma}} \right] \quad (18)$$

Similarly, for an isentropic expansion across the inlet guide vanes

$$\frac{T_1'}{T_{t0}} = \left(\frac{P_1}{P_{t0}} \right)^{\frac{\gamma-1}{\gamma}} \quad (19)$$

and

$$(\Delta T_{is})_{\text{guide vanes}} \equiv T_{t0} - T_1' = T_{t0} \left[1 - \left(P_1 / P_{t0} \right)^{\frac{\gamma-1}{\gamma}} \right] \quad (20)$$

The isentropic, or theoretical degree of reaction, r , represents that portion of the overall isentropic enthalpy drop which occurs in the rotor, or

$$r \equiv \frac{T_1' - T_2''}{\Delta T_{is}} \quad (21)$$

Therefore,

$$r = 1 - \frac{(\Delta T_{is})_{\text{guide vanes}}}{\Delta T_{is}} \quad (22)$$

and, from Equations (18) and (20),

$$r = 1 - \frac{\left[1 - (P_1/P_{t0})^{\frac{\gamma-1}{\gamma}} \right]}{\left[1 - (P_2/P_{t0})^{\frac{\gamma-1}{\gamma}} \right]} \quad (23)$$

The total-to-static efficiency of the turbine is defined as the ratio of the work actually produced by the turbine to that work which could ideally be accomplished by isentropic expansion from total inlet to static outlet conditions. For this case, the efficiency may be expressed by the ratio of the corresponding temperature drops,

$$\eta = \Delta T_w / \Delta T_{is} \quad (24)$$

The change in total enthalpy across the turbine is

$$\Delta H_w = c_p \Delta T_w = \frac{M \omega}{J \dot{W}} \quad (25)$$

where M is the net torque produced, ω is the rotational speed, and \dot{W} is the mass flow rate. Therefore, ΔT_w may be expressed as:

$$\Delta T_w = \frac{M \omega}{J c_p \dot{W}} \quad (26)$$

The efficiency given by Equation (24) was computed both for the case where bearing friction was considered and for the case where it was not. Bearing friction was calculated based on the results of coast-down

tests performed by Vavra (1). The friction horsepower is expressed by

$$HP_f = -0.6 + (N/1000)(.17143) \quad (27)$$

for $N \leq 10,500$ rpm, and by

$$HP_f = -0.6 + (N/1000)(.17143) - (4.898 \times 10^{-3})(N/1000 - 10.5)^2 \quad (28)$$

for $N > 10,500$ rpm. The bearing friction moment is then given by

$$M_f = \frac{HP_f \times 550}{\omega} \quad (29)$$

The net moment is then the sum of T , the moment measured by the dynamometer, and the bearing friction moment:

$$M = T + M_f \quad (30)$$

The velocity C_o corresponding to the isentropic enthalpy drop through the turbine is given by the expression

$$C_o^2 \equiv 2gJc_p \Delta T_{is} \quad (31)$$

and the peripheral speed of the rotor at the rotor inlet is

$$U_1 = \frac{\pi N D_1}{720} \quad (32)$$

where D_1 is the rotor inlet diameter in inches. By Equations (31) and (32), the isentropic head coefficient is given by

$$K_{is} \equiv (C_o / U_1)^2 \quad (33)$$

The absolute velocity V_1 is expressed by Equation (4). An alternate expression, obtained by substitution of Equation (23) into Equation (4), is

$$V_1 = \phi \sqrt{2gJc_p (1-r) \Delta T_{is}} \quad (34)$$

The temperature T_1 may then be obtained from

$$T_1 = T_{to} - \frac{V_1^2}{2gJc_p} \quad (35)$$

and M_1 , the Mach number at the rotor inlet, is

$$M_1 = \frac{V_1}{\sqrt{2gJc_p T_1}} \quad (36)$$

The results of the dummy rotor tests can now be used by introducing Equation (14) to obtain ϕ by an iterative procedure which is discussed in Appendix B. Equation (12) gives the nozzle loss coefficient as

$$\zeta_N = 1 - \phi^2 \quad (37)$$

Values for α_1 can now be taken from Equation (13) to determine the peripheral and meridional velocity components of V_1 .

$$V_{u1} = V_1 \sin \alpha_1 \quad (38)$$

$$V_{m1} = V_1 \cos \alpha_1 \quad (39)$$

From Figure 15 it is apparent that the peripheral component of the relative rotor inlet velocity W_1 is

$$W_{u1} = V_{u1} - U_1 \quad (40)$$

and W_1 is then found from

$$W_1 = \sqrt{V_{m1}^2 + W_{u1}^2} \quad (41)$$

The relative inlet flow angle β_1 is

$$\beta_1 = \sin^{-1} (W_{u1} / W_1) \quad (42)$$

At this point all conditions at the entrance to the rotor are known.

It is assumed that only the kinetic energy $V_{m1}^2 / 2gJC_p$ is useful in the rotor (since it has radial blades), and that the incidence loss at the rotor inlet is taken as $W_{u1}^2 / 2gJC_p$ (8). Thus, the effective relative velocity head is reduced, and static conditions at the rotor inlet are really those at T_1^* on Figure 14.

The equivalent state point E shown on Figure 14 is established from the energy equation for a rotating system in the following manner (6):

$$H_R = \text{constant} = h_1 + \frac{W_1^2}{2gJ} - \frac{\omega^2 R_1^2}{2gJ} = h_2 + \frac{W_2^2}{2gJ} - \frac{\omega^2 R_2^2}{2gJ} \quad (43)$$

where H_R is the relative total enthalpy. This equation may be rearranged in the form

$$H_E \equiv h_1 + \frac{W_1^2}{2gJ} - \left(\frac{U_1^2 - U_2^2}{2gJ} \right) = h_2 + \frac{W_2^2}{2gJ} \quad (44)$$

where the left side is equal to H_E , the total enthalpy at the state point E. Equation (44) clearly shows that state point E is the proper reference point from which to view the expansion process through the rotor in an analogous manner to that of the stator. The peripheral speed at the outer discharge radius, U_{20} , is given by Equation (32) with D_1 replaced by D_{20} , the outer diameter of the rotor discharge.

The work output of the turbine, represented by the change in total enthalpy, may be represented by Euler's turbine equation (6):

$$\Delta H_W = C_p \Delta T_W = \frac{U_1 V_{u1} - U_{20} V_{u20}}{gJ} \quad (45)$$

where U_{20} and V_{U20} occur at the outer discharge radius. Manipulating this equation and Equations (24) and (31), an expression for the peripheral component of the absolute discharge velocity, V_{U20} , is

$$\frac{V_{u20}}{U_1} = \frac{R_1}{R_{20}} \left[\frac{V_{u1}}{U_1} - \frac{\eta}{2} \left(\frac{C_o}{U_1} \right)^2 \right] \quad (46)$$

Using the velocity diagram of Figure 15, it can be shown that the relative velocity at the outer discharge radius, W_{20} , may be expressed by

$$\frac{W_{20}}{U_1} = \frac{(V_{u20}/U_1) - (R_{20}/R_1)}{\sin \beta_{20}} \quad (47)$$

where, in keeping with the stated assumptions,

$$\beta_{20} = -69.85^\circ \quad (48)$$

If the divergence of the pressure lines on the entropy diagram of Figure 14, in the direction of increasing entropy, is neglected, there is

$$T_1^* - T_2' = T_1' - T_2'' \quad (49)$$

By Equations (21) and (31), the right side of the expression is equivalent to

$$T_1' - T_2'' = r \frac{C_o^2}{2gJc_p} \quad (50)$$

From Figure 14, the left side may be expressed in terms of the velocities:

$$T_1^* - T_2' = \frac{W_{20th}^2}{2gJc_p} + \frac{U_1^2 - U_{20}^2}{2gJc_p} - \frac{V_{m1}^2}{2gJc_p} \quad (51)$$

Manipulation of Equations (50), (51), and (32) yields a relation for W_{20th} , the theoretical relative velocity at the rotor discharge:

$$\frac{W_{20th}}{U_1} = \left[\frac{r}{(U_1/C_o)^2} + \left(\frac{R_{20}}{R_1} \right)^2 + \left(\frac{V_{m1}}{U_1} \right)^2 - 1 \right] \quad (52)$$

Using Equations (47) and (52) it is now possible to define a velocity coefficient Ψ for the rotor, which is analogous to the velocity coefficient ϕ for the scroll and guide vanes given by Equation (2).

$$\Psi \equiv W_{20} / W_{20th} \quad (53)$$

The rotor loss coefficient, which is a measure of the kinetic energy loss through the rotor, is, then

$$\zeta_R \equiv 1 - \Psi^2 \quad (54)$$

The meridional velocity component of the absolute discharge velocity can be expressed by

$$V_{m20} = W_{20} \cos \beta_{20} \quad (55)$$

from Figure 15. The absolute discharge flow angle is then

$$\alpha_{20} = \tan^{-1} (V_{u20} / V_{m20}) \quad (56)$$

If consideration is given to the case where bearing losses are assumed to exist, the resulting efficiency will obviously be different from that for no bearing losses. Examination of the foregoing analysis shows that, correspondingly, different values for V_{u20} , V_{m20} , W_{20} , Ψ and ζ_R will result.

Thus, from the measured items of test data specified at the beginning of this section, the following performance parameters are obtained by the analysis technique: flow rate, head coefficient, degree of reaction, absolute and relative rotor inlet flow angles, velocity and loss coefficients for the scroll and guide vanes, the net torque produced, the absolute discharge flow angle, the rotor velocity and loss coefficients, and the total-to-static efficiency.

In this experiment the above parameters are referred to standard air in accordance with the NASA method, as described in (1). This method utilizes a total inlet pressure of 14.7 pounds per square inch absolute, a total inlet temperature of 518.7 degrees Rankine, a specific heat ratio of 1.4, and a constant pressure specific heat of 0.24 BTU per pound mass-degree Fahrenheit. The referral parameters are

$$\delta \equiv P_{t0} / 14.7 \quad (57)$$

$$\theta \equiv T_{t0} / 518.7 \quad (58)$$

and

$$\epsilon = \frac{0.810}{\gamma} \left(\frac{\gamma+1}{2} \right)^{\frac{\gamma+1}{2(\gamma-1)}} \quad (59)$$

The factor ϵ , which corrects the flow rate through the turbine for varying values of γ , is that given by Vavra (1) and is supposed to give a better correlation than the expression for ϵ used by NASA.

The referred speed is then given by

$$N_{ref.} \equiv N / \sqrt{\theta} \quad (60)$$

The referred flow rate is

$$\dot{W}_{ref.} \equiv \dot{W} \left(\sqrt{\theta} \frac{\epsilon}{\delta} \right) \quad (61)$$

Finally,, the referred moment is

$$M_{ref} \equiv M \left(\frac{\epsilon}{\delta} \right) \quad (62)$$

4.4 Data Reduction: Programs RADIAL and NOSP

The computer program RADIAL, listed in Appendix B, determines the turbine performance parameters described in Section 4.3 from the test data. In general, the specific techniques used by the computer in these computations are apparent from the program itself. However, Appendix B describes each subroutine briefly and elaborates on specific computational procedures which are not immediately obvious.

Program NOSP, listed in Appendix C, was written to compute the desired performance parameters from the locked rotor test data.

4.5 Discussion of Results

The input data and results of program RADIAL are listed in Tables B4 through B13, with input and output for a given clearance appearing in adjacent tables. The input data and results of program NOSP appear in Table C2.

Figure 27 shows the degree of reaction, r , as a function of head coefficient, k_{is} , for the clearances tested in this analysis as well as those of Riley (3) and Vavra (1). For each clearance, the degree of reaction was found to be a unique function of head coefficient, independent of turbine pressure ratio. This is in agreement with the findings of both Riley and Vavra. Riley further concluded that the degree of reaction is independent of axial clearance. The results of the present tests verify this for all clearances except for 0.081 inch. At this clearance, the values of r obtained were found to be approximately 1 to 1.5 per cent lower than those for the other clearances. This is shown on Figure 27, where the resulting curves for all clearances except 0.081 inch are represented by that for 0.061 inch, and the curve for 0.081 inch is plotted separately. This discrepancy implies that, for a given overall pressure

ratio, the pressure p_1 can no longer be maintained at a clearance of 0.081 inch.

It may be seen from the representative curve of Figure 27 that r decreases with increasing k_{is} (decreasing speed), from a value of approximately 0.75 at a k_{is} of 1.05 to 0.30 at a k_{is} of 6. This drop occurs because, with decreasing speed, a smaller pressure drop is required to pass the flow through the rotor.

The degree of reaction curves obtained in earlier tests by Vavra (1) and Riley (3) are superimposed on the curve of Figure 27. Vavra states that the value of r at design k_{is} of 2.3 should be approximately 0.486, as compared with the value of 0.395 obtained by him and with Riley's value of 0.402. The current tests yielded a value of 0.440 at design k_{is} , except for a clearance of 0.081 inch, for which the corresponding value of r was 0.434. This apparent increase in degree of reaction is due primarily to a more accurate determination of p_1 than was used by either Vavra or Riley. Boshoven (4) relocated the shroud pressure taps, which measure the pressure p_1 , to a position axially outward in the annulus around the periphery of the shroud. This was done to reduce the effects of local perturbations on the pressure readings and greatly improved the uniformity of the pressure distribution around the shrouds. This improvement in the accuracy of p_1 yields a more accurate value of r since degree of reaction is directly dependent on p_1 .

The degree of reaction remains lower than the design value because the guide vane exit area is too small to permit discharge of the design mass flow (1).

Significant plots resulting from the overall turbine efficiency calculations are given in Figures 28 through 31. Figure 28 depicts turbine efficiency as a function of referred speed for the case of no bearing

losses and a clearance of 0.081 inch. Figure 29 is a corresponding plot of efficiency versus head coefficient. Figures 30 and 31 represent these same respective parameters, also at a clearance of 0.081 inch, for the case where bearing losses are considered.

Efficiency was found to be essentially independent of clearance over the range of clearances tested. Figures 28 through 31 are therefore representative of the results for all clearances between 0.015 and 0.081 inch.

Values of turbine efficiency were obtained from measurements of the torque at the turbine shaft made with the air dynamometer and from the bearing loss values as determined from the results of coast-down tests conducted by Vavra (1). Because of the previously discussed problem of excessive bearing temperatures and seizing experienced during these tests, the bearing losses are probably greater than the maximum losses determined by Vavra. However, since time did not permit a repetition of the coast-down tests, Vavra's equations for maximum bearing losses [Equations (27) and (28)] were used.

A comparison of Figures 28 and 29 and of Figures 30 and 31 shows the advantage derived from representing efficiency as a function of head coefficient instead of referred speed. Use of the head coefficient effectively reduces a family of curves to a single curve. However, if the bearing losses are ignored, as in Figure 29, the resulting plot depends significantly on pressure ratio. In this figure only those curves representing the pressure ratios for maximum and minimum efficiencies are shown to avoid clutter.

Figure 31 shows that the efficiencies are nearly independent of pressure ratio in the case where allowance is made for bearing losses. If these bearing losses were accurately known, it would appear that the influence of pressure ratio would be completely eliminated from a plot of efficiency versus head coefficient.

In general, if bearing losses are not considered, a pressure ratio of 1.7 yields a maximum efficiency of 81.1 per cent at a k_{is} of 2.35 and an axial clearance of 0.015 inch. Minimum efficiencies are obtained for a pressure ratio of 1.2 and are in most cases 10 to 12 per cent lower than maximum efficiencies in the vicinity of the design k_{is} of 2.3. Vavra (1) reported a maximum efficiency of 81 per cent for the case of no bearing losses at a pressure ratio of 1.616, k_{is} of 2.37, and clearance of 0.062 inch. Riley (3) obtained a corresponding maximum efficiency of 82.52 per cent at a k_{is} of 2.26, pressure ratio of 1.678, and clearance of 0.027 inch.

For the case where bearing losses are taken into account, the maximum efficiency, η_L , was found to be 84.6 per cent at a pressure ratio of 1.7, head coefficient of 2.28, and clearance of 0.081 inch. This compares favorably with the design efficiency of 85.5 per cent at a pressure ratio of 1.7 and head coefficient of 2.3, as given by Vavra (1). Riley (3) obtained a maximum efficiency of 86.04 per cent at a pressure ratio of 1.678, head coefficient of 2.259, and clearance of 0.027 inch, based on the maximum values of bearing losses.

At minimum speed (maximum k_{is}) for a given pressure ratio and clearance, the efficiency in general is about 65 per cent. As speed is increased (k_{is} decreased), the efficiency increases to a maximum of about 84 per cent in the vicinity of a k_{is} of 2.3 and then falls off rapidly to 30 to 40 per cent at a k_{is} of about 1.05. Initially, then, the efficiency increases with speed because, by Equation (26), an increase in ω and decrease in \dot{W} offset the decrease in torque, resulting in increased turbine work and efficiency. As speed is further increased, the decreasing torque begins to predominate, causing the efficiency curve to peak and then rapidly decrease.

It was expected that, as the clearance was varied over the range encompassed by these tests, a "critical" clearance would be reached beyond which turbine efficiency would deteriorate rapidly. Riley (3) observed this to occur at a clearance of 0.052 inch. Such an occurrence was not observed in these tests over the range of clearances from 0.015 to 0.081 inch. Thus, it appears that axial clearance has no appreciable effect on turbine efficiency over this range of clearances.

It has been previously stated that Riley (3) was in all likelihood operating at a considerably greater clearance than he believed himself to be. This is substantiated to a degree by the fact that Vavra (1) did not experience this efficiency drop at a clearance of 0.062 inch. Since gaps also existed between the rotor and shrouds during Riley's tests, the blades would have left the wall boundary layer at a lesser axial clearance than in these tests where the blade and shroud contours were matched. Thus, it is reasonable to assume that the critical clearance is at some value greater than 0.081 inch.

That such a drop in efficiency should occur as clearance is increased to some critical value is explained in part by Csanady (9). The rotating blades "scrape up" the shroud boundary layer and produce vortices in the vicinity of the tips of the blades which, in turbines, tend to nullify the tip vortices themselves. At a particular tip clearance, then, these two vortices would neutralize each other, leaving only the passage vortex which causes secondary flow losses. This neutralization should produce a pronounced increase in efficiency at that clearance at which it occurs. For the subject turbine, it would appear that if this condition does exist, it occurs at a clearance less than 0.015 inch.

The efficiency is essentially independent of clearance because, although the tip vortices become more predominant as clearance increases,

there is also a buildup of the boundary layer. This buildup maintains a reasonably even relative balance between the tip vortices and the "scraped up" vortices. As clearance is extended beyond some critical value, however, the blades begin to operate near the edge of the wall boundary layer, and the countering vortices quickly cease to be effective in neutralizing the increasing tip vortices. The result is a pronounced increase in rotor loss and a corresponding decrease in turbine efficiency. It is also worthy of note that, for the test turbine, although the axial tip clearance is increased, the radial clearance between the shrouds and the rotor blades in the vicinity of the discharge remains essentially unchanged.

The rotor velocity coefficient, Ψ , is plotted as a function of the head coefficient in Figure 32, for the case where bearing losses are neglected. The clearance represented is 0.024 inch. Figures 33 through 37 show the curves of Ψ_L versus k_{is} , with bearing losses considered, for each of the five clearances tested. Again, it may be seen that if bearing losses are ignored, there is considerably more variation of the curves with pressure ratio than in the case where bearing losses are considered.

The only variation in rotor velocity coefficient with axial clearance which can be established is that values of Ψ for a clearance of 0.081 inch seem to be generally higher than for all other clearances. This variation is evident for both bearing loss cases, with values of Ψ_L being generally 10 to 15 per cent higher at a clearance of 0.081 inch. Because of the negligible effect of axial clearance and the doubtful significance of the case where bearing losses are neglected, Figure 32, for a clearance of 0.024 inch, is the only curve included for the case where bearing losses are not considered.

Figures 33 through 37 show that maximum values of ψ_L do not always occur at the higher pressure ratios, although ψ_L is more nearly constant over the range of k_{is} values for the higher pressure ratios.

At the design k_{is} of 2.3, a value for ψ_L of 0.960 was produced at a pressure ratio of 1.2 and clearance of 0.081 inch. The maximum value of ψ_L was found to occur at the same pressure ratio and clearance and at a k_{is} of 3.35. Its value is 0.990.

It can be seen from the curves for ψ_L given in Figures 33 through 37 that ψ_L remains relatively constant over a range of k_{is} between about 2.3 and the maximum value. As k_{is} is decreased below 2.3, ψ_L first decreases, with a minimum occurring at a k_{is} of 1.7 to 1.9. It then increases to a peak at a k_{is} of about 1.5, and falls off sharply as the head coefficient is further decreased. Examination of the tabulated performance data in Appendix B shows that the relative rotor inlet flow angle β_1 is positive at values of k_{is} greater than about 2.3, so that the relative flow strikes the pressure side of the blades. This produces the accompanying incidence losses, and further losses occur as the flow is turned through a relatively large angle to follow the flow channel.

As U_1 is increased (k_{is} decreased), β_1 becomes negative, so that impingement of the flow on the blades acts opposite to the direction of rotation. The incidence losses are not significantly changed; however, the flow must now be turned by a considerably smaller amount in order to follow the flow channel. Thus, the resultant sum of these three losses appears to be less, and an increase in ψ_L occurs at a k_{is} of about 1.5. Below this point, as β_1 becomes increasingly negative, the relative flow becomes almost perpendicular to the blades. Thus, the advantage is lost, and the rotor efficiency deteriorates rapidly.

A plot of referred moment with bearing losses included, as a function of referred speed, is shown in Figure 38 for data obtained at a clearance of 0.081 inch. The values of the torque at zero speed resulting from the locked rotor tests are also shown. The effects of clearance on this parameter were also found to be negligible over the range of clearances from 0.015 to 0.081 inch, there being only slight random variations present in the resulting data. Therefore, Figure 38 is a representative plot for all clearances.

As expected, the maximum moment of about 16.1 foot-pounds was found to occur at zero speed and at a pressure ratio of 1.7. For the maximum speed of about 18,000 rpm, this pressure ratio yielded 6.3 foot-pounds for zero bearing losses and 6.8 foot-pounds for maximum bearing losses. The lowest pressure ratio, 1.2, consistently yielded the lowest values of moment. The moment curves of Vavra (1) and Riley (3) are almost identical to those obtained in these tests, except for the results obtained by Riley beyond the "critical" clearance.

In general, the torque produced by the flow energy at a given pressure ratio is a maximum at zero speed and decreases with increasing turbine speed. This may be explained by the law of angular momentum, which, by reference to the velocity diagram of Figure 15, can be written as

$$M = \dot{W} R_{20} \left[\left(\frac{R_1}{R_{20}} \right) V_{u1} - V_{u2} \right] \quad (63)$$

For a given pressure ratio, V_{u1} is nearly constant with speed, and the mass flow rate \dot{W} decreases with increasing speed. From Figure 15, V_{u2} also increases with speed. Thus, it is seen that the torque produced, M , decreases with increasing turbine speed.

After completion of the test runs previously described, an informal trial run was made at a clearance of 0.100 inch in an attempt to determine the critical clearance. Although not conclusive, the results indicated no significant change in the values of the performance parameters. This implies that a reasonable overall efficiency may be maintained at clearances which might considerably exceed those tested in this analysis. Since these additional tests were not complete, the resulting data are not included in this report.

SECTION 5

CONCLUSIONS AND RECOMMENDATIONS

At a pressure ratio of 1.7, a clearance of 0.081 inch, and a head coefficient of 2.28, a maximum total-to-static overall efficiency of 84.6 per cent was obtained for the case where bearing losses were considered. The efficiency, referred moment, and degree of reaction were found to be independent of clearance over the range of clearances between 0.015 and 0.081 inch. A clearance tolerance of this sort is very important in small turbines and in turbines where thermal expansion must be considered. It is recommended that additional testing be performed in order to determine the precise clearance beyond which turbine performance deteriorates. Tests might also be conducted in which the clearance at the rotor discharge is varied in addition to the tip clearance, although this would require cutting the shrouds or the manufacture of additional shrouds with various annular openings.

The results of this investigation show that computations based on flow conditions at the outer discharge radius are simpler and more straightforward than those obtained by referring the losses to a calculated mass-average radius, and that this simplicity does not compromise the quality of the results. On the contrary, a correlation of the rotor velocity coefficient is obtained by this method, whereas previous efforts to obtain meaningful loss parameters were not successful (7).

There is strong evidence that the bearing loss data used in this investigation are no longer applicable. Correct data should be obtained either through new coast-down tests or through some implementation of the lubricating oil temperature differential across the bearings, as previously described. The latter method would be highly preferable since it

would provide accurate loss information on a current basis and would correctly reflect any change in the mechanical condition of the bearings. Successful implementation of such a method would probably be contingent on a complete redesigning of the test rig, so that the oil lines are routed outside of the discharge flow as much as possible and are thoroughly insulated.

Since any inaccuracies in torque measurement introduce considerable error into the calculations as performed herein, additional effort is required in order to determine how to properly compensate the torque capsule output for thermal effects. An alternative solution would be to utilize a force (reluctance) capsule and a moment arm arrangement. This capsule could be remotely located and shielded so as to be free of the effects of the dynamometer bearing heat and the cold turbine discharge air.

It is recommended that the modifications described by Vavra (1) be performed in order to improve the component matching of the turbine and that further tests be carried out in order to determine the effects of these modifications on the performance parameters. Specifically, the enlarging of the guide vane discharge area or the reduction of the rotor discharge area would ultimately increase the relative rotor discharge velocity W_2 , which would reduce the peripheral velocity V_{u2} . Greater turbine work, and thus higher efficiencies, should result.

It is felt that the turbine test rig is now in much better operating condition than for any previous tests. The instrumentation has been proven; and, for the first time, the axial clearances may be accurately set. Accordingly, further testing to verify and expand on the performance parameters obtained in this investigation is recommended.

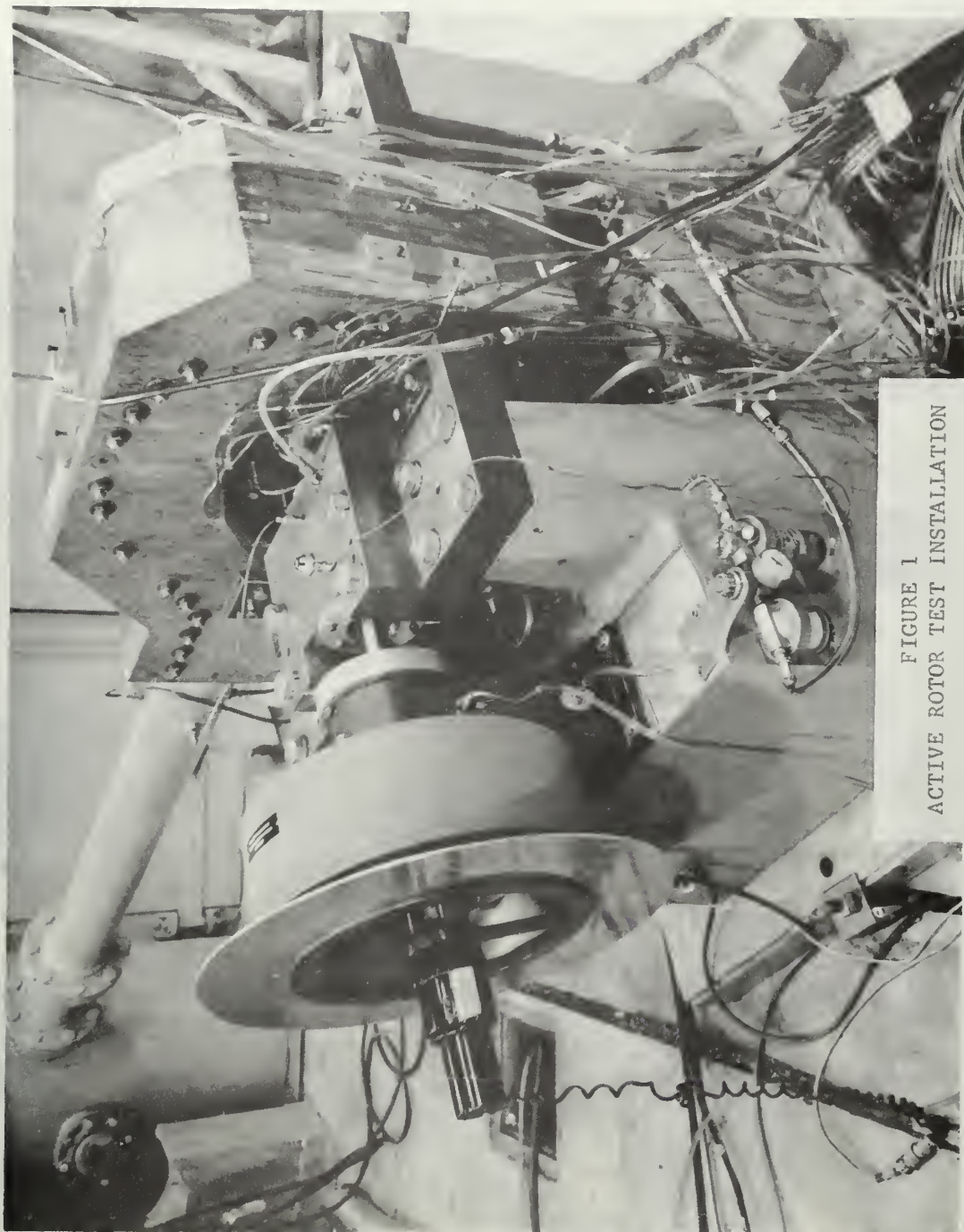


FIGURE 1
ACTIVE ROTOR TEST INSTALLATION

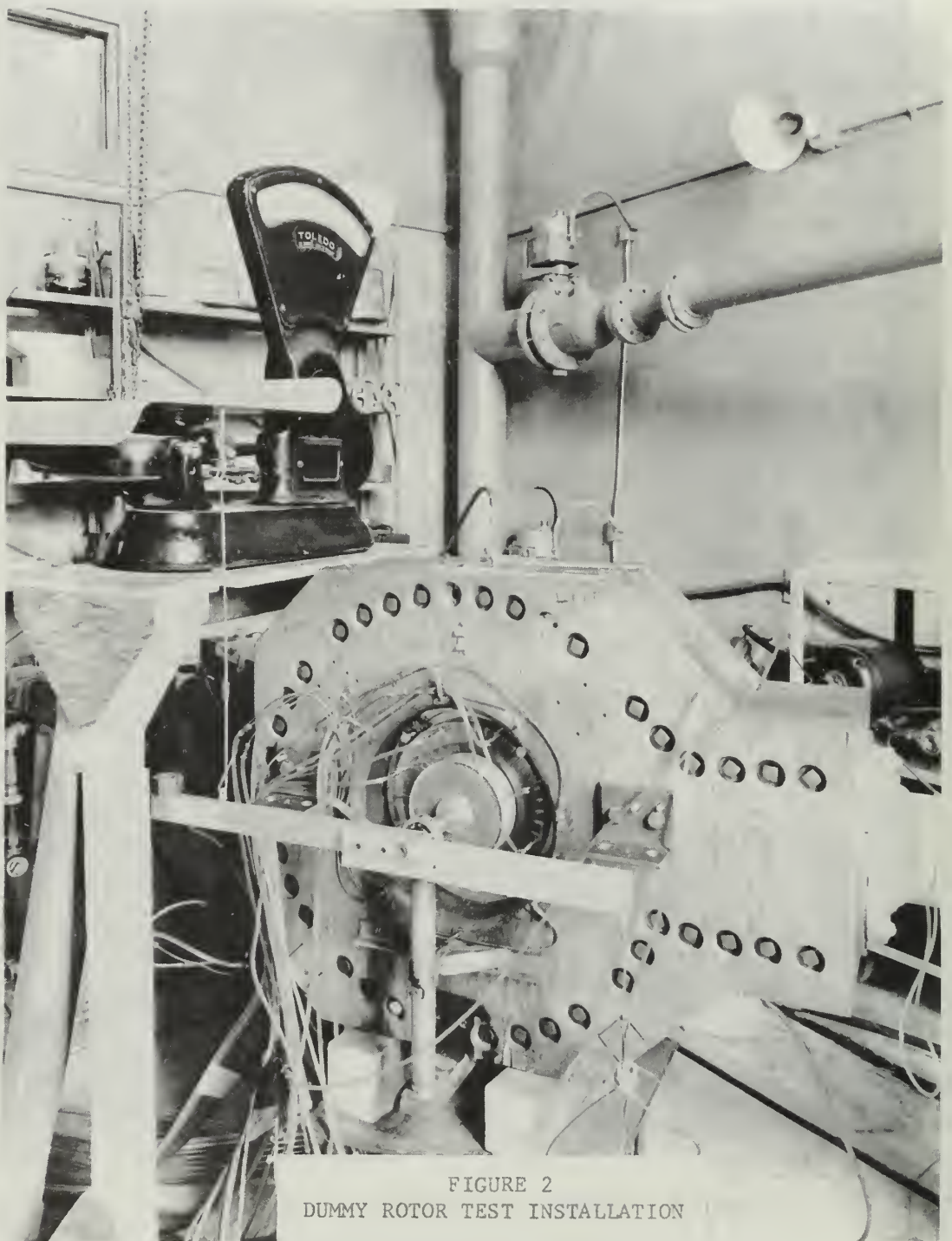


FIGURE 2
DUMMY ROTOR TEST INSTALLATION



FIGURE 3
WOODEN SCROLL INSERT

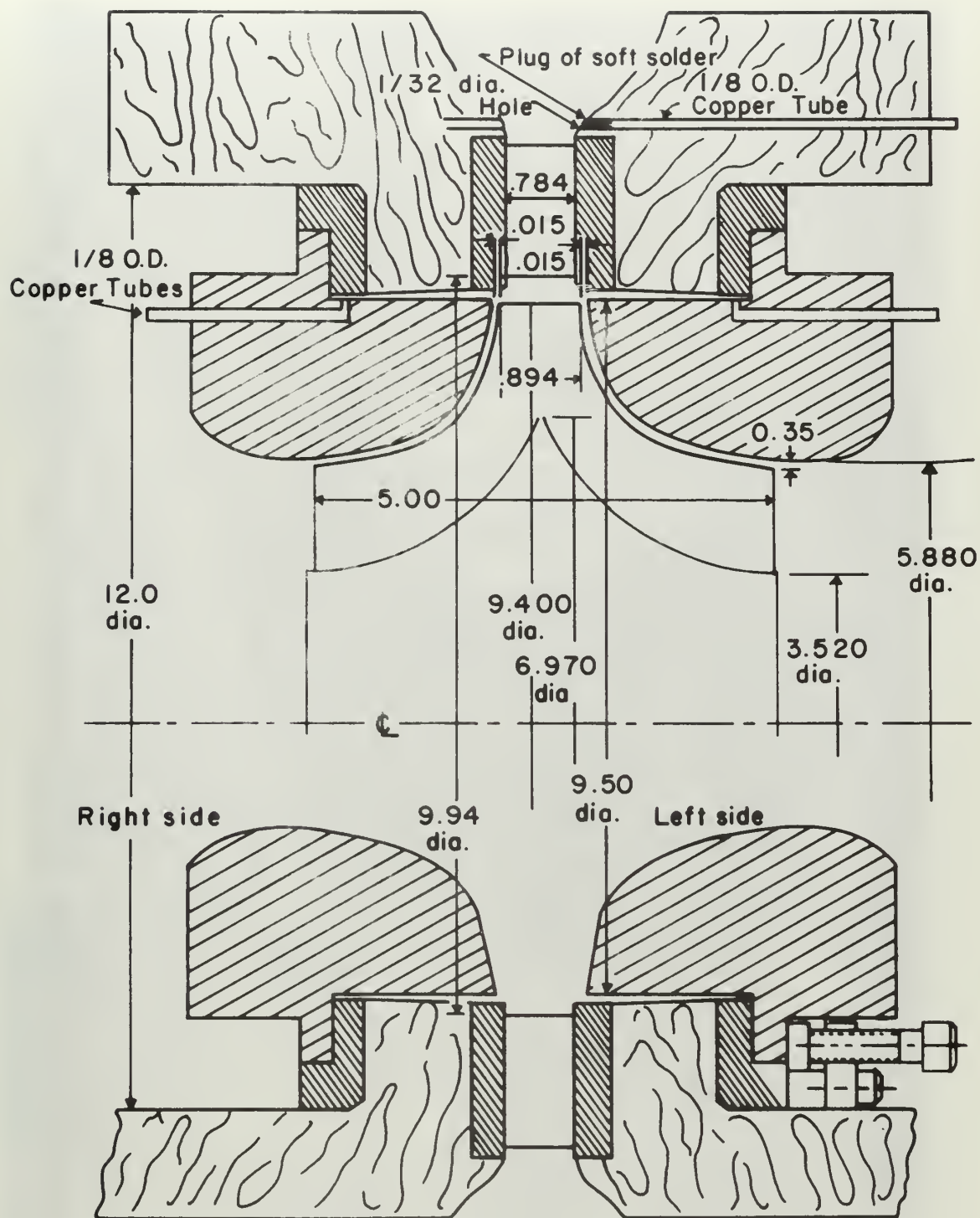


FIGURE 5
CROSS-SECTION OF TURBINE

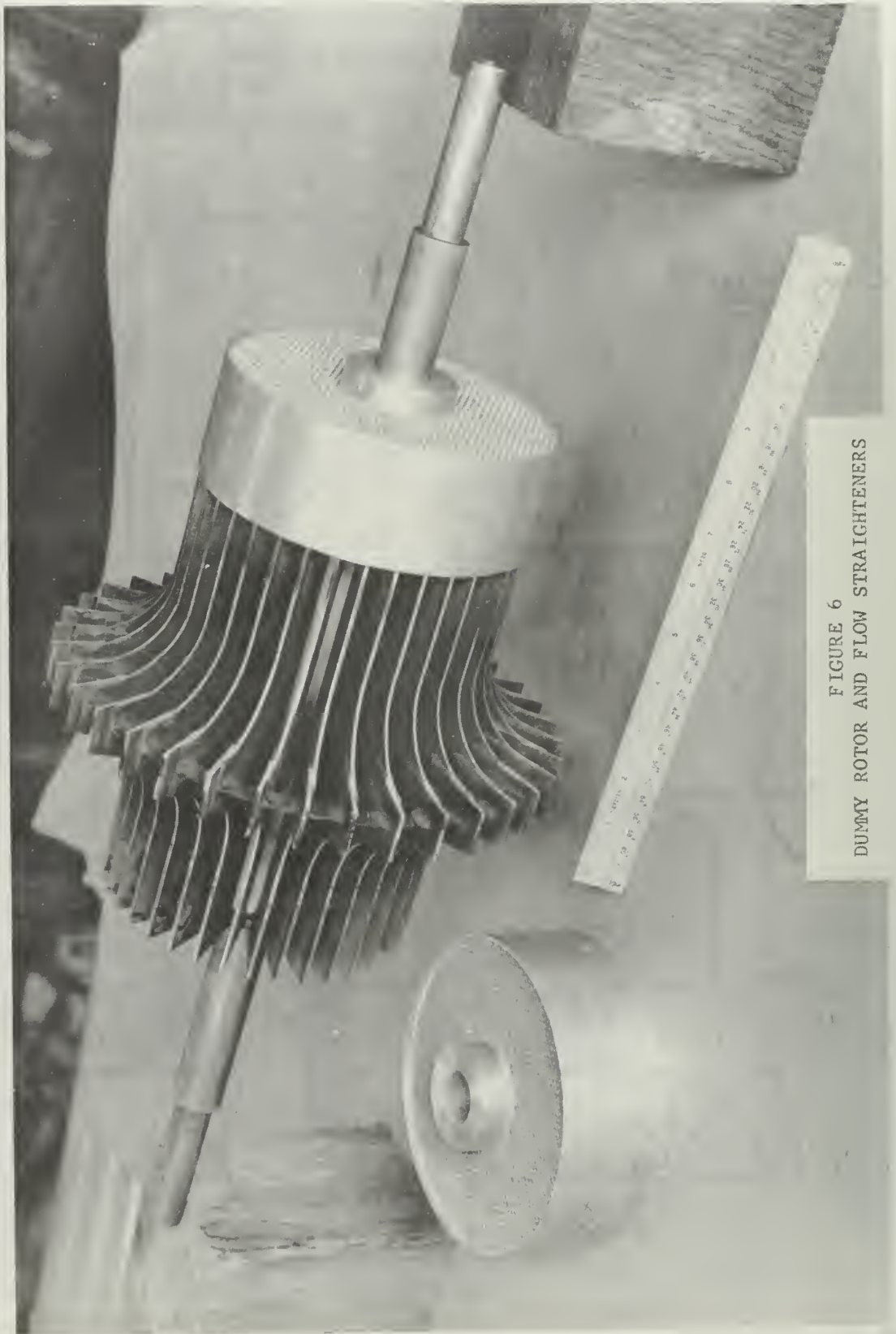


FIGURE 6
DUMMY ROTOR AND FLOW STRAIGHTENERS

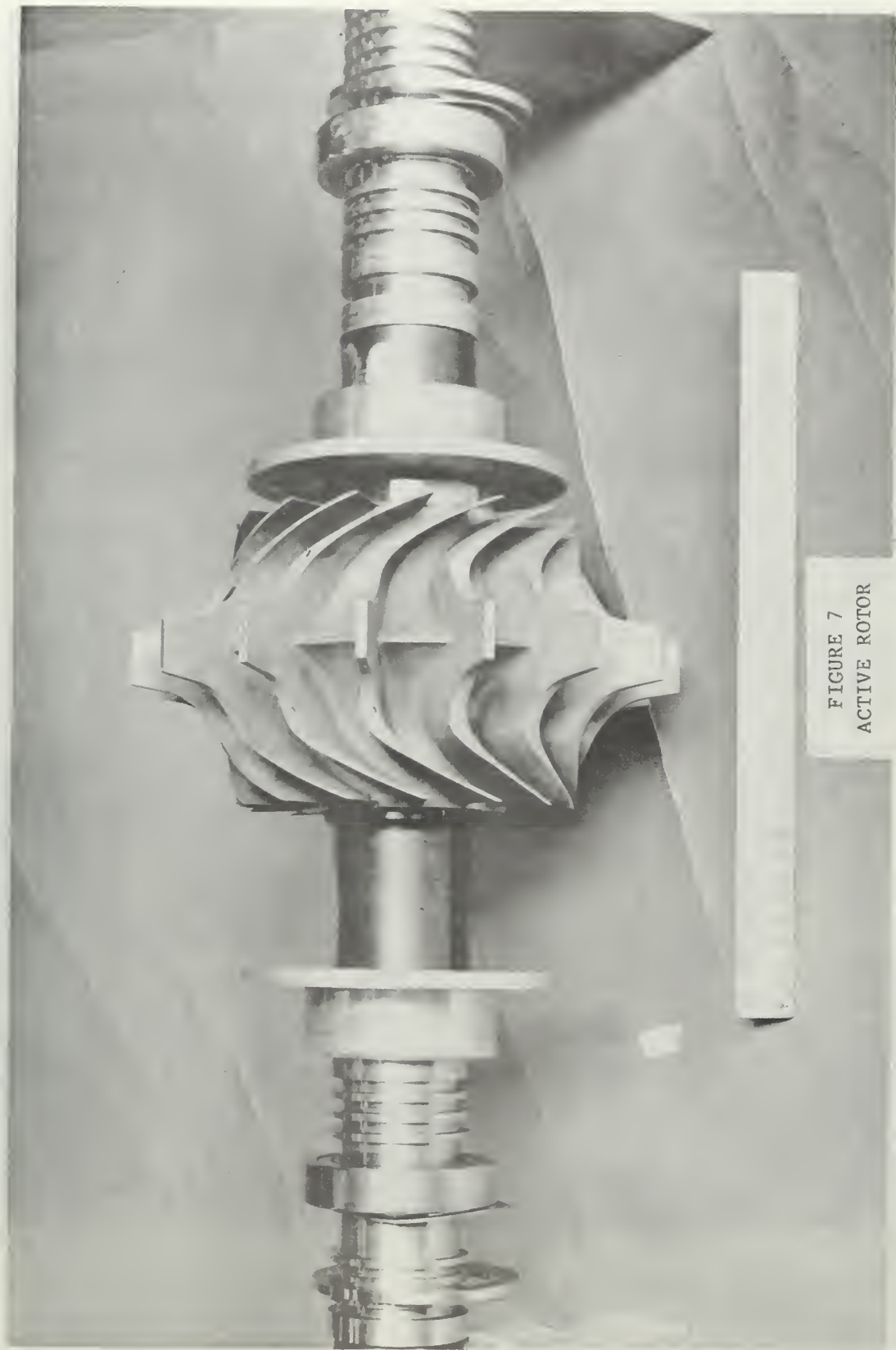


FIGURE 7
ACTIVE ROTOR

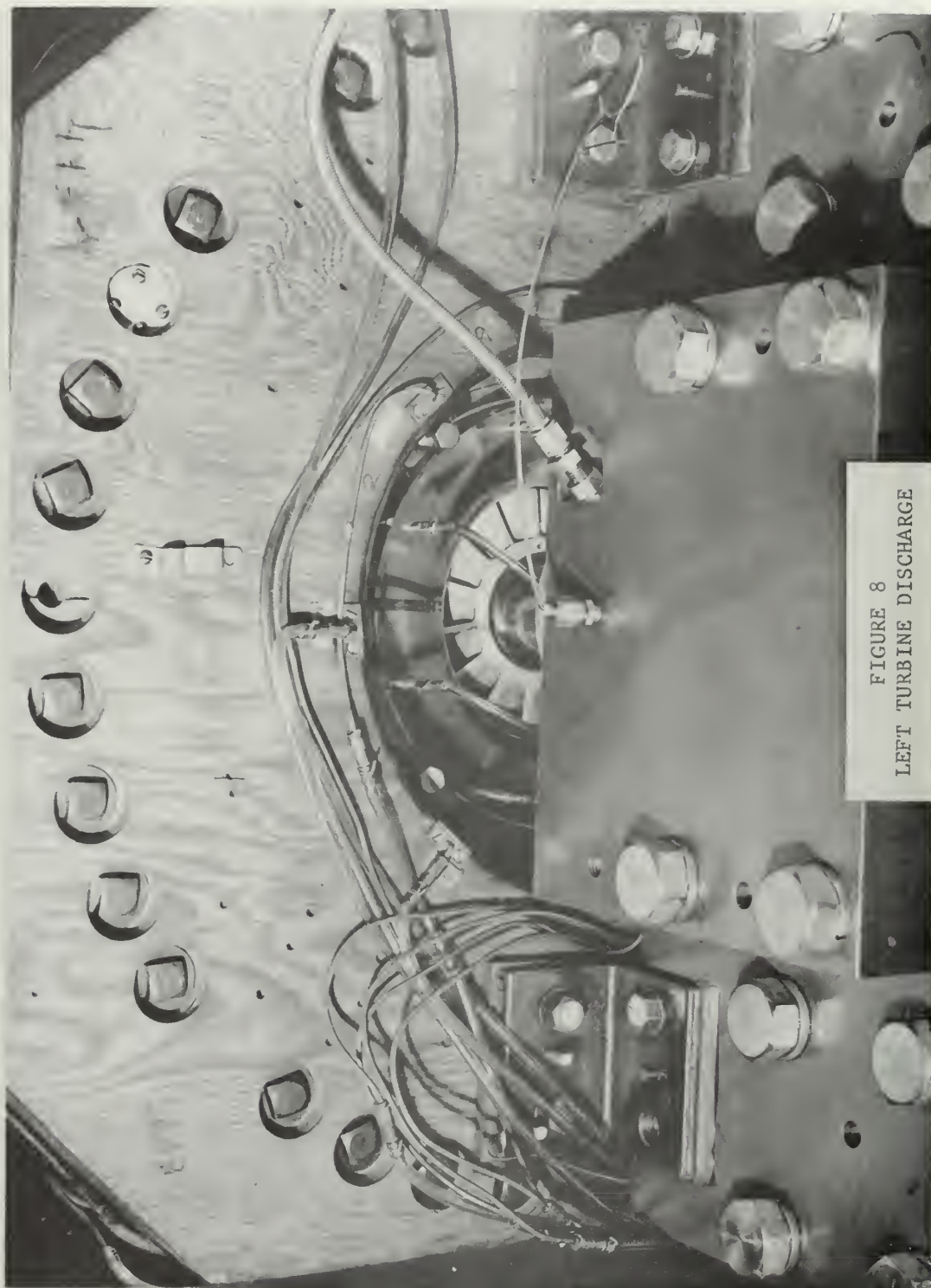


FIGURE 8
LEFT TURBINE DISCHARGE

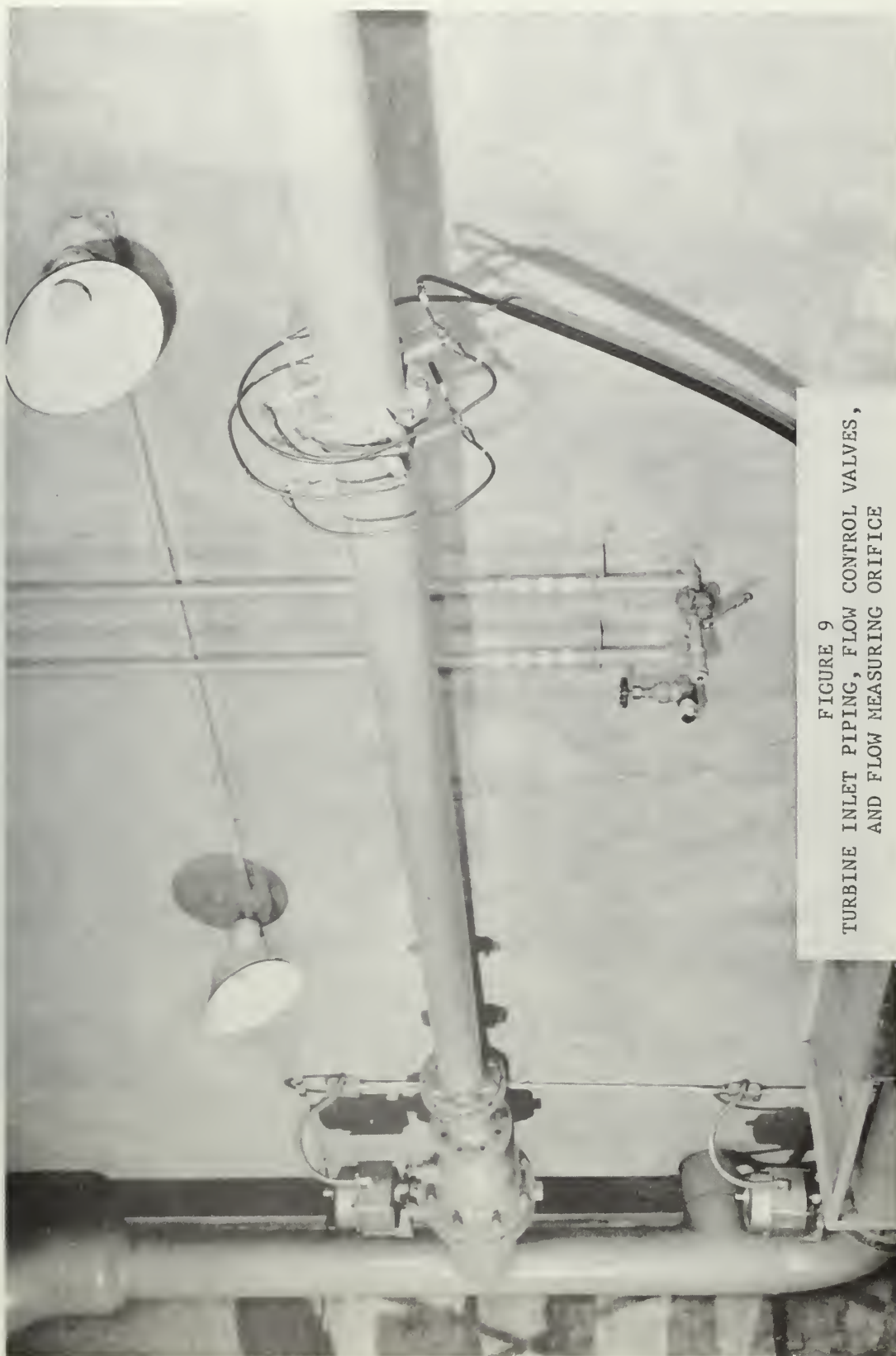


FIGURE 9
TURBINE INLET PIPING, FLOW CONTROL VALVES,
AND FLOW MEASURING ORIFICE

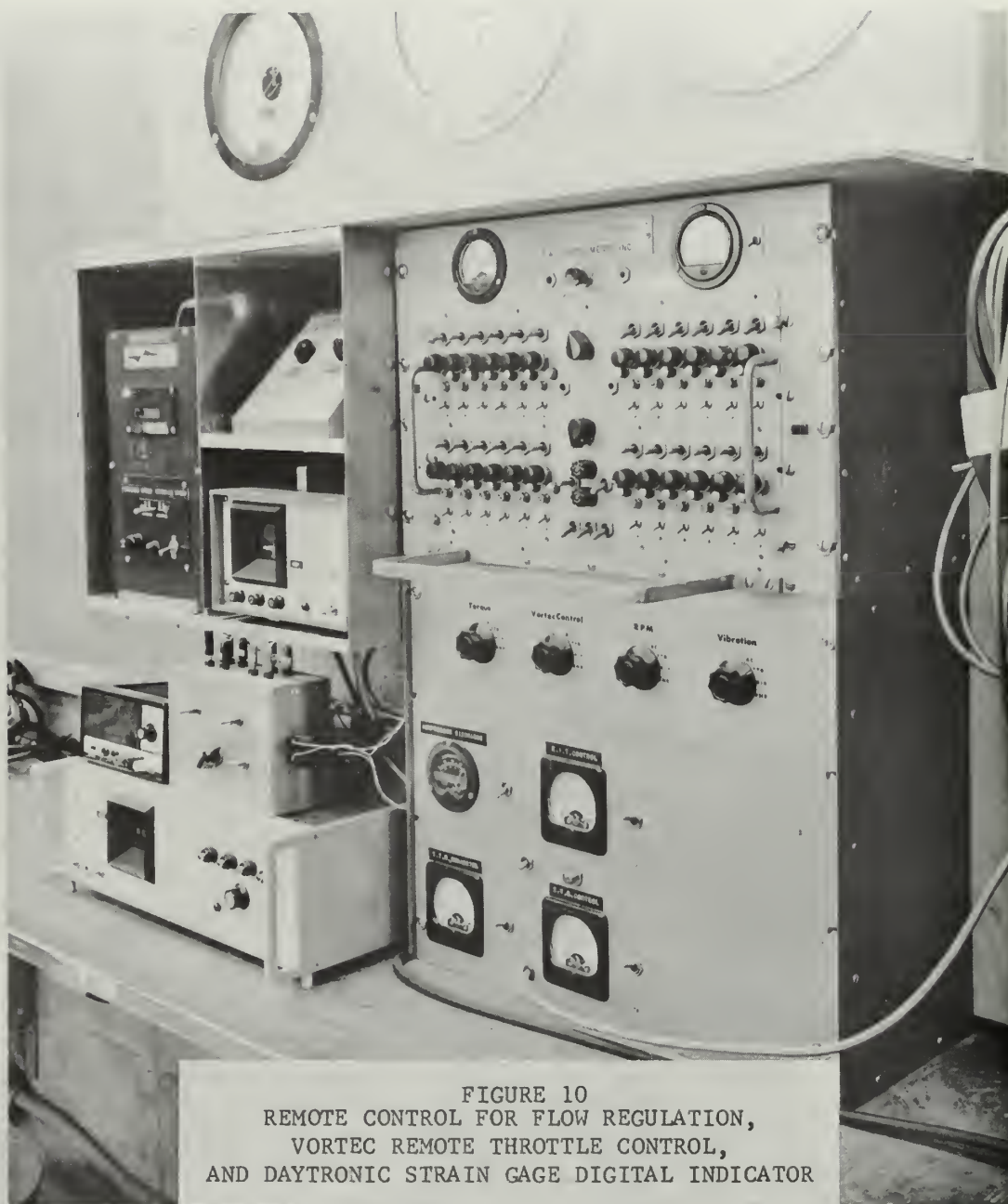


FIGURE 10
REMOTE CONTROL FOR FLOW REGULATION,
VORTEC REMOTE THROTTLE CONTROL,
AND DAYTRONIC STRAIN GAGE DIGITAL INDICATOR

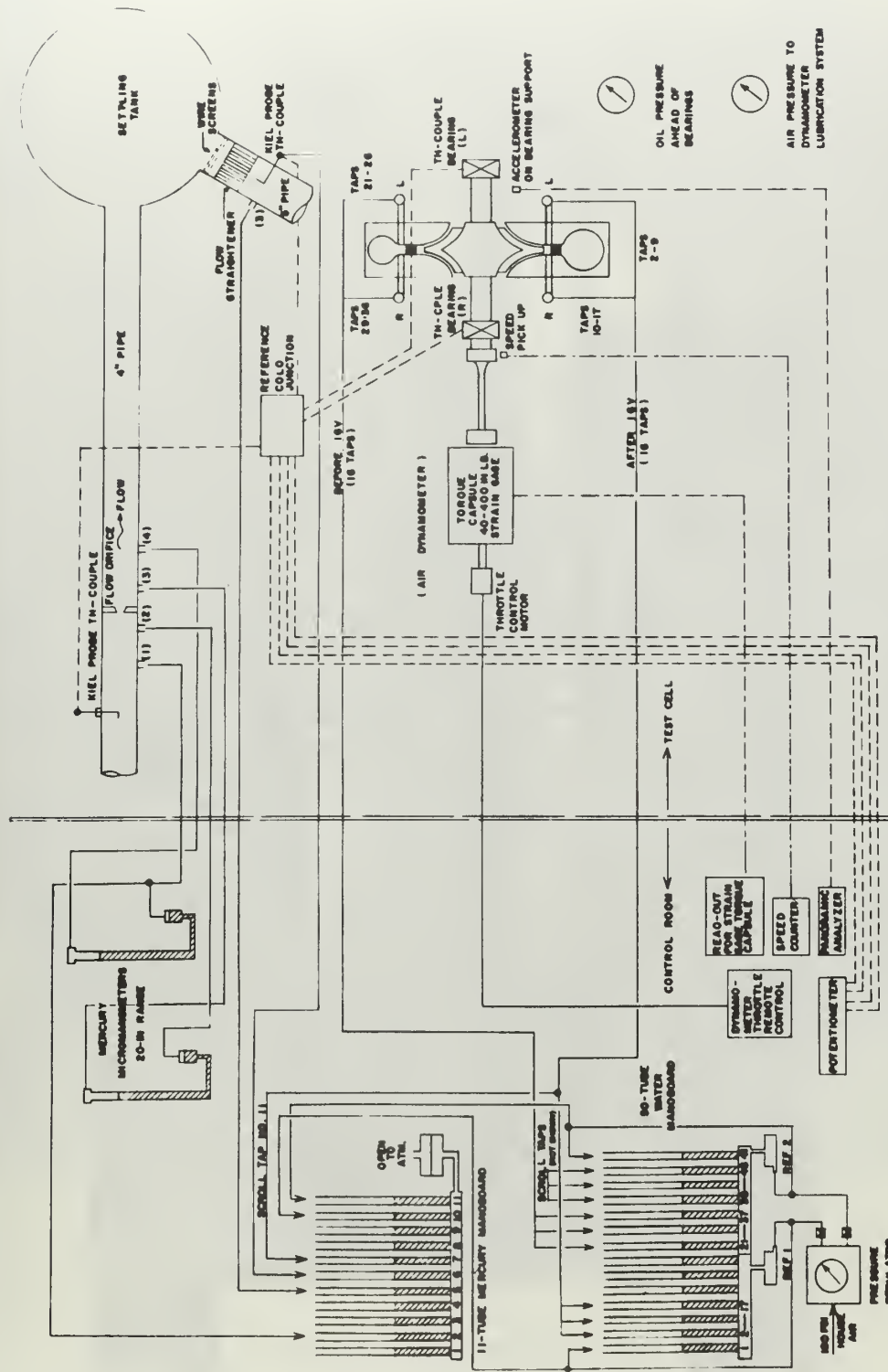


FIGURE 11
SCHEMATIC OF RADIAL TURBINE INSTRUMENTATION

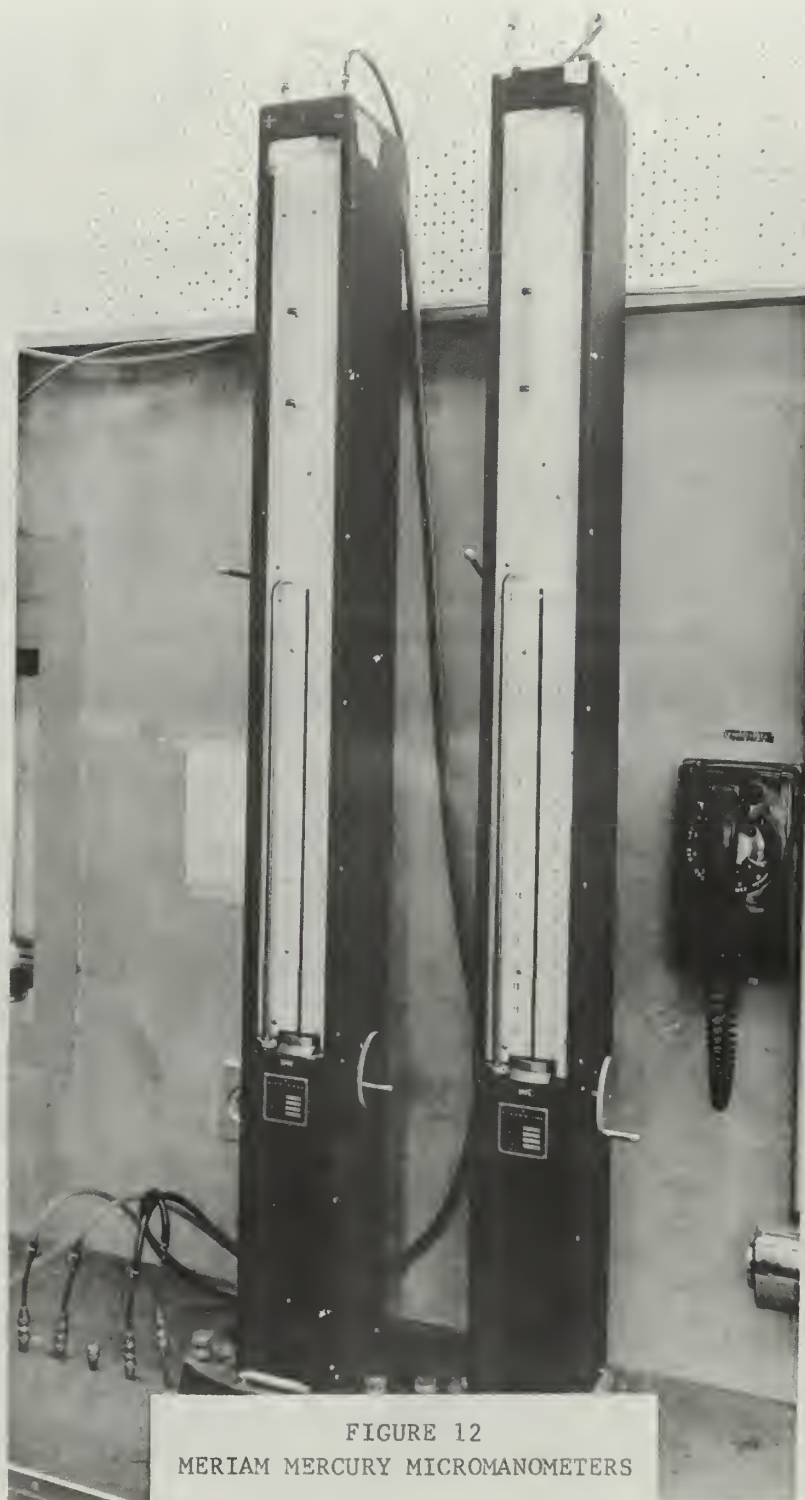


FIGURE 12
MERIAM MERCURY MICROMANOMETERS



FIGURE 13
BROWN POTENTIOMETER

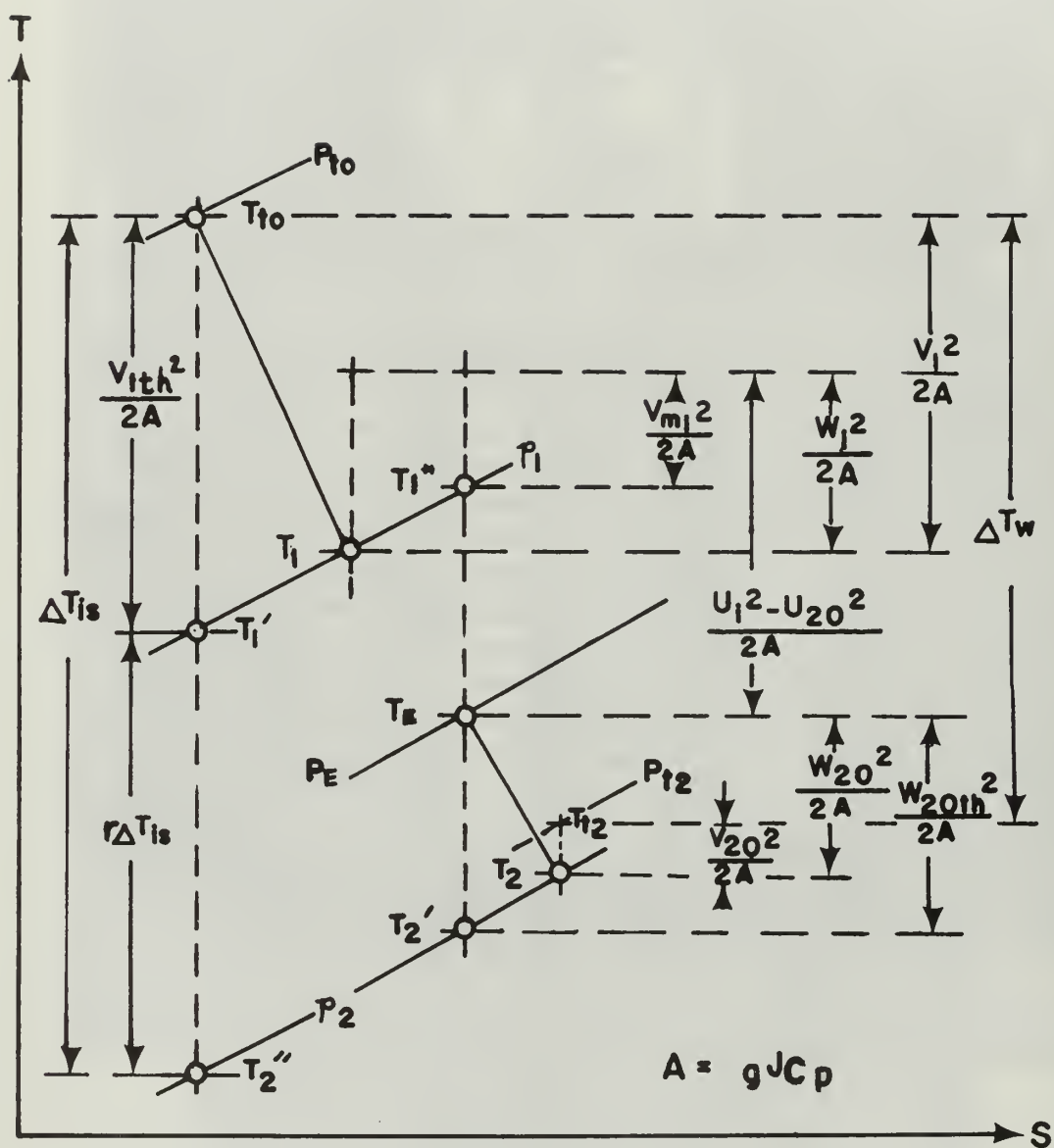


FIGURE 14
TEMPERATURE-ENTROPY DIAGRAM FOR RADIAL TURBINE

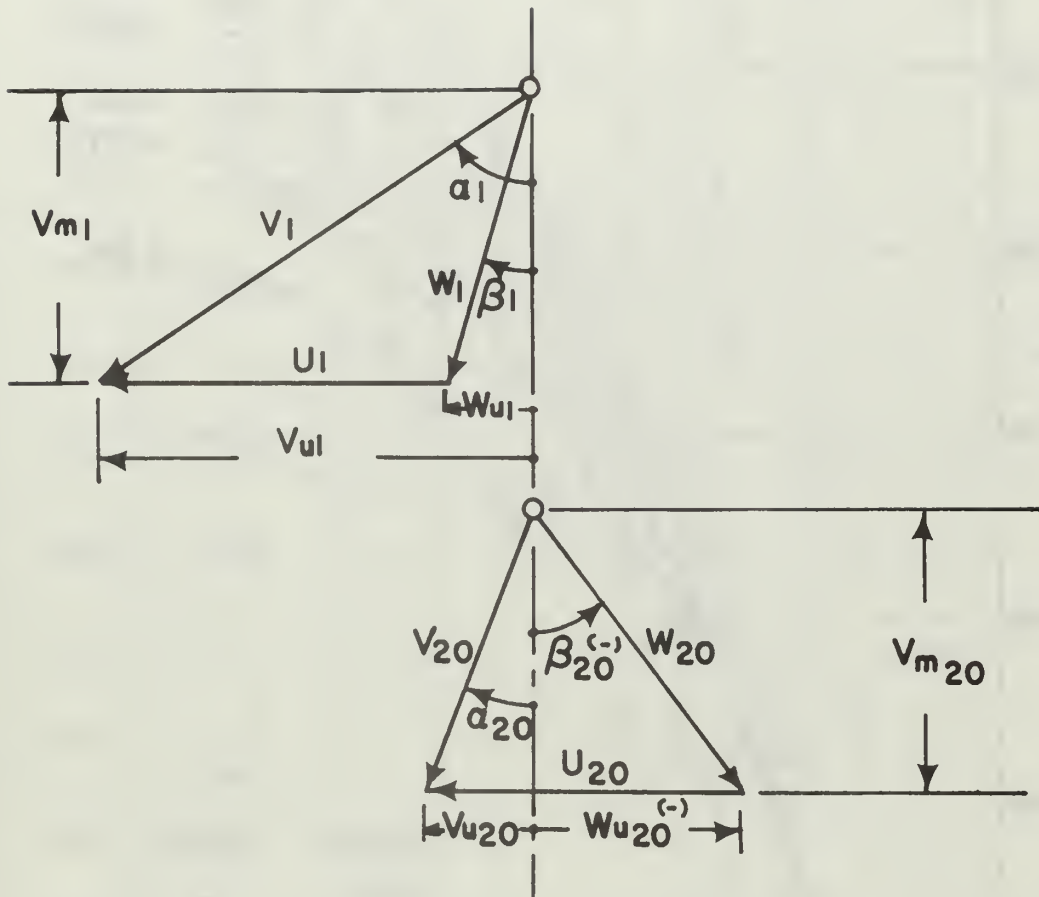


FIGURE 15
VELOCITY DIAGRAMS FOR RADIAL TURBINE

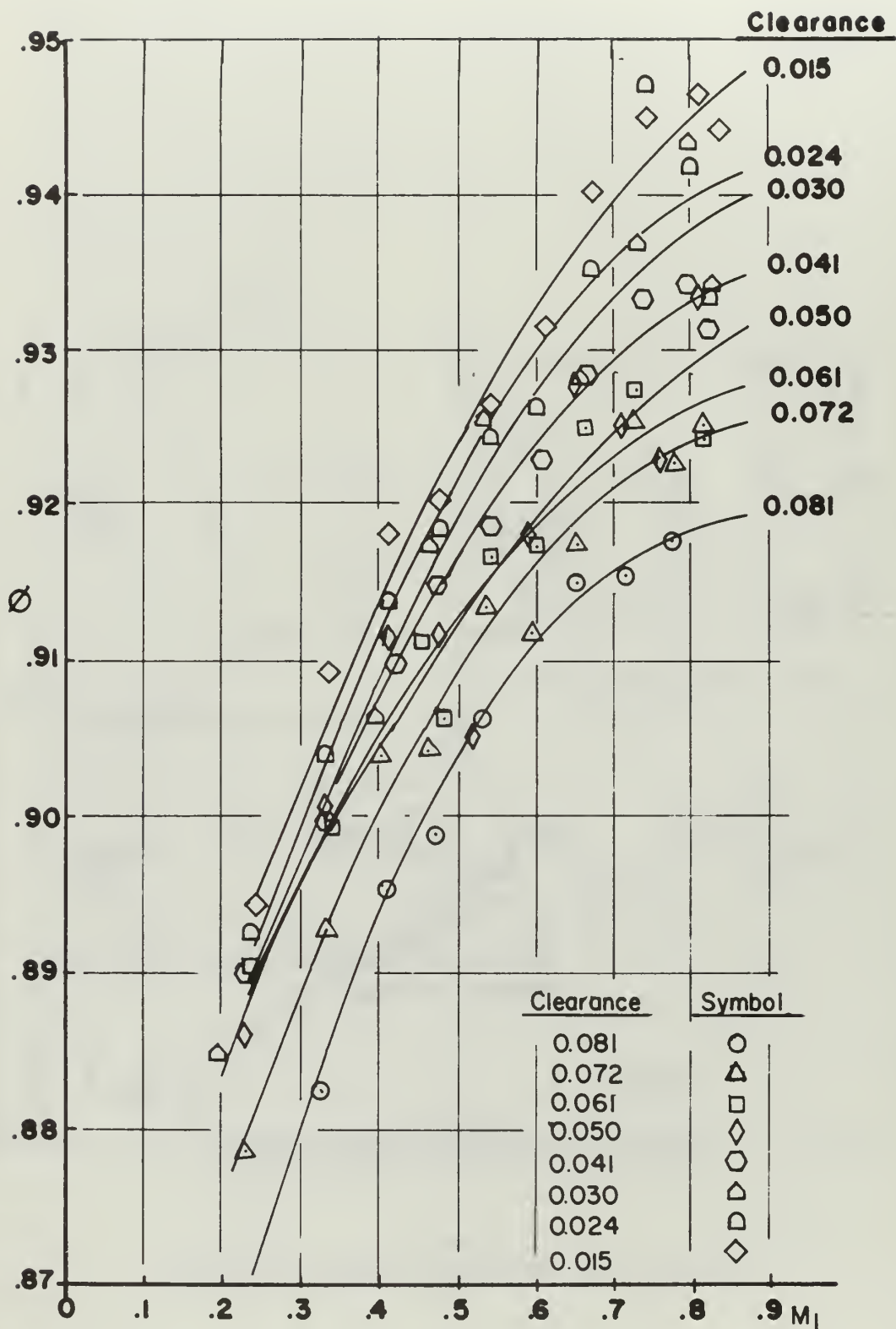


FIGURE 16
VELOCITY COEFFICIENT VS. MACH NUMBER

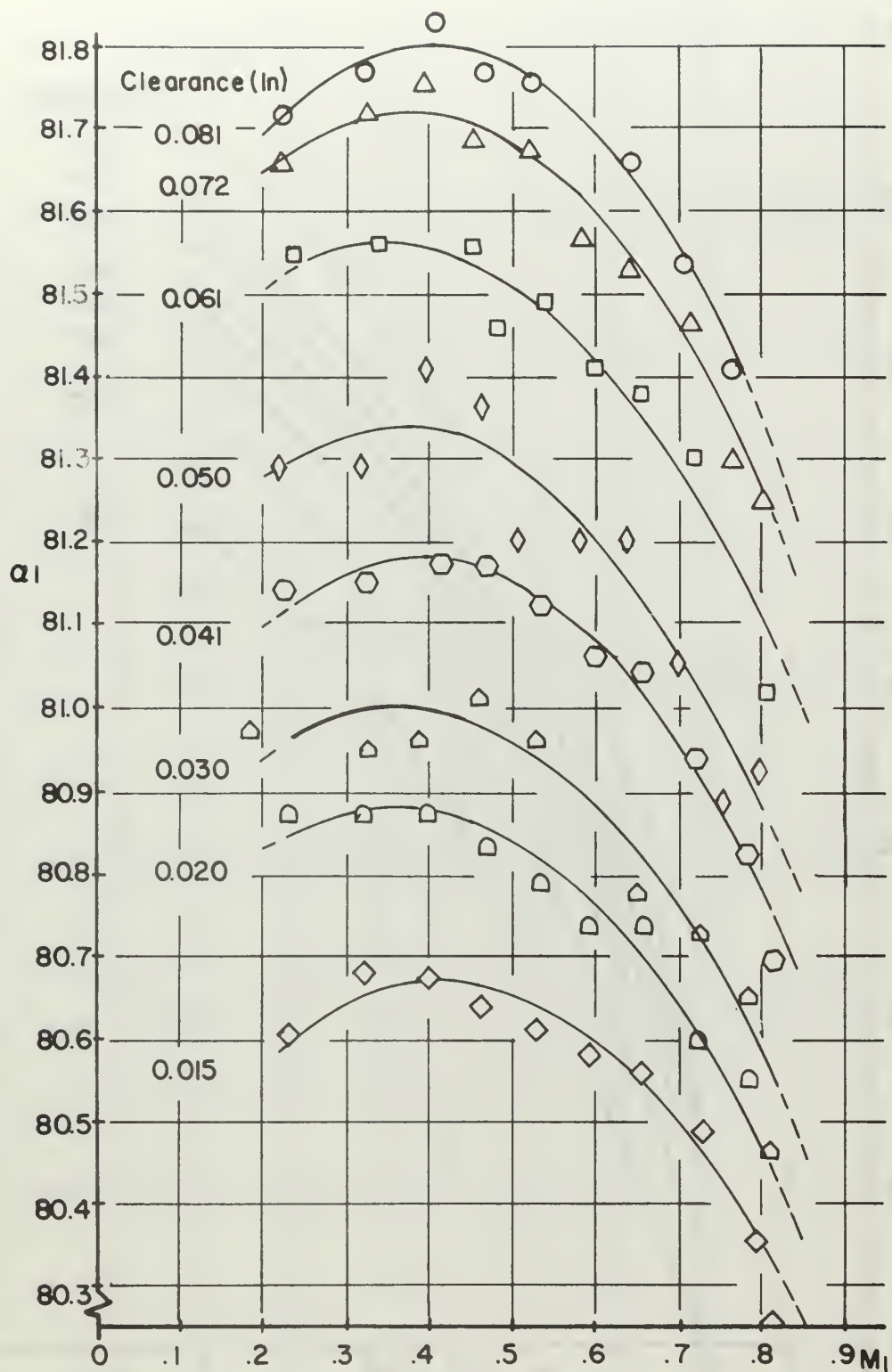


FIGURE 17
ABSOLUTE ROTOR INLET FLOW ANGLE VS. MACH NUMBER

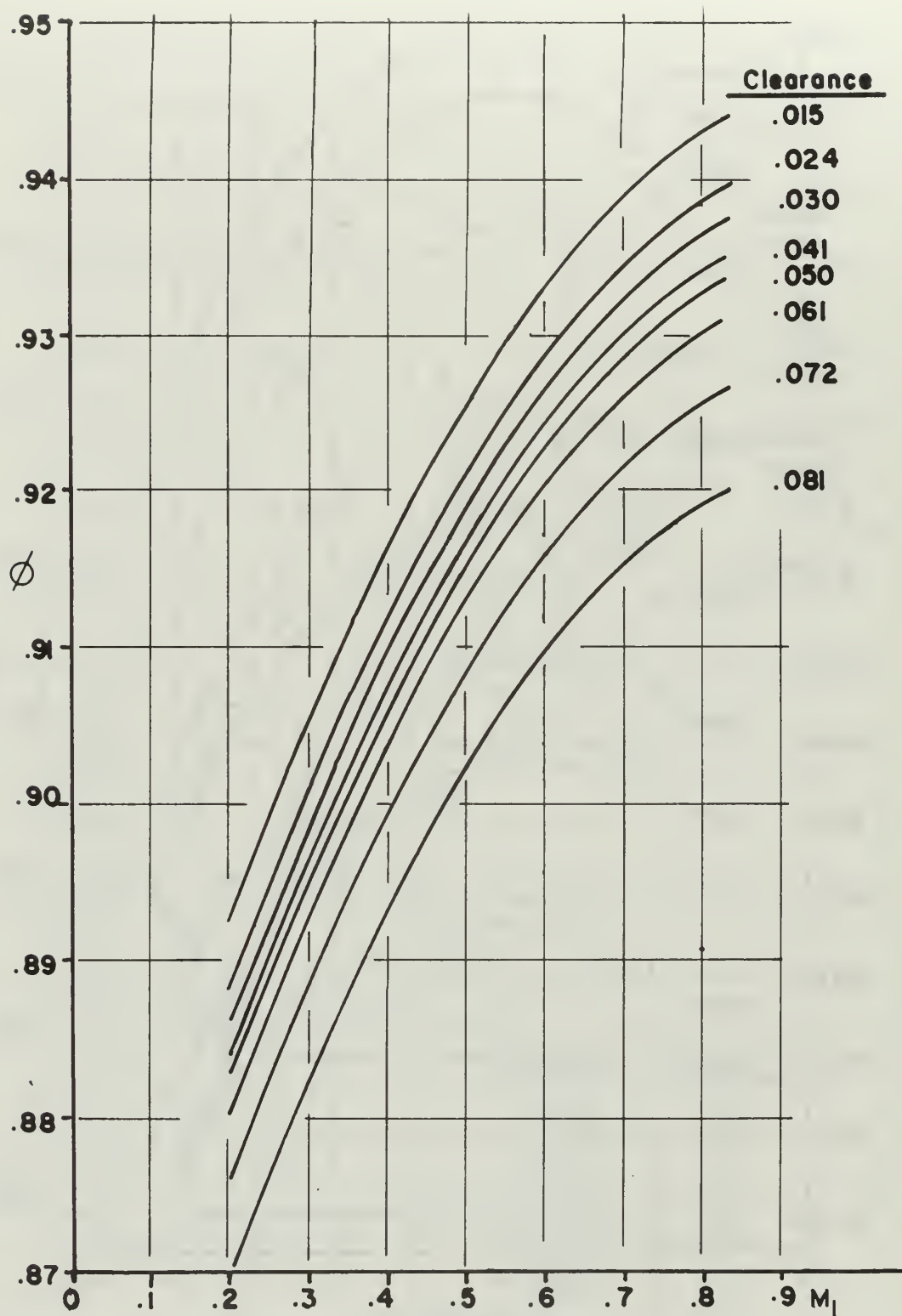


FIGURE 18
VELOCITY COEFFICIENT VS. MACH NUMBER
FROM DERIVED EQUATION

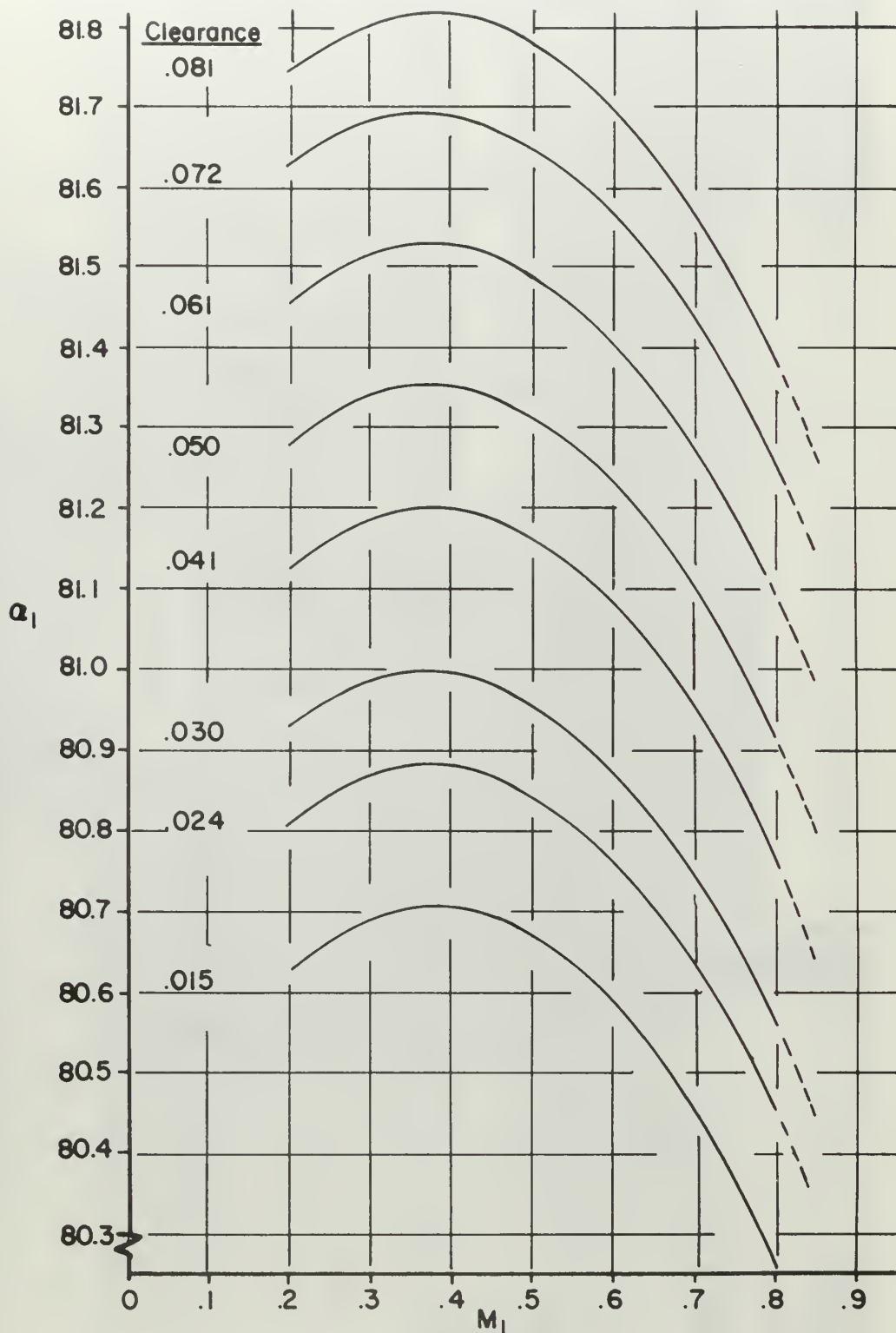


FIGURE 19
ABSOLUTE ROTOR INLET FLOW ANGLE VS. MACH NUMBER
FROM DERIVED EQUATION

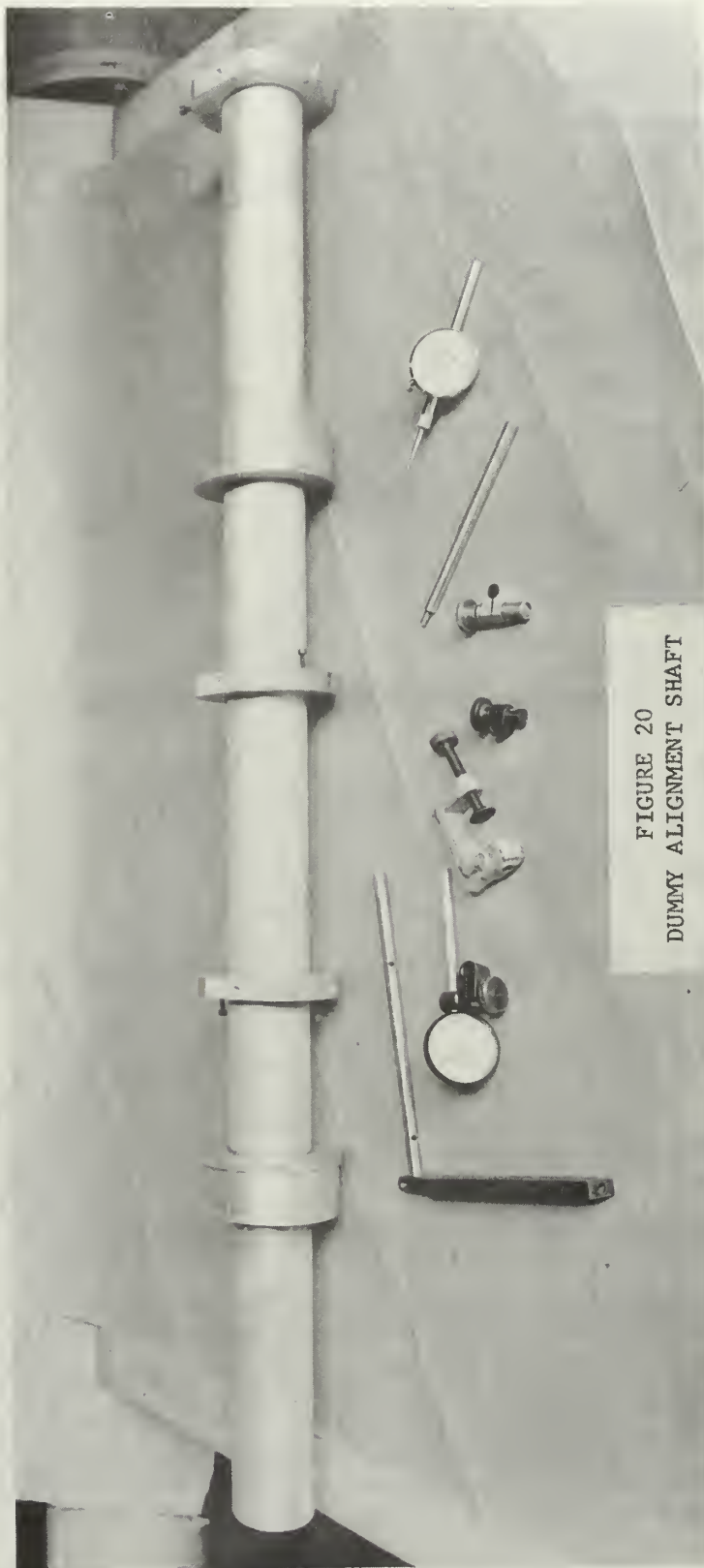


FIGURE 20
DUMMY ALIGNMENT SHAFT



FIGURE 21
FLUX CUTTER, QUILL SHAFT,
AND DYNAMOMETER TORQUE CAPSULE

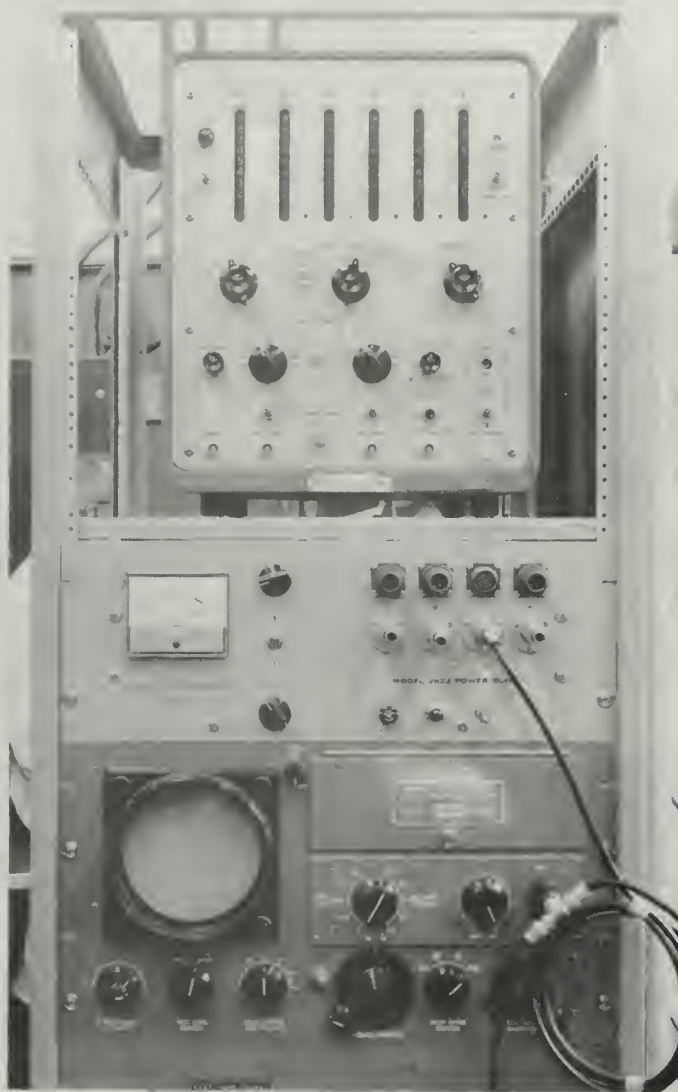


FIGURE 22
ELECTRONIC SPEED COUNTER
AND VIBRATION ANALYZER

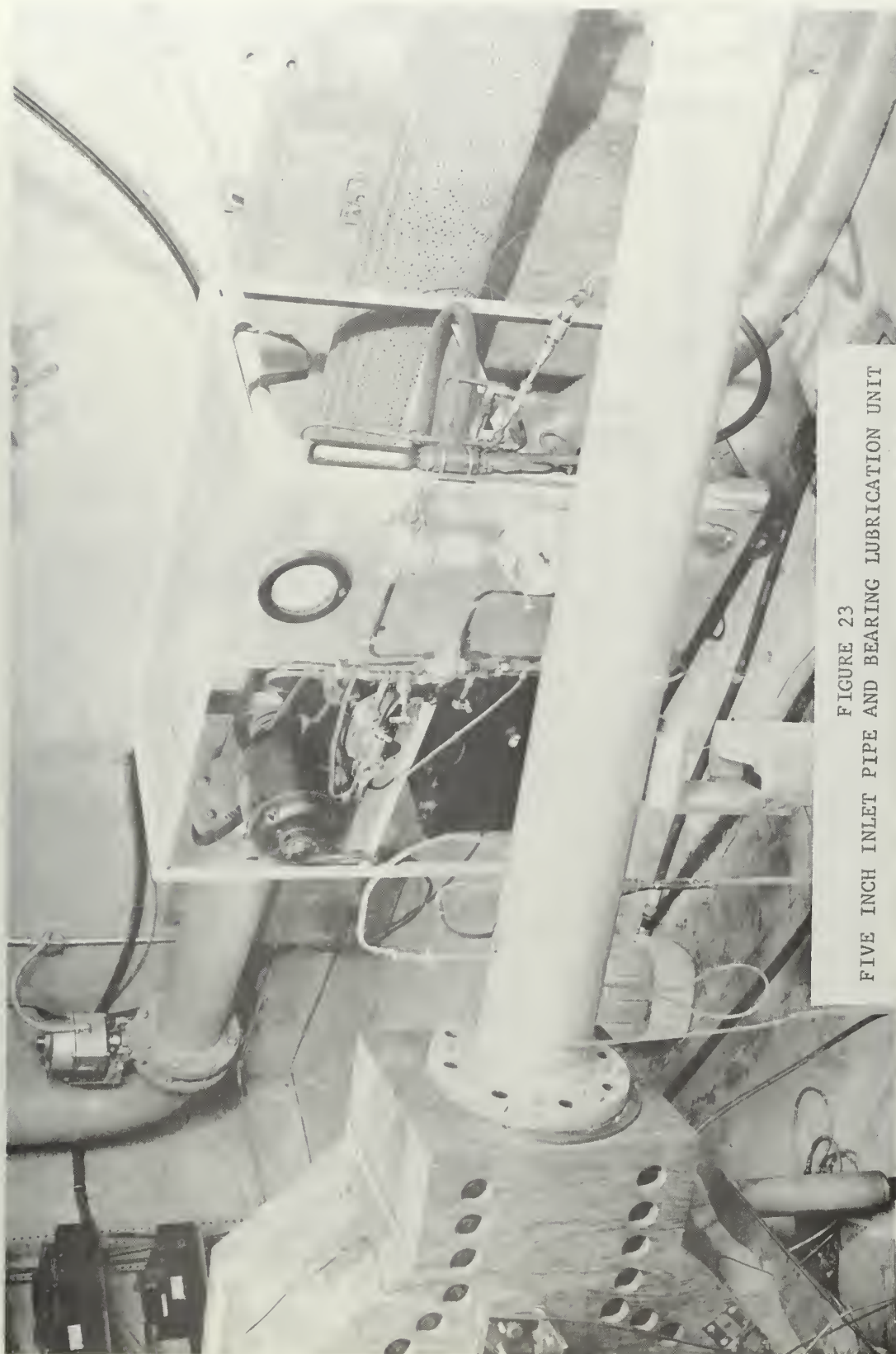


FIGURE 23
FIVE INCH INLET PIPE AND BEARING LUBRICATION UNIT

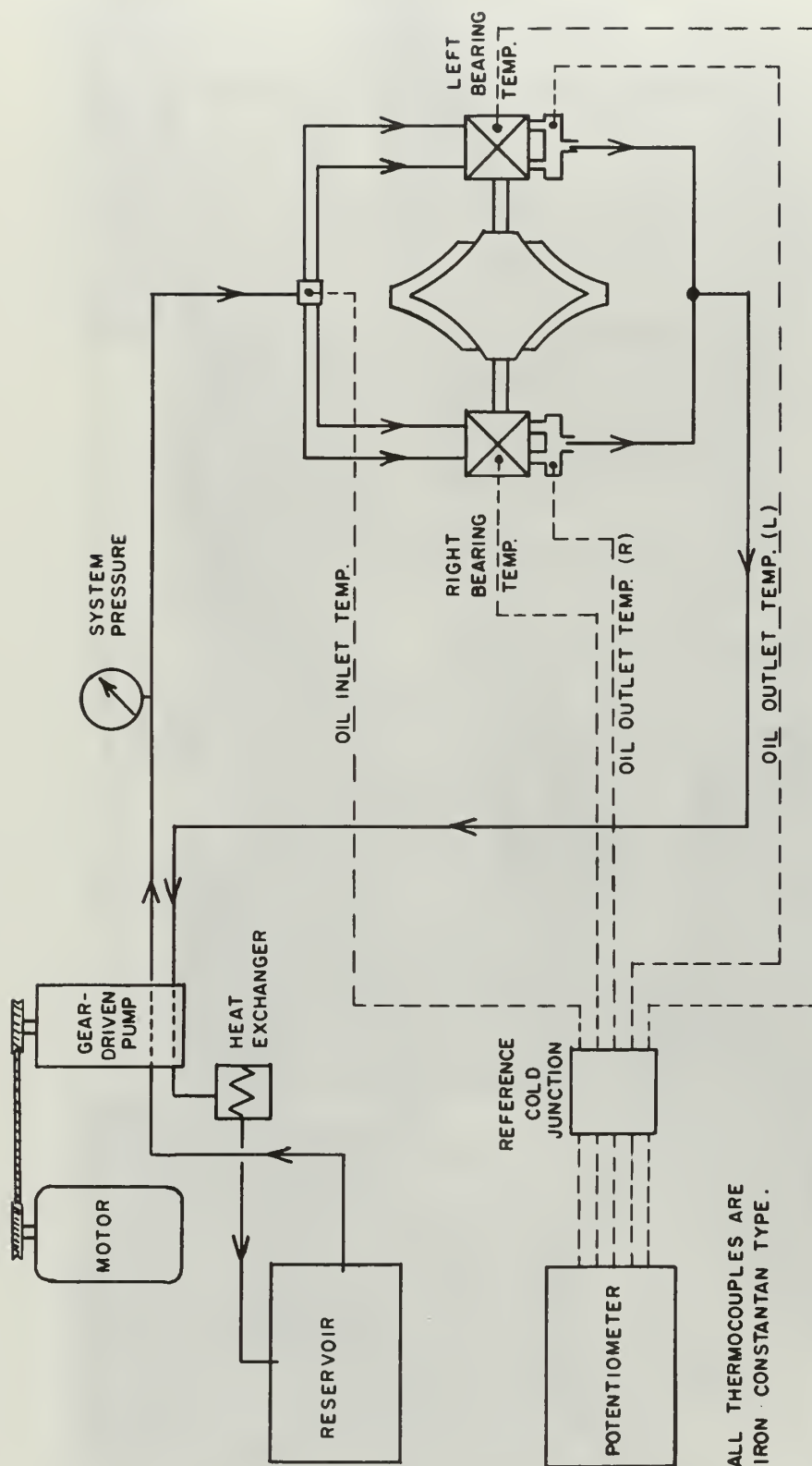
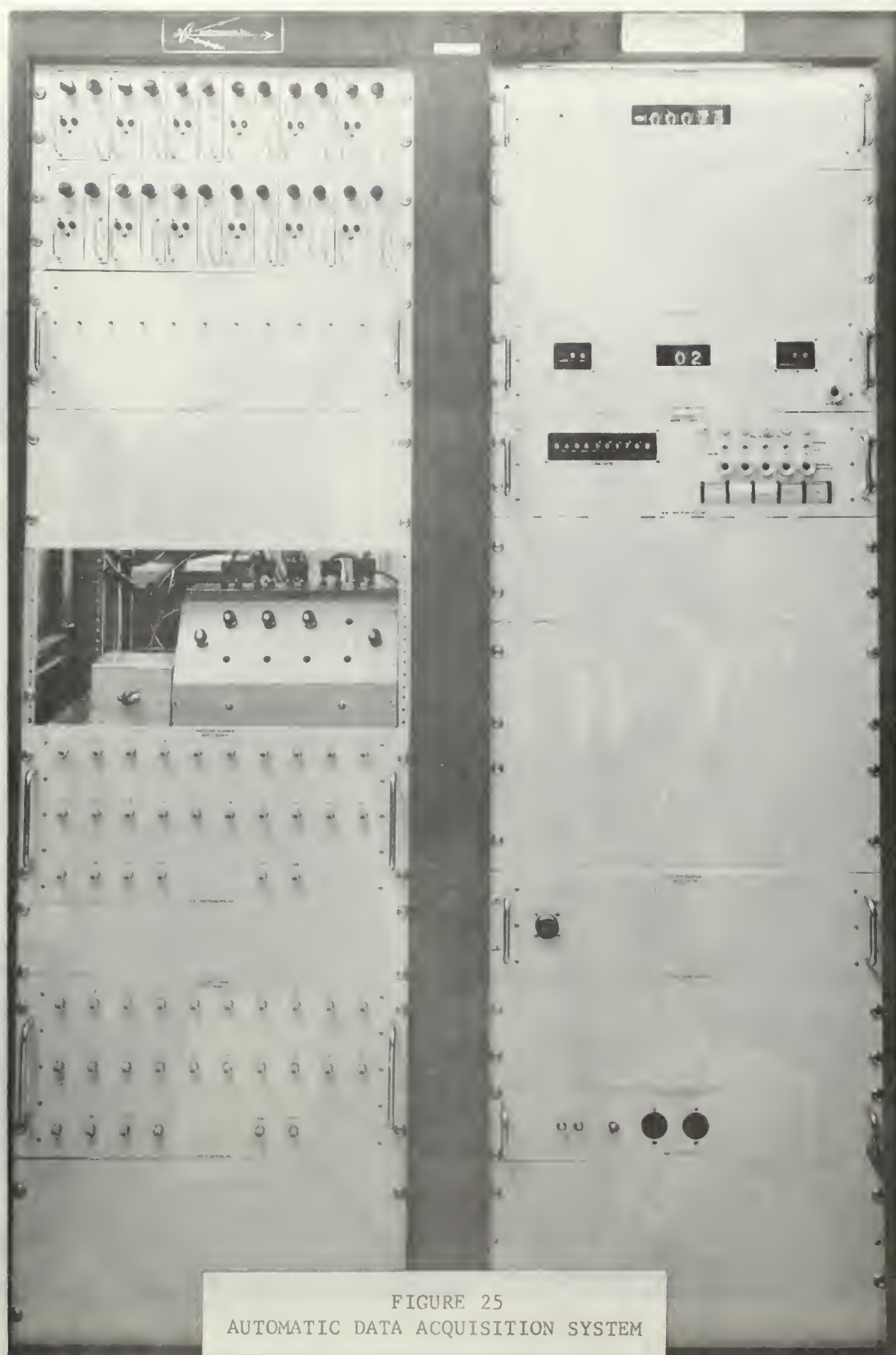


FIGURE 24
SCHEMATIC OF TURBINE LUBRICATION SYSTEM



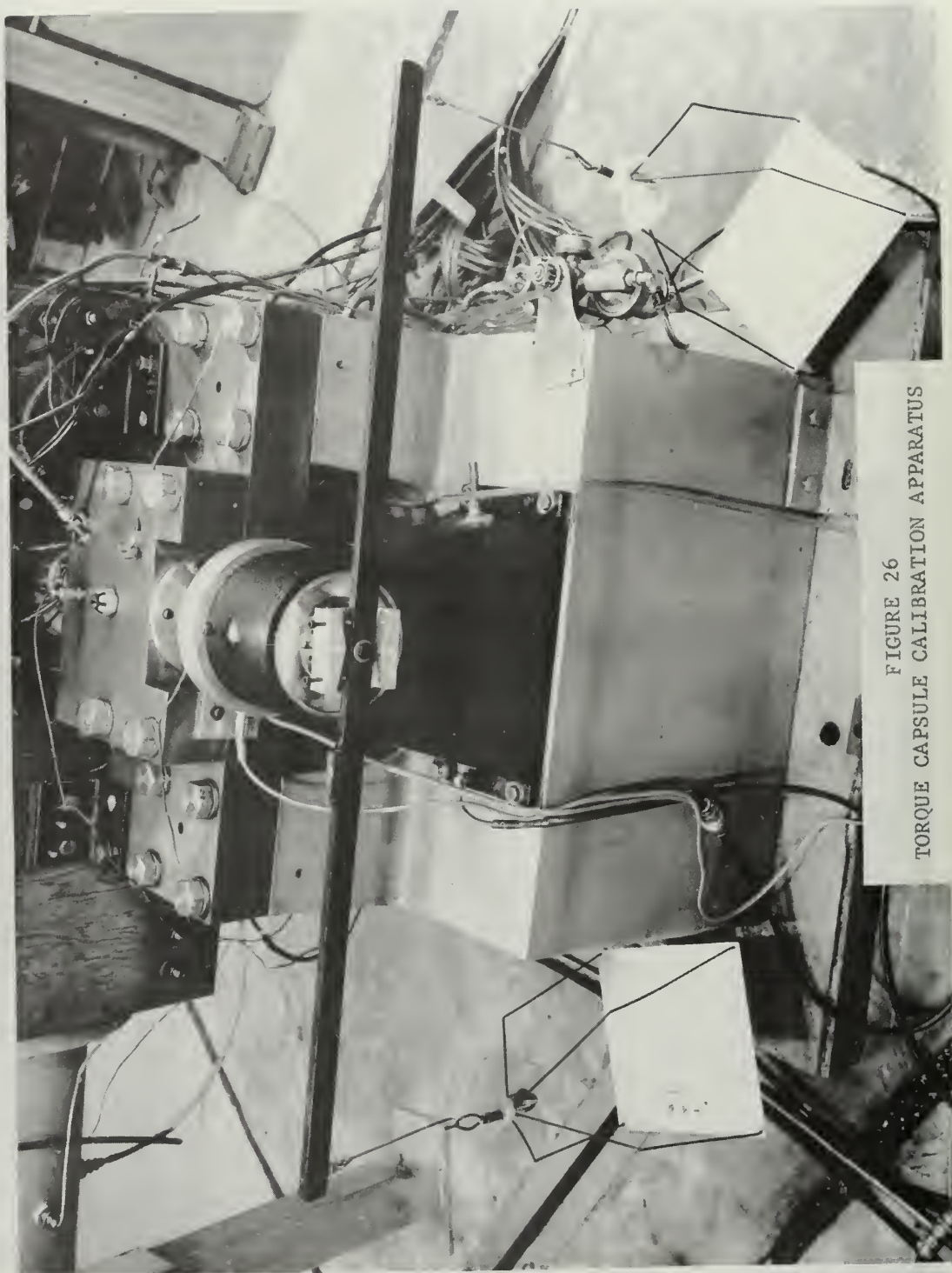


FIGURE 26
TORQUE CAPSULE CALIBRATION APPARATUS

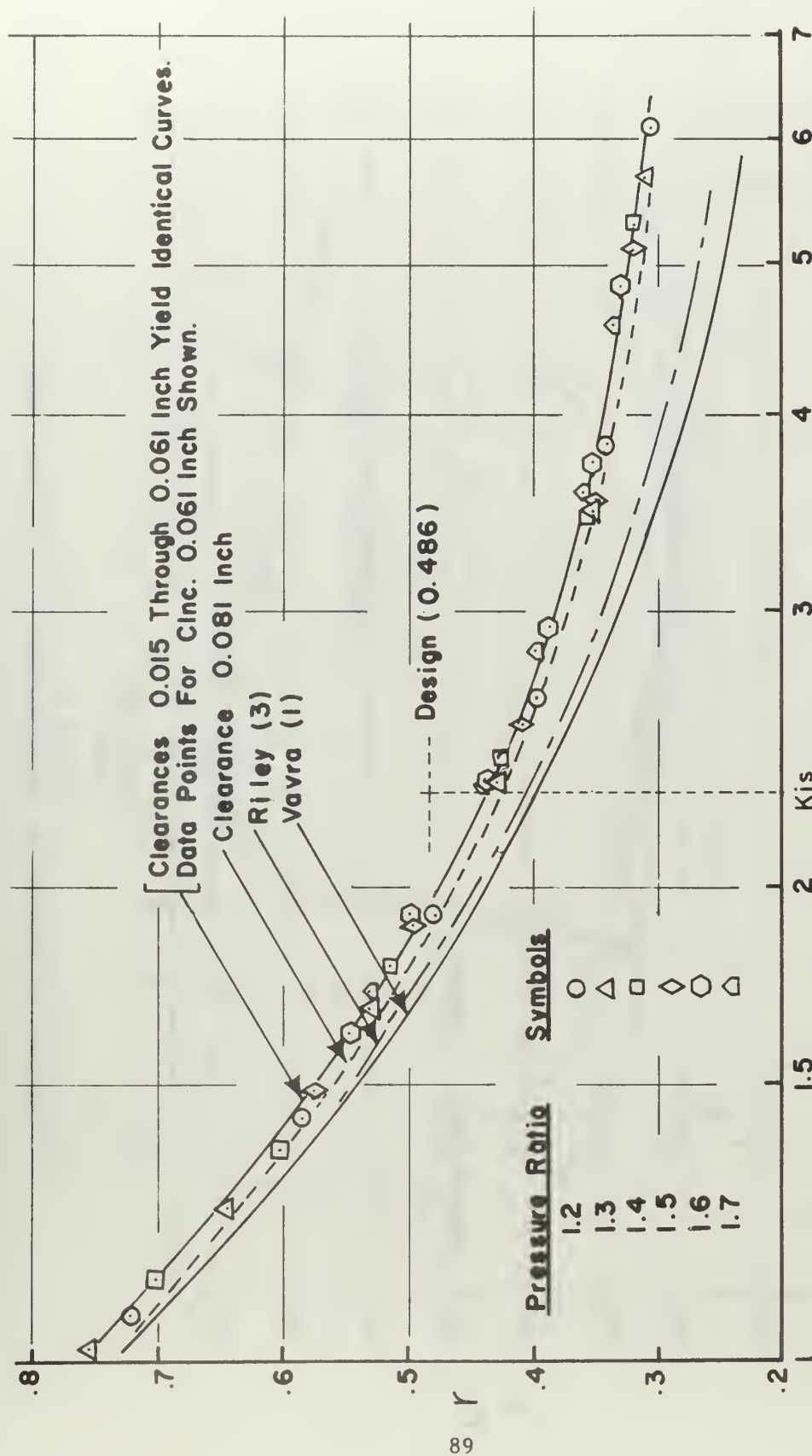


FIGURE 27
DEGREE OF REACTION VS. HEAD COEFFICIENT

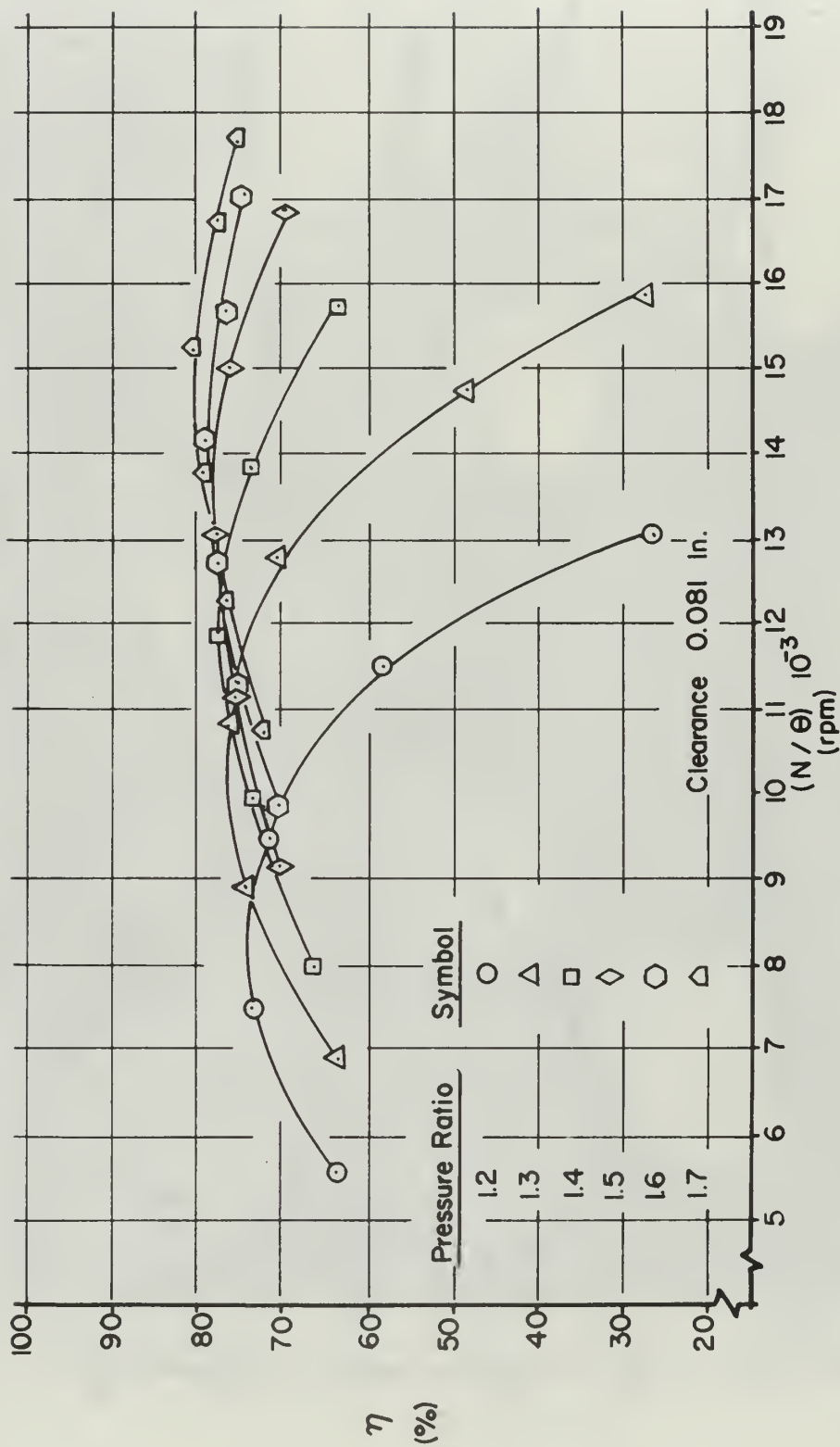


FIGURE 28
OVERALL EFFICIENCY (NO BEARING LOSSES) VS. REFERRED SPEED

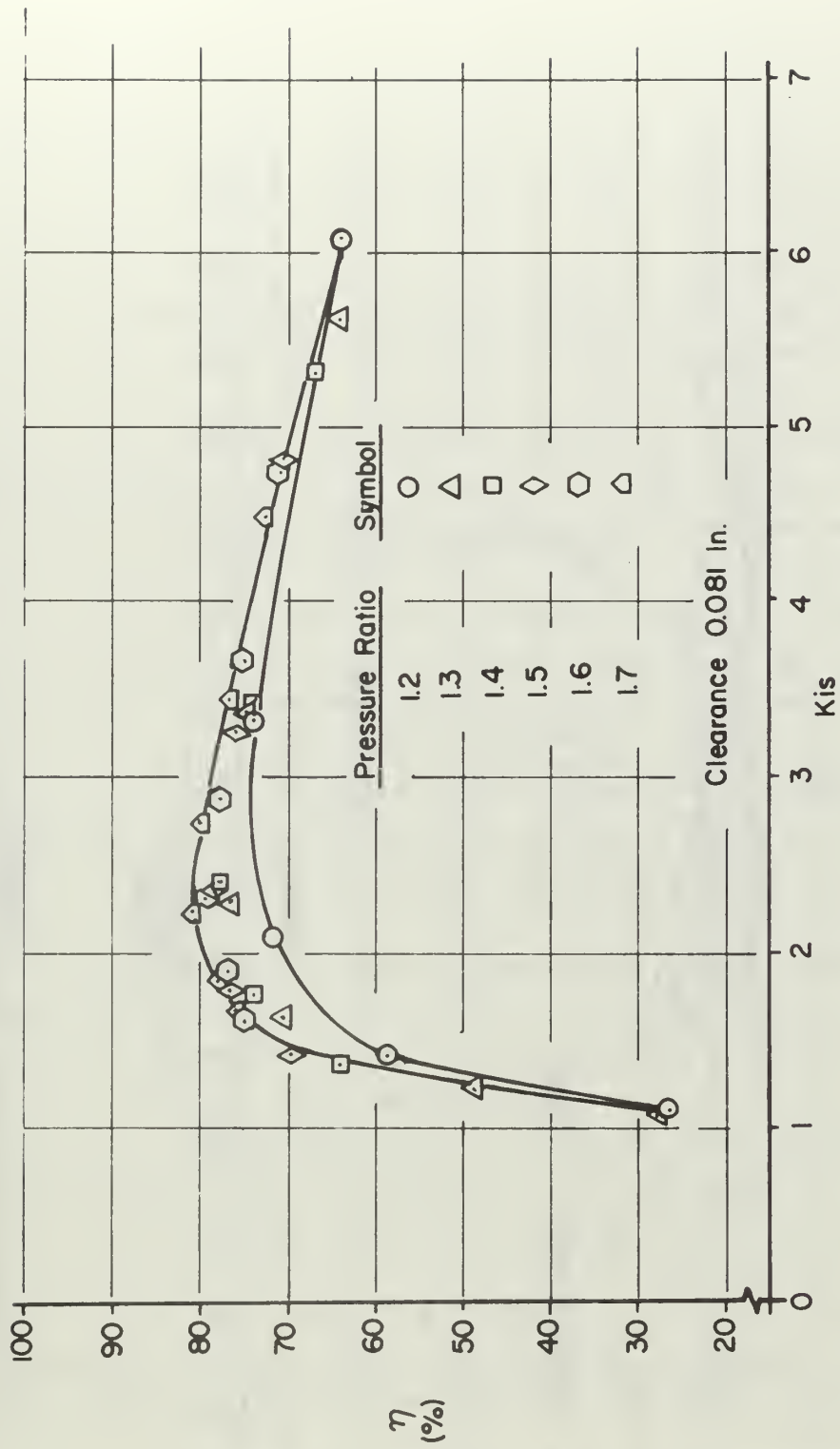


FIGURE 29
OVERALL EFFICIENCY (NO BEARING LOSSES) VS. HEAD COEFFICIENT

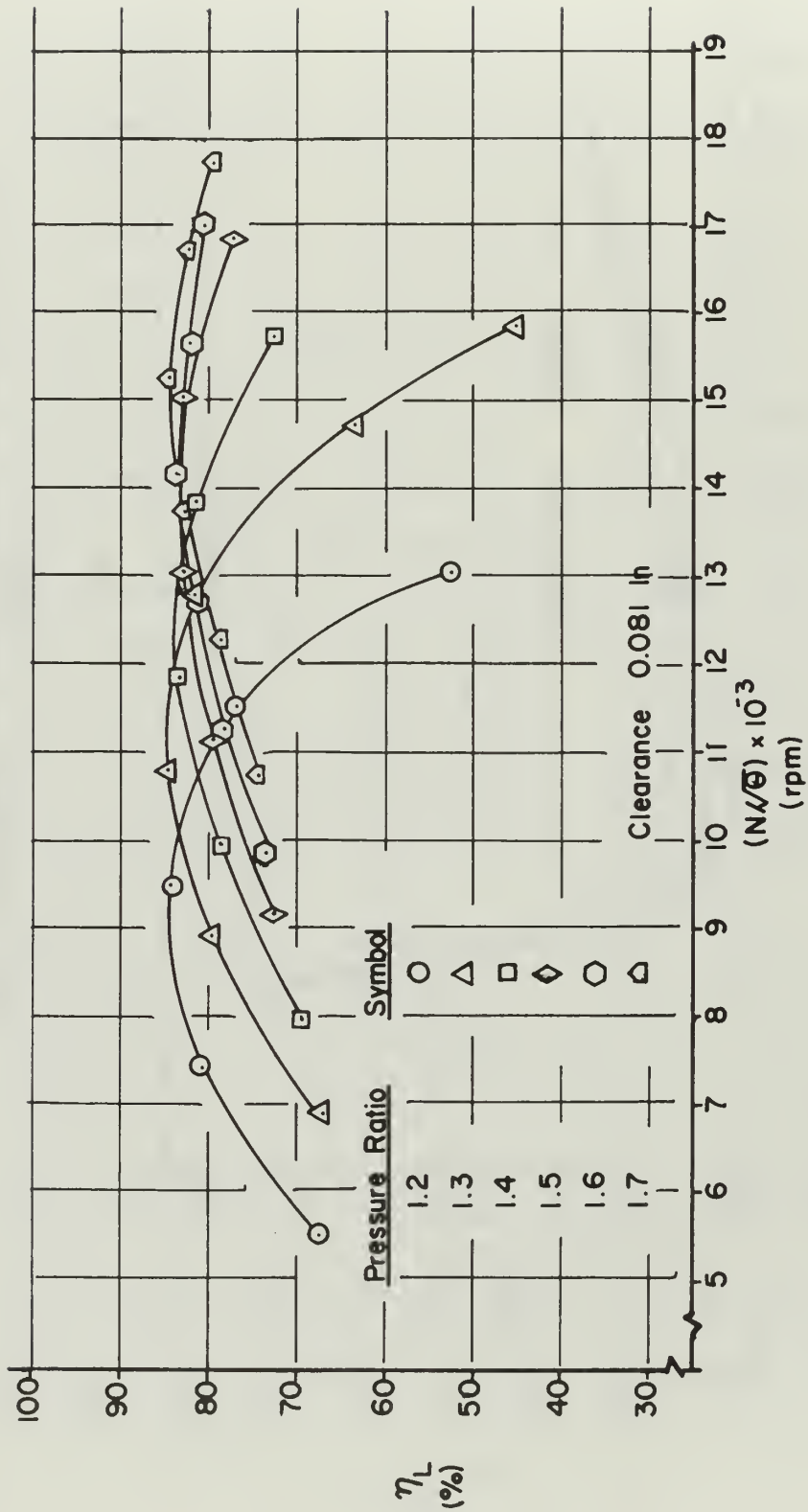


FIGURE 30
OVERALL EFFICIENCY (WITH BEARING LOSSES) VS. REFERRED SPEED

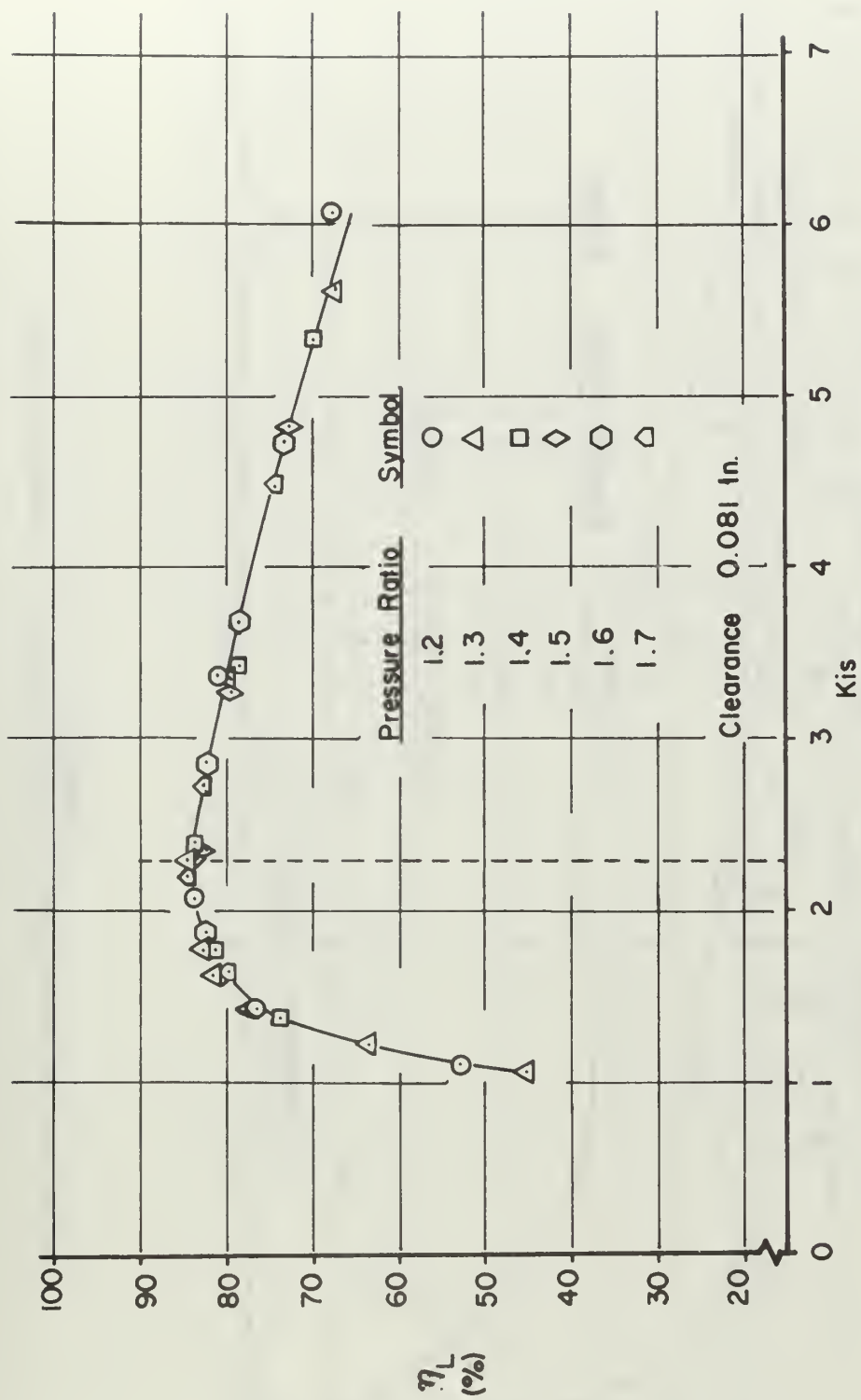


FIGURE 31
OVERALL EFFICIENCY (WITH BEARING LOSSES) VS. HEAD COEFFICIENT

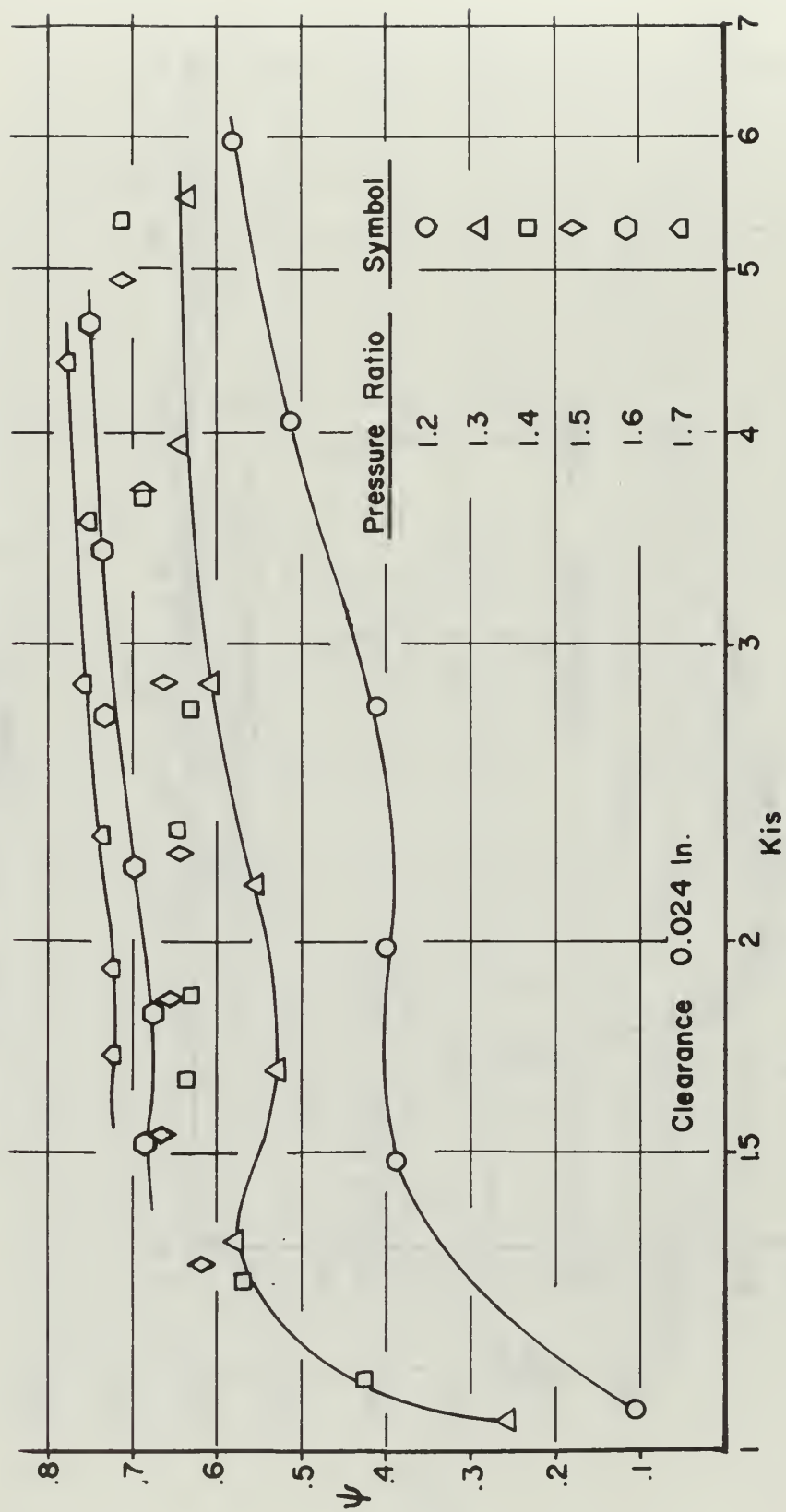


FIGURE 32
 ROTOR VELOCITY COEFFICIENT (NO BEARING LOSSES) VS. HEAD COEFFICIENT

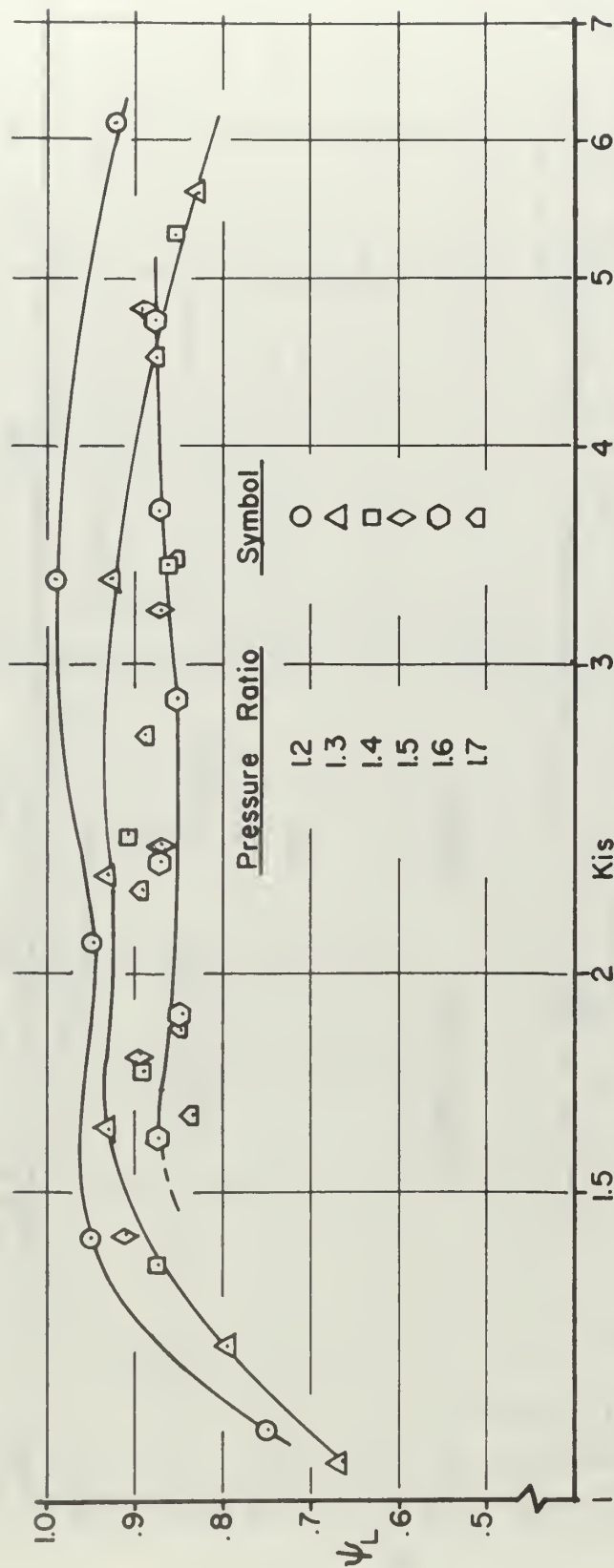


FIGURE 33
 ROTOR VELOCITY COEFFICIENT (WITH BEARING LOSSES) VS. HEAD COEFFICIENT
 CLEARANCE 0.081 IN.

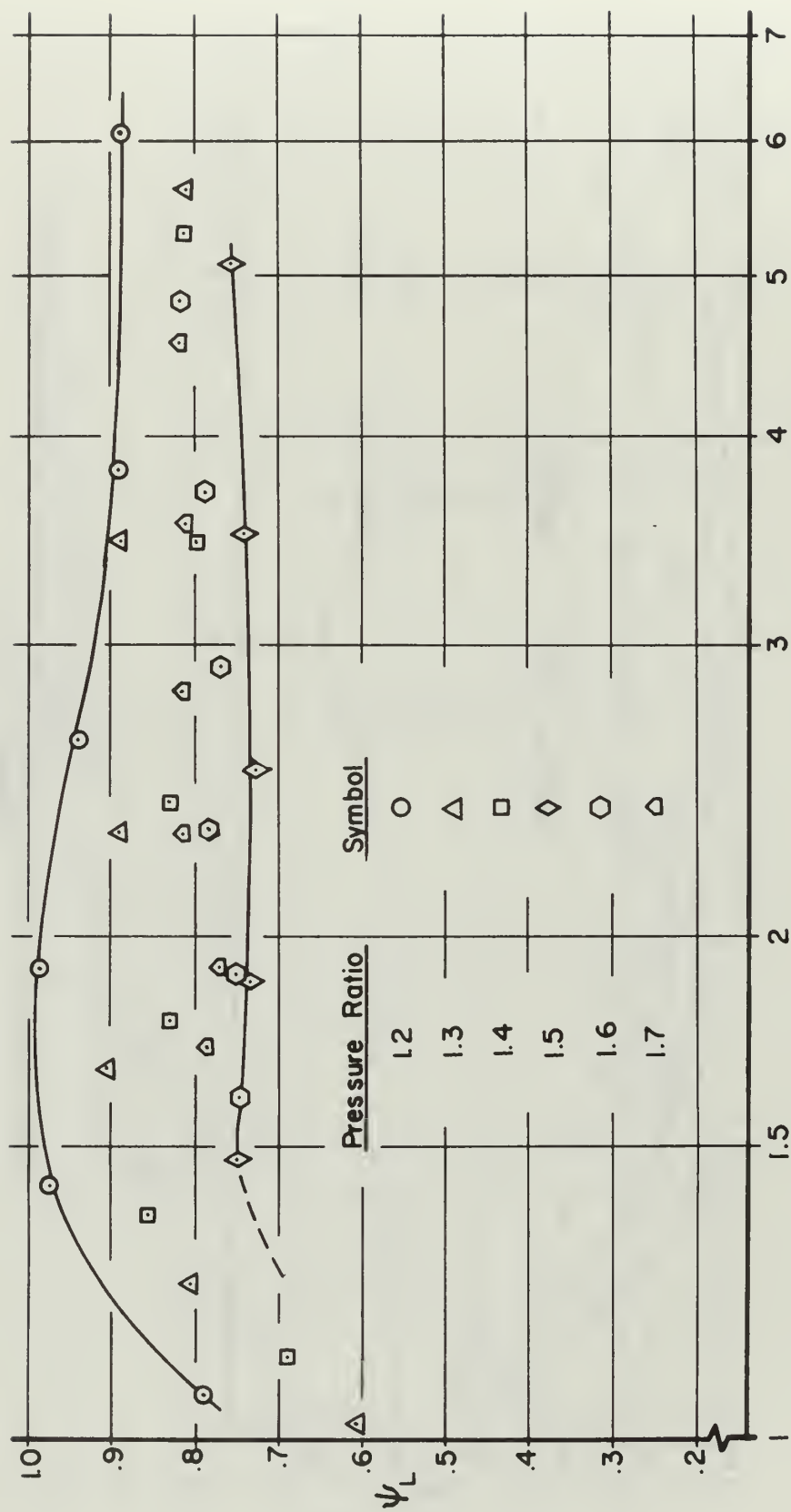


FIGURE 34
 ROTOR VELOCITY COEFFICIENT (WITH BEARING LOSSES) VS. HEAD COEFFICIENT
 CLEARANCE 0.061 IN.

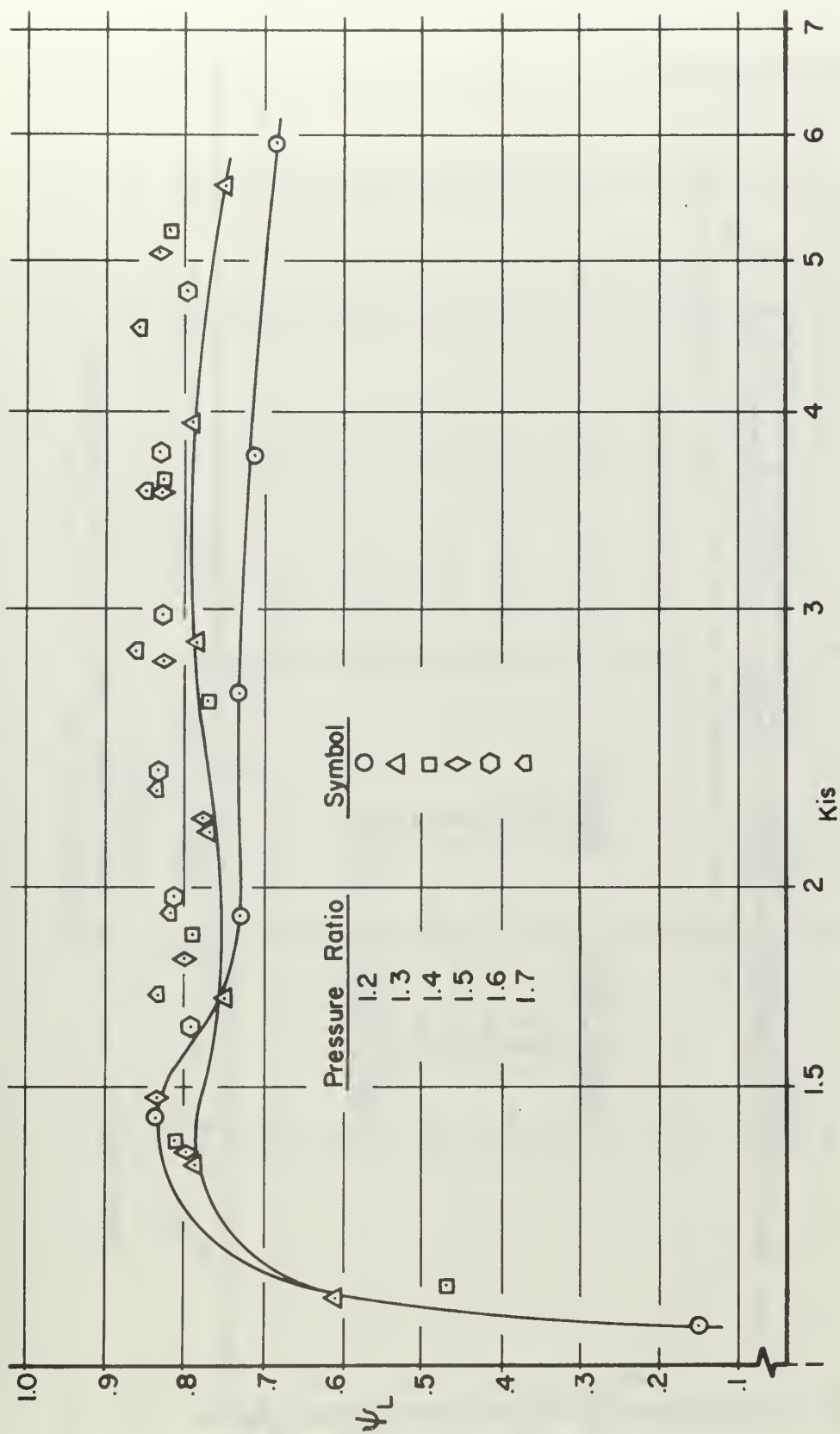


FIGURE 35
 ROTOR VELOCITY COEFFICIENT (WITH BEARING LOSSES) VS. HEAD COEFFICIENT
 CLEARANCE 0.041 IN.

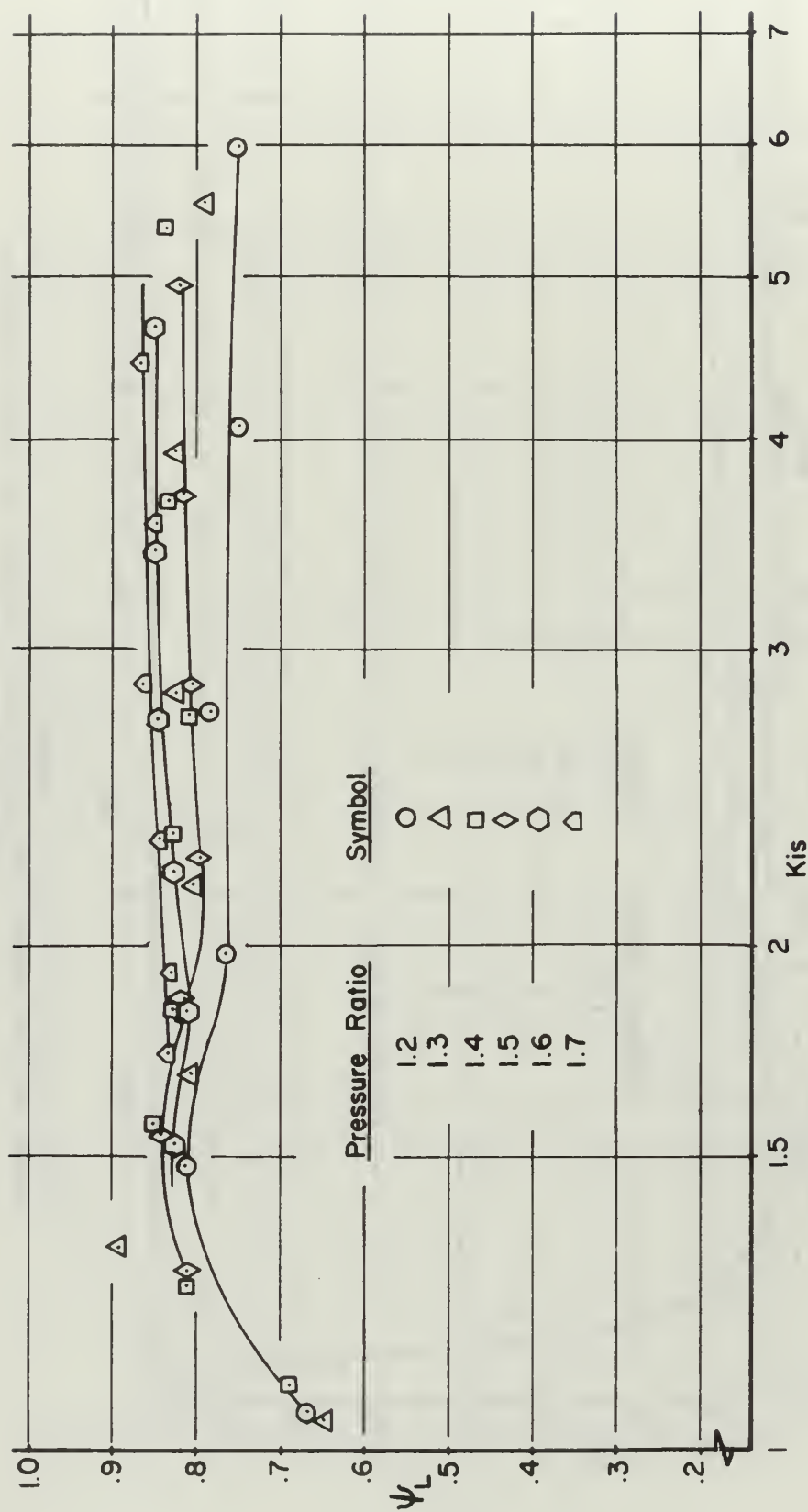


FIGURE 36
 ROTOR VELOCITY COEFFICIENT (WITH BEARING LOSSES) VS. HEAD COEFFICIENT
 CLEARANCE 0.024 IN.

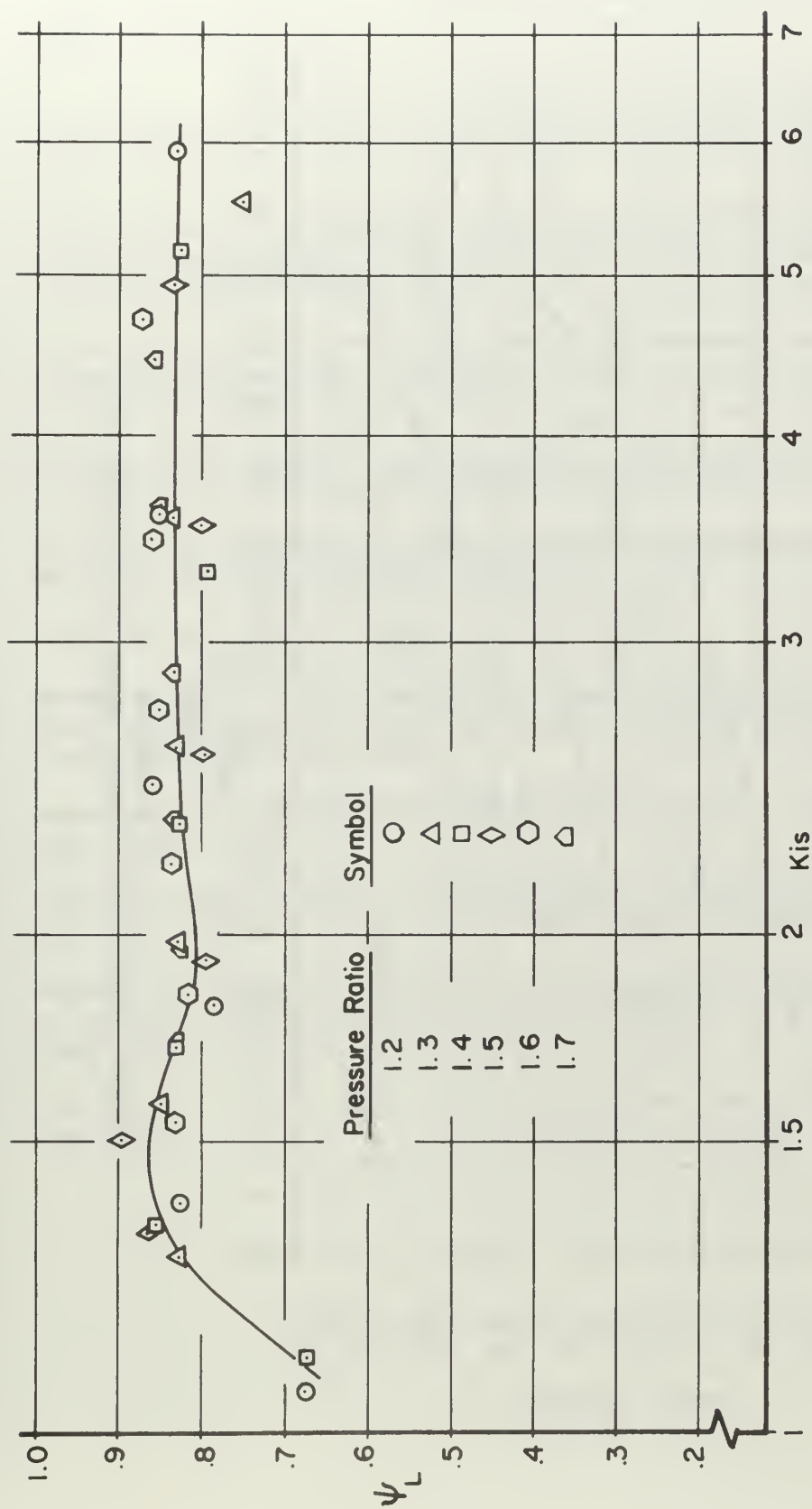


FIGURE 37
 ROTOR VELOCITY COEFFICIENT (WITH BEARING LOSSES) VS. HEAD COEFFICIENT
 CLEARANCE 0.015 IN.

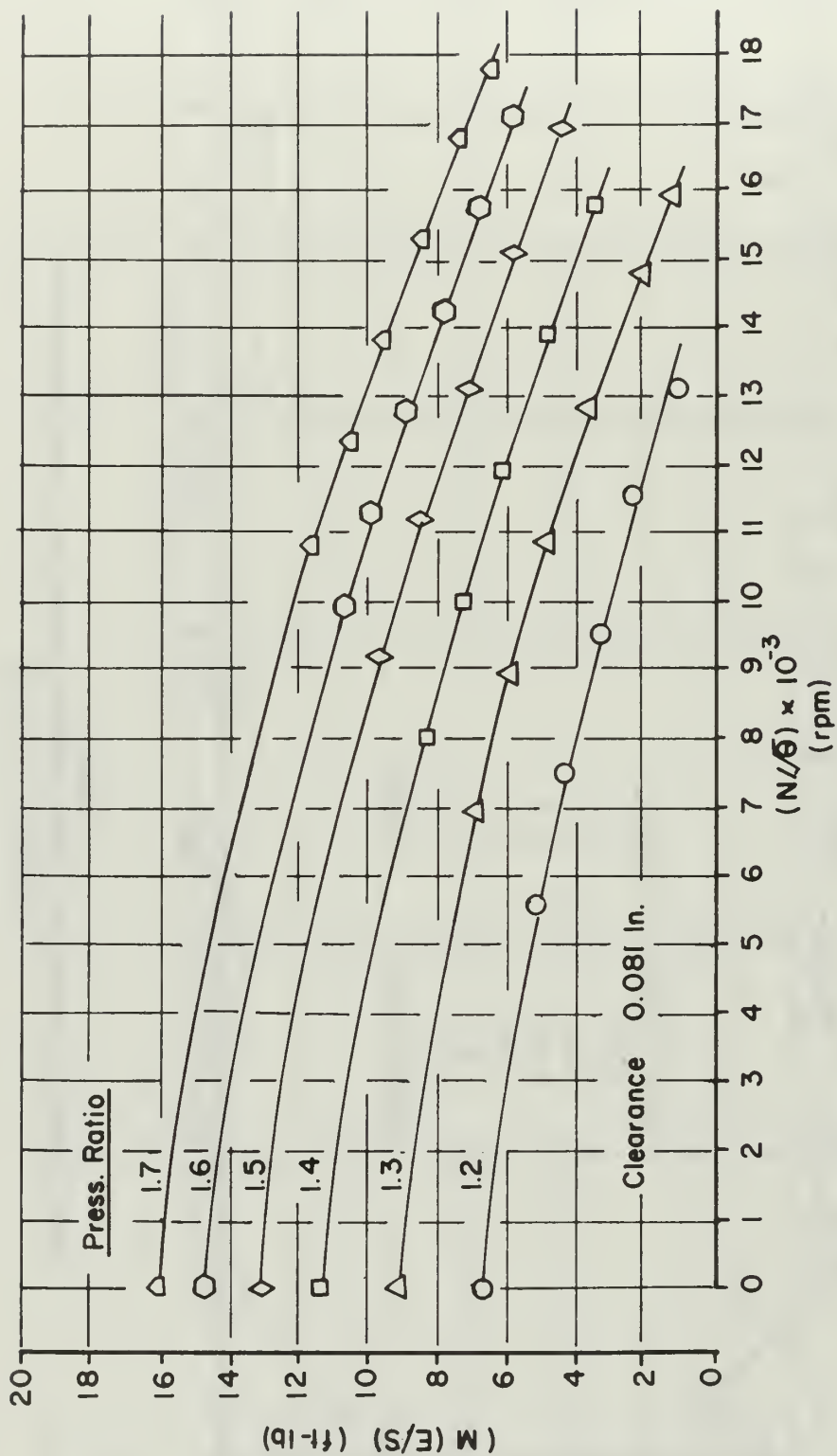


FIGURE 38
REFERRED MOMENT (WITH BEARING LOSSES) VS. REFERRED SPEED

REFERENCES

1. Vavra, M. H., Results of Turbine Air Testing Program, Phase II, Report AGLR-VA No. 29, for Aerojet General Corporation, January 1965.
2. Finn, W. A., "Performance Investigation of a Dual Discharge Radial Inflow Turbine." Master's thesis, Naval Postgraduate School, May 1966.
3. Riley, M. W., "The Effect of Axial Clearance on the Performance of a Dual Discharge Radial Turbine." Master's thesis, Naval Postgraduate School, December 1966.
4. Boshoven, R. L., "An Investigation of Compressible Flows with Large Whirl Components." Engineer's thesis, Naval Postgraduate School, June 1967.
5. Stearns, R. F., et al. Flow Measurement with Orifice Meters. New York: D. van Nostrand Company, 1951.
6. Vavra, M. H. Aero-Thermodynamics and Flow in Turbomachines. New York: John Wiley and Sons, 1960.
7. Vavra, M. H., Private communication, 1968.
8. Vavra, M. H., "Flow in Radial Turbines." Lecture notes for a short course on flow in turbines, von Karman Institute for Fluid Dynamics, March 1968.
9. Csanady, G. T. Theory of Turbomachines. New York: McGraw-Hill Book Company, 1964.
10. National Research Council. International Critical Tables, Vol. III. New York: McGraw-Hill Book Company, 1928.
11. Shenker, H. Reference Tables for Thermocouples. National Bureau of Standards, United States Department of Commerce, Circular 561. Washington: Government Printing Office, 1955.
12. Keenan, J. M. and J. Kaye. Gas Tables. New York: John Wiley and Sons, 1948.

APPENDIX A

PROGRAM SCROLL

Program SCROLL computes the losses in the scroll and guide vanes and the absolute rotor inlet flow angle from torque, mass flow rate, pressure, and temperature data obtained in the dummy rotor tests. The program is essentially that used by Riley (3) and by Boshoven (4), with several changes as specified below. It can process any number of runs, with a maximum of ten sets of data per run. A listing of program SCROLL is given in Table A1. The input and output values which constitute the results of the eight sets of dummy rotor test data obtained are presented in Tables A2 through A9.

A1 Main Program

The value of the specific gravity of mercury, G_{hg} , at room temperature t_{rm} , was determined from

$$G_{hg} = 13.63905 - (1.36303 \times 10^{-3}) t_{rm} \quad (A1)$$

for temperatures between 32°F and 113°F. The factor for converting inches Hg to lb/ft^2 is

$$C_{f1} = 70.438824 (G_{hg} / 13.54) \quad (A2)$$

The value of the specific gravity of water at room temperature is

$$G_{H_2O} = 0.9983763 + (1.060576 \times 10^{-4}) t_{rm} - (1.593186 \times 10^{-6}) t_{rm}^2 \quad (A3)$$

The specific gravity relations were obtained from the tabulated data of Reference 10.. These equations are slightly different from those used previously.

A2 Subroutine TEMP

The relations for the evaluation of the temperatures in this subroutine from the thermocouple readings in millivolts are different from those previously used because of the substitution of iron-constantan thermocouples for the chromel-alumel type. Thus, for iron-constantan thermocouples producing a millivolt output V , and using a cold junction reference temperature, t_{cj} , the temperature relations are

$$t = t_{cj} + 0.144 + 35.77 V - 0.4518 V^2 \quad (A4)$$

for $t \leq 100^\circ\text{F}$

$$t = t_{cj} + 1.252 + 34.86 V - 0.1855 V^2 \quad (A5)$$

for $100^\circ\text{F} < t \leq 200^\circ\text{F}$

Equations (A4) and (A5) were obtained from data tabulated in Reference 11.

A3 Subroutine FLOW

The evaluation of the flow rate using the measured data from the particular flow orifices employed in the radial turbine test setup was carried out in accordance with a method developed originally by Vavra (1), after the techniques given by Stearns, et al. (5). The values thus determined by Vavra applied to a sharp-edged orifice of 2.800 inches diameter. Before this series of tests was begun, the flow orifice diameter was measured and found to be 2.7965 inches. Additionally, the conversion factors and the value of the specific gravity of mercury used herein are slightly different than those previously used, the latter being 13.54 vice 13.59. The equations given below are thus those of Vavra (1), with these

modifications introduced. Computations were made for the vena contracta taps only, although flange tap data were available, because these data give a more accurate flow rate (1).

The relation for the flow rate is

$$\dot{W} = C \propto Y_1 F_r \sqrt{\frac{P_{1vc} \Delta h_{1vc}}{T_4}} \quad (A6)$$

where:

- C - factor dependent on orifice diameter, type of pressure taps, and dimensional units
- \propto - area multiplier to account for thermal expansion of orifice
- Y_1 - factor which accounts for compressibility effects
- F_r - Reynolds number correction factor
- P_{1vc} - absolute pressure at upstream tap
- Δh_{1vc} - pressure differential across orifice
- T_4 - temperature ahead of orifice

For vena contracta taps, $C = 0.9057$.

For a stainless steel orifice:

$$\propto = 1.0 + (1.85 \times 10^{-5}) (T_4 - 532.) \quad (A7)$$

$$Y_1 = 1.0 - 0.351 \frac{\Delta h_{1vc}}{P_{1vc}} \quad (A8)$$

Also,

$$F_r = 1.0 + \frac{0.001275}{X} \quad (A9)$$

where

$$X = 0.8131 \frac{\dot{W}}{Z} \quad (A10)$$

$$Z = 1.9 + (2.4 \times 10^{-3}) (T_4 - 559.69) \quad (A11)$$

where Equation (A11) is valid for air between 50°F and 300°F.

The resulting flow rate equation used herein is then given by

$$\dot{W} = 2.2854 \propto Y_1 F_r \sqrt{\frac{P_{1VC} \Delta h_{1VC}}{T_4}} \quad (A12)$$

where: \dot{W} is in lb_m/sec

P_{1VC} , Δh_{1VC} are in in. Hg.

T_4 is in °R

and where \propto , Y_1 and F_r are as given previously.

A4 Subroutine PRESS

It has been previously mentioned that a regulated reference pressure was used on the 96-inch water manometer board. This pressure must therefore be accounted for in computing p_1 , the absolute static pressure at the rotor inlet. This is done in the equation

$$p_1 = \frac{(P_{atm} + H_{refl})(G_{Hg}) + (H_L)(G_{H_2O})}{13.54} \quad (A13)$$

where the quantity $(P_{atm} + H_{refl})$ represents the total reference pressure applied to the manometer reservoir.

A5 Method of Assembly of Input Data

The items of input data necessary in performing computations with program SCROLL are given below in the order in which they must appear on the data cards. Specific formats for the numerical entries are given in the program listing.

<u>Card No.</u>	<u>FORTRAN</u>	<u>Description</u>
1	NRUNS	Number of runs (clearances) to be processed
2	NPTS	Number of points (pressure ratios) in run
3	DPVC	Measured pressure differential across flow orifice, from vena contracta taps (in. Hg)

<u>Card No.</u>	<u>FORTTRAN</u>	<u>Description</u>
	PUVC	Measured pressure upstream of flow measuring orifice, from vena contracta taps (in. Hg gage)
	P5P	Measured static pressure at turbine inlet (in. Hg gage)
	PATM	Barometric pressure (in. Hg)
	HREF1	Measured reference pressure applied to H ₂ O manometer board (in. Hg gage)
	H1	Average static pressure ahead of rotor (in. H ₂ O gage)
	SR	Torque scale reading (lb.)
	TRM	Control room temperature (°F)
	V4	Thermocouple reading ahead of orifice (mv.)
	V5	Thermocouple reading at turbine inlet (mv.)
4	TCJ	Cold junction temperature (°F)
	STARE	Torque scale tare (lb.)
	B1	Perpendicular distance between shroud inner extremities (in.)

Cards 3 and 4 comprise the input data for one test point and are repeated for a total of NPTS test points for each run. Each new run begins with card 2.

TABLE A1
LISTING OF PROGRAM SCROLL

```

C  PROGRAM SCROLL
  DIMENSION DPVC(10),PUVC(10),P5D(10),PATM(10),HREF1(10),H1(10),
  1SR(10),TRM(10),V4(10),V5(10),WVCP(10),PRP(10),PHIP(10),ALPH(10),
  2VEL(10),TS(10),ACH(10),PS(10)
  COMMON GHG,GWR,CFL,TCJ,STARE,T4,T5,WVC,PR,PI,PHI,ALF1,PAT,V1,T1,
  *ACH1,B1
  READ(5,10) NRUNS
  DC 99 J=1,NRUNS
  READ(5,10) NPTS
  READ(5,11) (DPVC(K),PUVC(K),P5D(K),PATM(K),HREF1(K),H1(K),SR(K),
  *TRM(K),V4(K),V5(K),K=1,NPTS)
  READ(5,12) TCJ,STARE,B1
  CLNC=(R1-.894)/2.
  WRITE(6,20) CLNC
  *WRITE(6,20) (K,DPVC(K),PUVC(K),P5D(K),PATM(K),HREF1(K),H1(K),SR(K)
  *WRITE(6,24) TCJ,STARE,B1
  DO 100 K=1,NPTS
    GHG=13.039C5-1.363C3OF-3*TRM(K)
    GWR=.0983763+1.060576E-4*TRM(K)-1.593186E-6*TRM(K)**2
    CFL=70.438824*GHG/13.54
    DPV=DPVC(K)
    PUV=PUVC(K)
    P5=P5P(K)
    PAT=PATM(K)
    HFF1=HREF1(K)
    PIP=H1(K)
    S=SR(K)
    V4T=V4(K)
    V5T=V5(K)
    CALL TEMP (V4T,V5T)
    CALL FLOW (DPV,PIV)
    CALL PRESS (P5,HFF1,PIF)
    CALL ALPSI (S)
    WVCP(K)=WVC
    PRP(K)=PR
    PHIP(K)=PHI
    ALPH(K)=ALF1
    VEL(K)=V1
    TS(K)=T1
    ACH(K)=ACH1
    PS(K)=PI
  CONTINUE
  100 WRITE(6,22) (K,PRP(K),WVCP(K),PHIP(K),ALPH(K),

```

```

1 VEL(K), TS(K), ACH(K), PS(K), K=1, NPTS)
99 CONTINUE
10 FORMAT(I4)
11 FORMAT(10F7.3)
12 FORMAT(3F7.3)
20 * FORMAT(1H1, 'PROGRAM SCROLL', T74, 'D.D. WILLIAMS', //, T21,
* 'SCROLL AND GUIDE VANE TESTS OF ICP RADIAL TURBINE', //, T17, 'TABLE
* ', T53, 'CLEARANCE = ', F5.3, 'IN.', //, T41, 'INPUT DATA', //, T5, 'PT
* ', DPVC PUVV P5P PATM HREF1 H1 SR TRM
* V4 V5, //)
21 FORMAT(I6, J0F8.3)
22 * FORMAT(//, T40, 'OUTPUT DATA', //, T1C, 'PT PTO/PI WVC PHI
* ALPH(1) V1 MACH1 P1, //)
23 * FORMAT(5X, I6, 2F8.3, F8.4, 3F9.2, 2F9.3)
24 * FORMAT(//19X5HTCJ -F6.2, 9X7HSTARE -F5.2, 9X4HB1 -F6.3)
RETURN
END

```

C

```

SURROUTINE TEMP (V4, V5)
COMMON GHG, GWR, CF1, TCJ, STARE, T4, T5, WVC, PR, P1, PHI, ALP1, PAT, V1, T1,
* ACH1, B1
V=V4
J=1
100 T=TCJ+J.144+35.77-V-C.4518*V**2
101 IF(T-100.) 102, 101
102 T=TCJ+1.252+34.86*V-C.1855*V**2
103 T=T+459.69
104 IF(J-1) 103, 103, 104
J=2
T4=T
V=V5
GO TO 100
T5=T
RETURN
END

```

C


```

SUBROUTINE FLOW (DPVC,PUVC)
COMMON GHG,GWR,CFL,TCJ,STARF,T4,T5,WVC,PR,PI,PHI,ALPI,PAT,VJ,TI,
*ACH1,R1
DVC=DPVC*GHG/13.54
PVC=(PUVC+PAT)*GHG/13.54
A=1.+1.85E-5*(T4-532.)
Z=1.9+2.4E-3*(T4-560.)
Y=1.-.351*(PVC/PVC
WVC=2.2854*A*Y*SQRT(PVC*DVC/T4)
X=WVC*.8131/Z
WVC=(1.+0.001275/X)*WVC
RETURN
END

```

C

```

SUBROUTINE PRESS(PSF,HOF1,H1)
COMMON GHG,GWP,CFL,TCJ,STARE,T4,T5,WVC,PR,PI,PHI,ALPI,PAT,V1,T1,
*ACH1,B1
A=T5-459.69
CP=.23943+3.4E-6*A+2.F-8*A**2
PI=((PAT+HOF1)*GHG+H1*GWP)/13.54
PS5=(PAT+PSF)*GHG/13.54
TT=T5
100 RHO=PS5*CFL/(TT*53.3448)
VO=WVC/(RHO*3.14159*6.25/144.)
TO=T5-(VO**2)/(2.*32.174*778.16*CP)
DTT=TT-TO
TT=TO
IF(ABS(DTT)-.01)101,101,100
101 PTO=PS5+RHO*(VO**2)/(2.*32.174*CFL)
PR=PTO/PI
RETURN
END

```

C

```

SUBROUTINE ALPSI (SR)
COMMON GHG,GWR,CFI,TCJ,STAPE,T4,T5,WVC,PR,PL,PHI,ALP1,PAT,VJ,T1,
*ACH1,B1
T=T5-459.6C
GAM=1.4018-2.E-5*T
EXP=(GAM-1.)/GAM
CP=.23943+3.4E-6*T+2.E-8*T**2
G=2.*32.174*778.16*CP
RM=(SR-STAPE)*12.0
VUI=RM*32.174/(WVC*4.75)
B=T5*(1.-1./PR**EXP)
A1=2.*3.14159*4.75*B1/144.
PHI=1.
100 V1=PHI*SQRT(G*B)
TI=T5-(V1**2)/G
RHO=P1*CF1/(T1*53.3448)
VM1=WVC/(A1*RHO)
V1A=SQRT(VM1**2+VUI**2)
IF(ABS(V1-V1A)-.5)102,102,101
101 PHI=PHI-.0001
GO TO 100
102 ALP1=57.29578*ATAN(VUI/VM1)
ACH1=V1/SQRT(32.174*GAM*53.3448*T1)
RETURN
END

```

SCROLL AND GUIDE VANE TESTS OF ICP RADIAL TURBINE

TABLE A2

CLEARANCE = 0.081 IN.

INPUT DATA									
PT	CPVC	PVVC	P5P	PATM	HREF1	H1	SR	TRM	V4
1	1.134	2.640	1.520	30.040	C.C	2.089	1.820	83.000	1.597
2	2.259	5.350	3.160	30.040	0.0	4.306	3.800	83.600	1.625
3	3.399	8.310	4.990	30.040	0.0	6.799	6.010	84.000	1.643
4	4.410	11.000	6.700	30.040	0.0	9.103	8.040	84.500	1.660
5	5.443	14.000	8.640	30.040	0.0	11.781	10.330	85.000	1.655
6	6.619	18.600	12.080	30.030	0.0	15.045	13.060	85.000	1.660
7	7.768	21.290	13.550	30.030	C.C	18.561	15.940	85.200	1.665
8	9.278	26.410	17.210	30.030	0.0	24.234	19.850	85.600	1.675
9	10.795	31.850	21.110	30.030	0.0	30.913	24.000	86.000	1.680
10	11.582	37.830	23.250	30.030	C.C	34.725	26.300	86.000	1.685
TCJ - 32.00									V5
STARE - 0.0									1.495
R1 - 1.056									1.540
									1.560
									1.582
									1.600
									1.605
									1.615
									1.630
									1.635

OUTPUT DATA				
PT	PTO/PI	WVC	PHI	PI
1	1.047	0.590	81.72	30.162
2	1.097	0.855	81.77	30.324
3	1.152	1.081	81.83	30.506
4	1.203	1.263	81.77	30.674
5	1.260	1.445	81.76	30.869
6	1.363	1.666	81.49	31.099
7	1.400	1.843	81.66	31.357
8	1.499	2.101	81.54	31.773
9	1.600	2.364	81.41	32.263
10	1.654	2.567	80.87	32.543
				MACH1
				0.223
				0.322
				0.405
				0.466
				0.526
				0.580
				0.645
				0.710
				0.769
				0.778
			T1	
			538.93	
			534.73	
			529.13	
			524.51	
			518.83	
			513.32	
			506.01	
			498.20	
			490.88	
			489.82	

PROGRAM SCROLL

D.D. WILLIAMS

SCROLL AND GUIDE VANE TESTS OF ICP RADIAL TURBINE

TABLE A3

CLEARANCE = 0.072 IN.

INPUT DATA									
PT	DPVC	PVVC	PSP	PATM	HREF1	H1	SR	TRM	V4
1	1.147	2.690	1.550	29.880	0.0	2.308	1.860	79.100	1.675
2	2.278	5.460	3.210	29.880	0.0	4.708	3.880	80.000	1.702
3	2.234	7.960	4.750	29.880	0.0	6.958	5.750	80.200	1.710
4	2.232	10.660	6.460	29.880	0.0	9.406	7.750	81.300	1.755
5	3.392	13.960	8.180	29.880	0.0	12.517	10.300	82.200	1.785
6	6.653	17.750	11.180	29.880	0.0	16.517	13.160	83.000	1.800
7	7.823	21.560	13.780	29.880	0.0	20.593	16.100	84.000	1.820
8	9.392	26.950	17.560	29.880	0.0	26.829	20.330	84.700	1.830
9	10.837	32.200	21.330	29.880	0.0	33.722	24.210	85.000	1.835
10	11.796	35.780	24.020	29.880	0.0	38.925	26.990	85.500	1.840

TCJ - 32.00

STARE - 0.0

B1 - 1.038

OUTPUT DATA

PT	PTO/PI	WVC	PHI	ALPH(1)	V1	T1	MACH1	PI
1	1.048	0.591	0.8789	81.66	259.13	541.12	0.227	30.031
2	1.098	0.856	0.8929	81.72	372.74	537.03	0.328	30.204
3	1.145	1.047	0.9038	81.76	451.70	532.47	0.399	30.369
4	1.195	1.228	0.9043	81.69	518.06	528.60	0.460	30.546
5	1.257	1.430	0.9134	81.68	592.06	523.01	0.528	30.784
6	1.331	1.645	0.9116	81.57	658.04	517.00	0.590	31.064
7	1.403	1.843	0.9174	81.53	718.94	510.61	0.649	31.361
8	1.504	2.111	0.9252	81.47	791.94	502.04	0.721	31.817
9	1.599	2.361	0.9225	81.30	843.57	495.25	0.773	32.323
10	1.664	2.528	0.9249	81.25	878.58	490.51	0.809	32.704

PROGRAM SCRCLL

D.O. WILLIAMS

SCRCLL AND GUIDE VANE TESTS OF ICP RADIAL TURBINE

TABLE A4
CLEARANCE = 0.061 IN.

INPUT DATA										
PT	DPVC	PVVC	P5P	PATM	HPEF1	H1	SR	TRM	V4	V5
1	1.185	2.785	1.600	29.970	0.00	2.512	1.940	82.000	1.625	1.540
2	2.393	5.765	3.390	29.970	0.00	5.337	4.100	82.000	1.630	1.560
3	4.012	10.015	6.060	29.970	0.00	9.401	7.310	82.500	1.645	1.590
4	4.610	11.700	7.130	29.970	0.00	11.001	8.510	83.100	1.635	1.595
5	5.554	14.410	8.900	29.970	0.00	13.866	10.640	83.600	1.640	1.605
6	6.720	17.590	11.310	29.970	0.00	17.546	13.350	83.400	1.642	1.610
7	7.912	21.880	13.920	29.970	0.00	21.975	16.370	83.000	1.650	1.620
8	9.405	26.560	17.580	29.970	0.00	28.241	20.320	83.300	1.660	1.630
9	10.924	32.500	21.580	29.970	0.00	35.484	24.180	83.300	1.660	1.630
10	11.886	36.100	24.170	29.970	0.00	40.753	27.080	83.400	1.660	1.630
TCJ - 32.00 STARE - 0.0 RI - 1.016										
OUTPUT DATA										
PT	PTO/PI	WVC	PHI	ALPH(1)	V1	T1	MACH1	PI		
1	1.049	0.603	0.8901	81.55	265.03	540.00	0.233	30.127		
2	1.102	0.883	0.8991	81.56	381.76	534.39	0.337	30.335		
3	1.181	1.193	0.9100	81.56	503.00	526.44	0.448	30.634		
4	1.263	1.301	0.9060	81.49	539.00	523.64	0.480	30.748		
5	1.331	1.466	0.9164	81.41	597.19	518.08	0.535	30.057		
6	1.402	1.666	0.9171	81.41	650.13	511.91	0.594	31.228		
7	1.499	1.871	0.9247	81.38	719.80	505.12	0.653	31.556		
8	1.599	2.126	0.9271	81.30	796.26	495.13	0.719	32.017		
9	1.666	2.391	0.9155	81.02	832.78	491.20	0.767	32.548		
10		2.566	0.9238	81.02	871.05	485.77	0.806	32.936		

PRCGRAM SCROLL

SCROLL AND GUIDE VANE TESTS OF ICP RADIAL TURBINE

D.O. WILLIAMS

TABLE A5

CLEARANCE = 0.050 IN.

INPUT DATA									
PT	DPVC	PLVC	P5P	PATM	HREF1	H1	SP	TRM	V5
1	1.158	2.720	1.560	29.920	0.0	2.547	1.880	78.000	1.493
2	2.305	5.480	3.190	29.920	0.0	5.204	3.900	79.000	1.530
3	3.285	8.110	4.840	29.920	0.0	7.926	5.860	79.200	1.540
4	4.423	11.280	6.860	29.920	0.0	10.989	8.200	79.200	1.500
5	5.333	13.820	8.540	29.920	0.0	13.858	10.040	79.600	1.530
6	6.676	17.800	11.170	29.920	0.0	18.247	13.180	80.000	1.540
7	7.788	21.460	13.610	29.920	0.0	22.750	16.020	80.000	1.550
8	9.262	26.400	17.110	29.920	0.0	29.118	19.740	80.200	1.560
9	10.712	31.350	20.690	29.920	0.0	35.069	23.520	80.600	1.575
10	11.753	35.500	23.700	29.920	0.0	42.194	26.780	80.600	1.595
TCJ - 32.00 STARE - 0.0 RI - 0.994									
OUTPUT DATA									
PT	PTO/PI	WVC	PHI	ALPH(1)	V1	T1	MACH1	PI	
1	1.047	0.598	0.8857	81.29	259.21	536.64	0.228	30.091	
2	1.096	0.866	0.9005	81.29	370.67	532.69	0.328	30.284	
3	1.145	1.063	0.9111	81.41	453.76	527.85	0.403	30.484	
4	1.204	1.275	0.9112	81.36	529.32	520.63	0.473	30.709	
5	1.251	1.433	0.9049	81.20	576.79	517.12	0.517	30.919	
6	1.325	1.662	0.9177	81.20	652.60	509.70	0.590	31.241	
7	1.390	1.854	0.9271	81.14	711.14	503.40	0.647	31.572	
8	1.481	2.106	0.9249	81.05	771.79	496.95	0.707	32.041	
9	1.574	2.351	0.9226	80.88	823.91	489.95	0.759	32.477	
10	1.641	2.539	0.9328	80.92	868.80	484.21	0.805	33.002	

PROGRAM SCRCLL

SCRCLL AND GUIDE VANE TESTS OF ICP RADIAL TURBINE

D.D. WILLIAMS

TABLE A6

CLEARANCE = 0.041 IN.

INPUT DATA										
PT	DPVC	PLVC	P5P	PATM	HREF1	HI	SP	TRM	V4	V5
1	1.159	2.700	1.560	30.010	0.0	2.696	1.890	80.000	1.610	1.530
2	2.348	5.610	3.310	30.010	0.0	5.815	3.980	80.200	1.620	1.560
3	3.549	8.770	5.260	30.010	0.0	9.279	6.310	80.900	1.625	1.585
4	4.422	11.170	6.800	30.010	0.0	11.986	8.120	80.000	1.635	1.595
5	5.682	14.810	9.170	30.010	0.0	16.047	10.870	80.100	1.635	1.605
6	6.823	18.700	11.770	30.010	0.0	22.842	13.800	80.000	1.645	1.640
7	8.094	22.450	14.390	30.010	0.0	25.428	16.750	81.000	1.675	1.665
8	9.715	27.990	18.280	30.010	0.0	33.019	21.020	81.900	1.675	1.665
9	11.254	33.650	22.400	30.010	0.0	41.769	25.290	82.000	1.702	1.670
10	12.258	37.450	25.200	30.010	0.0	47.581	28.050	82.000	1.720	1.690
ICJ - 32.00										
STARE - 0.0										
R1 - 0.976										

OUTPUT DATA										
PT	PTO/PI	WVC	PHI	ALPH(1)	V1	T1	MACH1	P1		
1	1.047	0.596	0.890	81.14	259.91	539.83	0.228	30.186		
2	1.098	0.874	0.899	81.15	374.02	534.83	0.331	30.415		
3	1.155	1.110	0.909	81.17	458.02	528.99	0.415	30.668		
4	1.199	1.269	0.914	81.12	526.87	524.63	0.469	30.870		
5	1.265	1.489	0.918	81.12	600.87	517.78	0.539	31.169		
6	1.335	1.704	0.922	81.06	666.68	511.08	0.602	31.522		
7	1.405	1.900	0.928	81.04	725.68	505.44	0.653	31.855		
8	1.503	2.177	0.933	80.94	795.31	497.31	0.723	32.412		
9	1.601	2.445	0.934	80.82	852.15	490.03	0.785	33.055		
10	1.666	2.620	0.931	80.69	882.28	486.20	0.816	33.481		

SCROLL AND GUIDE VANE TESTS OF ICP RADIAL TURBINE

TABLE A7
CLEARANCE = 0.030 IN.

INPUT DATA									
PT	DPVC	PLVC	P5P	PATM	HREF1	H1	SR	TRM	V5
1	0.840	2.000	1.150	30.000	0.0	2.096	1.360	75.200	1.390
2	0.352	5.670	3.350	30.000	0.0	6.133	4.000	76.000	1.420
3	0.228	7.900	4.750	30.000	0.0	8.606	5.670	76.300	1.435
4	0.555	10.900	6.620	30.000	0.0	12.080	7.900	78.000	1.440
5	0.538	14.450	8.920	30.000	0.0	16.384	10.630	78.400	1.485
6	0.202	18.950	11.980	30.000	0.0	22.088	13.940	78.800	1.505
7	0.295	22.830	14.600	30.000	0.0	27.082	16.940	78.800	1.520
8	0.406	28.550	18.650	30.000	0.0	35.422	21.450	79.000	1.555
9	0.473	34.000	22.550	30.000	0.0	45.122	25.657	79.300	1.570
10		37.600	25.400	30.000	0.0	50.191	28.350	79.800	1.595

TCJ - 32.00 STARE - 0.0 RI - 0.954

OUTPUT DATA					
PT	PTO/PI	WVC	PHI	ALPH(1)	VI
1	1.034	0.508	0.8848	80.97	221.00
2	1.099	0.881	0.8956	80.95	374.05
3	1.139	1.056	0.9063	80.96	442.45
4	1.193	1.255	0.9174	81.01	518.62
5	1.256	1.475	0.9254	80.96	593.79
6	1.339	1.728	0.9193	80.78	664.69
7	1.407	1.929	0.9280	80.73	723.72
8	1.504	2.216	0.9366	80.73	797.67
9	1.597	2.477	0.9432	80.65	853.65
10	1.663	2.654	0.9342	80.46	880.95

PI	T1	MACH1
30.147	536.79	0.195
30.442	529.72	0.332
30.623	525.59	0.394
30.873	519.67	0.464
31.189	514.43	0.532
31.603	507.69	0.602
31.975	501.38	0.659
32.589	493.05	0.733
33.302	485.97	0.790
33.673	482.96	0.818

PROGRAM SCROLL

D.D. WILLIAMS

SCROLL AND GUIDE VANE TESTS OF ICP RADIAL TURBINE

TABLE A8

CLEARANCE = 0.024 IN.

INPUT DATA											
PT	DPVC	PVVC	P5P	PATM	HREF1	H1	SR	TRM	V4	V5	
1	1.237	2.920	1.700	29.560	0.0	3.193	2.020	72.900	1.520	1.435	
2	2.295	5.500	3.250	29.560	0.0	6.135	3.890	73.900	1.535	1.465	
3	3.391	8.340	5.000	29.560	0.0	9.529	5.990	74.500	1.540	1.495	
4	4.514	11.400	6.930	29.560	0.0	13.098	8.270	75.100	1.543	1.525	
5	5.747	14.930	9.230	29.560	0.0	17.457	10.960	75.800	1.560	1.523	
6	6.904	18.540	11.660	29.560	0.0	21.845	13.680	76.200	1.580	1.545	
7	8.201	22.750	14.570	29.570	0.0	27.859	17.000	77.000	1.590	1.555	
8	9.913	28.600	18.200	29.970	0.0	35.859	21.440	77.900	1.600	1.565	
9	11.395	34.050	22.700	29.970	0.0	44.934	25.670	78.800	1.610	1.580	
10	12.397	37.900	25.420	29.970	0.0	51.838	28.210	79.000	1.625	1.598	
								STARE - C.0	R1 - C.942		
								TCJ - 32.00			

OUTPUT DATA								
PT	PTO/PI	WVC	PHI	ALPH(1)	V1	T1	MACH1	PI
1	1.050	0.619	0.8922	80.87	269.11	536.20	0.237	30.195
2	1.096	0.866	0.9036	80.87	370.47	531.84	0.328	30.408
3	1.146	1.083	0.9134	80.87	455.73	527.01	0.405	30.655
4	1.200	1.288	0.9181	80.83	529.07	521.34	0.473	30.917
5	1.263	1.502	0.9242	80.79	601.13	515.18	0.540	31.236
6	1.329	1.701	0.9260	80.74	662.65	509.46	0.599	31.558
7	1.405	1.923	0.9349	80.74	728.65	502.16	0.663	31.980
8	1.492	2.215	0.9469	80.60	797.81	493.72	0.732	32.595
9	1.600	2.474	0.9415	80.55	855.57	485.28	0.791	33.260
10	1.658	2.650	0.9333	80.33	877.98	483.67	0.814	33.767

PROGRAM SCROLL
 D.D. WILLIAMS

SCROLL AND GUIDE VANE TESTS OF ICP RADIAL TURBINE

TABLE A9
 CLEARANCE = 0.015 IN.

INPUT DATA									
PT	DPVC	PUVC	P5P	FATM	HREF1	H1	SR	TRM	V5
1	1.309	3.070	1.780	30.120	0.0	3.548	2.120	75.000	1.545
2	2.428	5.820	3.430	30.120	0.0	6.792	4.120	76.000	1.562
3	3.503	8.590	5.130	30.120	0.0	10.197	6.170	76.900	1.580
4	4.611	11.960	7.090	30.120	0.0	13.879	8.440	77.200	1.590
5	5.776	14.960	9.250	30.120	0.0	18.168	10.970	78.100	1.605
6	7.046	18.900	11.910	30.060	0.0	23.169	13.980	79.000	1.620
7	8.328	23.050	14.710	30.060	0.0	28.179	17.240	79.200	1.615
8	9.992	28.890	18.840	30.060	0.0	38.109	21.790	80.100	1.620
9	11.853	35.650	23.810	30.060	0.0	50.909	26.050	80.600	1.635
10	12.683	38.820	26.150	30.060	0.0	56.909	29.050	80.600	1.580

TCJ - 32.00
 STARE - 0.0
R1 - 0.924

OUTPUT DATA					
PT	PTO/P1	WVC	PHI	ALPH(1)	V1
1	1.052	0.639	0.8542	80.60	273.91
2	1.099	0.894	0.9090	80.68	379.91
3	1.147	1.104	0.9177	80.67	460.69
4	1.202	1.305	0.9201	80.64	533.13
5	1.260	1.507	0.9262	80.61	600.20
6	1.332	1.724	0.9305	80.58	668.98
7	1.404	1.943	0.9397	80.56	732.53
8	1.503	2.230	0.9447	80.49	802.81
9	1.612	2.553	0.9462	80.36	865.47
10	1.660	2.698	0.9440	80.26	888.48

T1	MACH1	P1
536.85	0.241	30.374
531.94	0.336	30.610
527.15	0.409	30.858
522.01	0.476	31.128
516.20	0.539	31.441
508.98	0.604	31.747
493.09	0.666	32.160
484.07	0.737	32.843
481.50	0.802	33.771
	0.826	34.225

APPENDIX B

PROGRAM RADIAL

Program RADIAL computes the referred flow rate, head coefficient, degree of reaction, relative and absolute rotor inlet flow angles, velocity and loss coefficients for the scroll and guide vanes, referred moment, absolute discharge flow angle, velocity and loss coefficients for the rotor, and efficiencies from the torque, speed, mass flow rate, and the pressure and temperature data obtained during the active rotor tests. The calculation technique generally follows that given in the theory of Section 4.3. It can process any number of clearances (sets) and any number of pressure ratios (runs) per clearance with a maximum of ten different speed settings (points) per run. A listing of program RADIAL is given in Table B1.

In program RADIAL, use was made of temporary memory disc storage of the input data in order to avoid the awkward procedure of subscripting the input variables. This procedure permits the processing and printing of the input data on a point-by-point basis and the presentation of the results in a compact, tabular form. Appropriate comments appear in the main program at the points where this procedure was used. The additional control cards required to implement this technique and to obtain necessary additional memory core storage space are shown in Table B2. As the table indicates, these cards are inserted just ahead of the data cards in the assembled deck.

The torque calibration data used for all runs are given in Table B3. The input and output values resulting from the five sets of test data are presented in Tables B4 through B13.

B1 Subroutines TEMP and FLOW

These subroutines perform the same functions as in program SCROLL, namely those of obtaining temperatures from the thermocouple readings and calculating mass flow rate, respectively. Subroutine TEMP has been expanded to include calculation of the temperatures of the bearing lubricating oil at the inlet and at the discharge of each bearing. However for reasons discussed in Section 4, these values were not used in this experiment.

B2 Subroutine PRESS

Subroutine PRESS establishes the total-to-static pressure ratios across the scroll and guide vanes (P_{to}/p_1) and across the turbine (P_{to}/p_2) and the ratio p_1/p_2 . An iteration process is necessary in order to determine an average value of the total pressure at the turbine inlet, P_{to} . Three relations are used to accomplish this, these being the gas law,

$$\rho_o = C_{f1} \frac{P_o}{R_g T_o} \quad (B1)$$

the continuity equation,

$$\dot{V}_o = \frac{\dot{W}}{\rho_o A_5} \quad (B2)$$

and the energy equation,

$$T_o = T_{to} - \frac{V_o^2}{2gJc_p} \quad (B3)$$

where A_5 is the area of the five-inch inlet pipe and C_p is the specific heat of air at the temperature T_{to} . Using T_{to} as a first approximation of ρ_o , an initial value of V_o is found, and from this, by Equation (B3), a new value of T_o . The iteration continues until a difference of 0.01

degrees or less exists between any two successive values of T_0 . Since velocities are low, the total pressure P_{t0} is then obtained from

$$P_{t0} = P_0 + \frac{\rho_0 V_0^2}{2 g C_{f1}} \quad (B4)$$

B3 Subroutine EDC

This subroutine computes the mean values of γ and C_p based on the arithmetic mean of total turbine inlet and static isentropic discharge temperatures. From Reference 3, the variations of γ and C_p with temperature are

$$\gamma = 1.4018 - (2 \times 10^{-5}) t \quad (B5)$$

$$C_p = 0.23943 + (3.4 \times 10^{-6}) t + (2 \times 10^{-8}) t^2 \quad (B6)$$

These relations were originally obtained from data tabulated in Reference 12 and are valid from approximately 40°F to 170°F.

The values of γ_{avg} and $C_{p(avg)}$ correspond to the average temperature through the turbine based on an isentropic expansion. This average temperature, t , is given by

$$t = (T_{t0} - 459.69) - \frac{\Delta T_{is}}{2} \quad (B7)$$

where

$$\Delta T_{is} = T_{t0} \left[1 - (P_2 / P_{t0})^{\frac{\gamma-1}{\gamma}} \right] \quad (B8)$$

Using an iteration process, the first approximation of ΔT_{is} is based on a value of γ corresponding to T_{t0} . The value of t resulting from Equation (B6) is compared with the previous value of t in each iteration until the difference between any two successive values of t is less than

1.0°. Using the final value of t , values of γ_{avg} , $C_{P(avg)}$, and ΔT_{is} are computed from Equations (B5), (B6), and (B8), respectively. The reference parameter Θ , given by

$$\Theta = (\gamma_{avg}/1.4) (T_5/518.7) \quad (B9)$$

is also computed in this subroutine.

The subscript indicating the average values of γ and C_p will be dropped in subsequent discussions. The average values of these quantities are assumed in the remainder of the program unless otherwise stated.

B4 Subroutines TORQ and DYNA

These subroutines compute the net torque produced by the turbine by evaluating the bearing friction moment and the torque measured by the dynamometer.

In subroutine TORQ, the bearing friction moment is evaluated from turbine rpm by Equations (27), (28), and (29). The net moment is calculated by Equation (30), where the dynamometer torque output is found in subroutine DYNA, called from subroutine TORQ.

Subroutine DYNA determines the torque from the dynamometer calibration data obtained for each run. These data are tabulated in Table B3 for all runs.

The values of the torque calibration data constitute a one-dimensional array with five elements, representing the torque scale reading for loads of zero to 400 inch-pounds, respectively, taken at 100 inch-pound intervals. Thus, TCD(1) represents the torque scale readout value for the no load condition. Using a DO loop with index I , the torque indicator reading for the test point being processed, TQ , is compared with the values of TCD(I) to determine the interval ($I, I+1$) within which TQ lies. Since

the calibration curve data are very nearly linear, the torque is computed assuming a straight line approximation between TCD(I) and TCD(I-1), by the equation

$$T = 100(I-1) + 100 \left[\frac{TQ - TCD(I)}{TCD(I+1) - TCD(I)} \right] \quad (B10)$$

This procedure was adapted from that used by Riley (3).

B5 Subroutine TURB

The turbine performance parameters described in Section 4 are calculated by subroutine TURB in a manner which follows the theory previously given. No iterations are involved, and the equations used are self-explanatory. Therefore, the steps will not be discussed here. The velocity coefficient, ϕ , and the absolute rotor inlet flow angle, α_1 , are provided from subroutine PHIAL, for which TURB is the calling subroutine.

B6 Subroutine PHIAL

This subroutine calculates the values of ϕ , α_1 , V_1 , and ζ_N , from the results of program SCROLL. The values of γ and C_p used are based on the total inlet temperature, rather than the average temperature as computed in subroutine EDC, because the values of ϕ and α_1 obtained in program SCROLL were computed in this manner.

The values of ϕ and α_1 are obtained from Equations (13) and (14), for which the entering arguments are CLNC, the axial clearance, and ACH1, or M_1 , the Mach number at the rotor inlet. Since V_1 and T_1 are not known at this point in the computations, they must be obtained by iteration. An initial value of V_1 is obtained from Equation (4) by assuming $\phi = 1.0$, and initial values of T_1 and M_1 are obtained from Equations (35) and (36), respectively. Using this value of M_1 , called ACHIA, and CLNC, a value of

ϕ , called PHIA, is obtained from Equation (13). The assumed value of ϕ is reduced in increments of 0.001 until succeeding values of ϕ and ϕ_A differ by no more than 0.001. Thus, values of V_1 , M_1 , and ϕ are established, and α_1 is then computed from Equation (14). The loss coefficient for the scroll and guide vanes, ζ_N , is then obtained from Equation (12).

B7 Subroutine REFER

This subroutine computes the referred speed, referred flow rate, and referred moment in accordance with Equations (60), (61), and (62), respectively.

B8 Method of Assembly of Input Data

In order to facilitate future use of program RADIAL, the order of assembly of the input data cards is given. The actual formats for the numerical entries may be obtained directly from the program listing. All items of data are given in the order in which they must appear on the data cards. For convenience, the symbols are redefined.

<u>Card No.</u>	<u>FORTTRAN</u>	<u>Description</u>
1	NSETS	Number of sets of data (clearances to be processed)
2	CLNC	Clearance for set
3	NRUNS	Number of runs (pressure ratios) in data set
4	TCD	Torque calibration data for run (5 values).
5	NPTS	Number of data points (speeds) in run
6	RPM	Measured turbine speed (rpm)
	TQ	Torque indicator reading (counts)
	PUVC	Measured pressure upstream of flow measuring orifice, from vena contracta taps (in. Hg gage)

<u>Card No.</u>	<u>FORTTRAN</u>	<u>Description</u>
	P5P	Measured static pressure at turbine inlet (in. Hg gage)
	H1	Average static pressure ahead of rotor (in H ₂ O gage)
	DPVC	Measured pressure differential across flow orifice, from vena contracta taps (in. Hg)
	PATM	Barometric pressure (in. Hg)
	HREF1	Measured reference pressure applied to water manometer board (in. Hg gage)
	V4	Thermocouple reading ahead of orifice (mv.)
	V5	Thermocouple reading at turbine inlet (mv.)
7	V20	Thermocouple reading at lube oil inlet (mv.)
	V21	Thermocouple reading at lube oil discharge from right bearing (mv.)
	V22	Thermocouple reading at lub oil discharge from left bearing (mv.)
	TRM	Control room temperature (°F)
	TCJ	Cold junction temperature (°F)

Cards 6 and 7 comprise the input data for one test point and are repeated for a total of NPTS test points for each run. Each new run begins with card 4, and each new set begins with card 2.

TABLE B1

www

```

C WRITE INPLT DATA.
  WRITE(6,7) J,K,RPM(K),TQ(K),PUVC(K),P5P(K),H1(K),DPVC(K),PATM(K),
  *HREF1(K),V4(K),V5(K),V20(K),V21(K),V22(K),TRM(K),TCJ(K)
  7 FORMAT(2X,2I3,1X,F7.0,2X,F6.0,3F8.2,F9.3,2F8.2,5F8.3,2F7.1)
  IF(K.EQ.NPTS) GC TO R
    GC TC 12
  R WRITE(6,1C3)
  1C3 FORMAT(/)
  13 CONTINUE
C WRITE DATA FOR CNE RUN CN TEMPORARY DATA SET.
  WRITE(8)(RPM(I),TC(I),PUVC(I),P5P(I),H1(I),DPVC(I),PATM(I),HREF1(I)
  *,V4(I),V5(I),V20(I),V21(I),V22(I),TRM(I),TCJ(I),I=1,NPTS)
  12 CONTINUE
C WRITE HEADING FOR PRINTOUT OF RESULTS.
  WRITE(6,2C0)
  2C0 FORMAT(1F1,///,T44,'PERFORMANCE EVALUATION OF ICP RADIAL TURRINE',
  *///)
  2C1 FORMAT(1F1,2C1) CLNC
  2C1 FORMAT(T22,'TABLE',T61,'OUTPUT DATA',T91,'CLEARANCE = ',F5.3,1X,
  *IN,///)
  2C2 FORMAT(T25,'REDUCED TC STANDARD AIR IN ACCORDANCE WITH NASA METHOD
  *,/,T25,'TCTAL INLET PRESS. = 14.7 PSIA, TCTAL INLET TEMPERATURE',
  *,/,T35,'= 518.7 DEG.R., GAMMA = 1.4, CP = 0.24 BTU/LBM-DEG.F.,//)
  2C3 FORMAT(/,T76,'NO BEARING LCASSES',T106,'MAXIMUM BEARING LOSSES',/,
  *T69,/,T10,'PRESS REF. REF. HEAD DEG ANGLE ANGLE VEL LOS
  *S,/,T2,'RUN/PT REF ANGLE REF ANGLE VEL LOSS EFF
  *IC-,/,T2,'RATIO SPEED FLOW COEFF REACT ALPHA1 BETAL CO
  *EFF CCEFF WCM ALF20 CCEFF IENCY DEG GV ROTOR',/)
  *EFF IENCY,/,T17,'RPM FT.LR DEG ROTOR',/)
  2C4 FORMAT(T2,/,T17,'RPM FT.LR DEG ROTOR',/)
  *-----)
C PROCESS DATA POINTS.
DO 21 J=1,NRUNS
C READ TOPQUE CALIBRATION DATA FROM TEMPORARY DATA SET.
  READ(8)(TCD(I),I=1,5)
  READ(8) NPTS
C READ DATA FOR CNE RUN FROM TEMPORARY DATA SET.
  READ(8)(PPM(I),TQ(I),FUVVC(I),P5P(I),H1(I),DPVC(I),PATM(I),HREF1(I)

```

```

* ,V4(I),V5(I),V20(I),V21(I),V22(I),TRM(I),TCJ(I),I=1,NPTS)
WRITE(6,205)
205 FORMAT(/)
DO 22 K=1,NPTS
  GHG=13.63905-1.363030E-3*TRM(K)
  GWR=.9983763+1.060576E-4*TRM(K)-1.593186E-6*TRM(K)**2
  CF1=70.428824*GHG/13.54
  CALL TEMP (V4(K),V5(K),V20(K),V21(K),V22(K),TCJ(K))
  CALL FLCW (GHG,DPVC(K),PUVC(K),PATM(K))
  CALL PRESS (PATM(K),HREF1(K),GHG,GWR,H1(K),P5P(K),CF1)
  CALL EDC (THETA)
  CALL TCRC (RPM(K),ICD,TQ(K))
  CALL TURB (RPM(K),CLNC)
  CALL REFER (RPM(K),THETA,GHG)
C WRITE OUTPUT DATA.
  WRITE(6,9) J,K,PR2,RPMR,WVCR,HEAD,DR,ALPH1,RETAL,PHI,ZETAN,TR,ALF2
  * ,PSI,ZETR,ETA,TNETR,ALF2L,PSIL,ZETRL,ETAL
  9 FORMAT(2I3,F8.3,F7.0,F7.3,2F6.3,F6.2,F7.2,2F6.3,
  * F6.2,F8.2,F7.2,2F6.3,F6.2)
  22 CCNTINUE
  21 CCNTINUE
  11 RETURN
END

```

```

C SUBROUTINE TEMP (V4,V5,V20,V21,V22,TCJ)
C CALCULATES TEMPERATURES FROM THERMOCOUPLE READINGS.
C THERMOCOUPLE EQUATIONS VALID FOR IRON-CONSTANTAN ONLY.
COMMON T4,T5,T20,T21,T22,WVC,P1,PTO,PR1,PR2,PSR,DTIS,
*XP,TNETR,ROSP,T,ETA,ETAL,ACH1,PHI,V1,ALPH1,ZETAN,BETAL,PSIL,
*ZETR,ZETRL,TR,TNETR,ALF2,ALF2L,RPMR,WVCR,BFM,HEAD,DR
DO 122 J=1,5
  GO TO (110,111,112,113,114),J
110 V=V4
111 GC TO 123
112 V=V5
113 GC TO 123
114 V=V20

```



```

113 GC TC 123
114 V=V21 GC TC 123
115 V=V22
116 T=TCJ+C.144+35.77*V-0.4518*V**2
117 IF(T.LE.100.) GO TO 115
118 T=TCJ+1.252+34.86*V-0.1855*V**2
119 IF(J.GT.2) GC TC 116
120 T=T+455.69
121 GO TO (117,118,119,120,121),J
122 T4=T GC TC 122
123 T5=T GC TC 122
124 T20=T GC TC 122
125 T21=T GC TC 122
126 T22=T GC TC 122
127 CONTINUE
128 RETURN
129 END

```

```

C CAL SUBROUTINE FLOW (GHG,DPVC,PVVC,PATM)
CALCULATES FLOW RATE FROM ORIFICE MEASUREMENTS.
COMMON T4,T5,T20,T21,T22,WVC,P1,PTO,PR1,PR2,PSR,DTIS,DHIS,CP,GAM,E
*XP,TNET,RCSP,T,FETA,ETAL,ACH1,PHI,V1,ALPH1,ZETAN,RETAL,PSI,PSIL,
*ZETR,ZETPL,TR,TNETR,ALF2,ALF2L,RPMR,WVCR,BFM,HEAD,DR
DVC=DPVC*GHG/13.54
PVC=(PLVVC+PATM)*GHG/13.54
A=1.+1.85E-5*(T4-532.)
Z=1.9+2.4E-3*(T4-560.)
Y=1.-.351*DVC/PVC
WVC=.2+.2854*A*Y*SQRT(PVC*DVC/T4)
X=WVC*.8131/Z
WVC=(1.+0.001275/X)*WVC
RETURN
END

```

```

C   SUBROUTINE PRESS (PATM,HREF1,GHG,GWR,H1,P5P,CF1)
CALCULATES INLET TOTAL PRESSURE AND PRESSURE RATIOS WITHIN TURBINE.
COMMON T4,T5,T20,T21,T22,WVC,P1,PTO,PR1,PR2,PSR,DTIS,DHIS,CP,GAM,E
*XP,TNET,ROSP,T,ETA,ETAL,ACH1,PHI,V1,ALPH1,ZETAN,BETA1,PSI,PSIL,
*ZETR,ZETRL,TR,TNETR,ALF2,ALF2L,RPMR,WVCR,BFM,HEAD,DR
A=T5-459.69
CP5=.23943+3.4E-6*A+2.E-8*A**2
P1=((PATM+HREF1)*GHG+(H1*GWR))/13.54
PS5=(PATM+P5F)*GHG/13.54
TT=T5
100 RHO=PS5*CF1/(TT*53.3448)
VO=WVC/(RHO*3.14159*6.25/144.)
TO=T5-(VC**2)/(2.*32.174*778.16*CP5)
DTT=TT-TC
TT=TO
IF(ABS(CIT)-.01) 101,101,100
101 PTO=PS5+RHC*(VO**2)/(2.*32.174*CF1)
PR1=PTC/P1
PR2=PTC/(PATM*GHG/13.54)
PSR=P1/(PATM*GHG/13.54)
RETURN
END

```

```

C   SUBROUTINE ECC (THETA)
CALCULATES AVERAGE TEMP. FOR DETERMINATION OF CP,GAMMA, AND SQ. ROOT
OF TEMP. RATIO (THETA), AND ISENTROPIC ENTHALPY DROP (DHIS).
COMMON T4,T5,T20,T21,T22,WVC,P1,PTO,PR1,PR2,PSR,DTIS,DHIS,CP,GAM,E
*XP,TNET,ROSP,T,ETA,ETAL,ACH1,PHI,V1,ALPH1,ZETAN,BETA1,PSI,ZETAR,AL
*F20,RPMR,WVCR,TNETR,BFM,HEAD,DR
A=T5-459.69

```

```

105 GA=1.4C1E-2.E-5*A
   EX=(GA-1.)/GA
   DT=T5*(1.-1./PR2**EX)
   AA=T5-459.69-DT/2.
   AAA=ABS(AA-A)
   IF(AAA-1.) 1C7,107,1C6
106 A=AA
   GC TG 1C5
1C7 GAM=GA
   EXP=EX
   DTIS=CT
   CP=.23942+3.4E-6*AA+2.E-8*AA**2
   DHIS=CP*DTIS
   IF(GAM*T5) 2C50,2C51,2C51
2C50 WRITE(6,2052) K,GAM,T5
2C52 FORMAT(//,6X,I4,2F8.3)
2051 CONTINUE
   THETA=(GAM/1.4)*(T5/518.7)
   RETURN
   END

C  CALCULATES NET TORQUE (MEASURED PLUS THAT DUE TO BEARING FRICTION).
   DIMENSION TCD(5)
   COMMON T4,T5,T2C,T21,T22,WVC,P1,PTO,PR1,PR2,PSR,DTIS,DHIS,CP,GAM,E
   *XP,TNET,ROSP,T,ETA,ETAL,ACH1,PHI,V1,ALPH1,ZETAN,BETA1,PSI,PSIL,
   *ZETR,ZETRL,TR,TNETR,ALF2,ALF2L,RPMR,WVCR,BFM,HEAD,DR
   ROSP=3.14159*RPM/30.
C  COMPUTE BEARING FRICTION MCMNT FROM COAST-DOWN DATA OF VAVRA, FOR
C  MAXIMUM LCSS CONDITION.
   IF(RPM.LE.10500.) GO TO 99
   HPF=-.6+((.17143)*(RPM/1000.)-(4.898E-3)*(RPM/1000.-10.5)**2
   GC TO 1CC
99 HPF=-.6+((.17143)*(RPM/1000.)
100 BFM=(HPF*550.)/RCSP
   CALL CYNA (TC,TCD,T)
   TNET=T+BFM
   RETURN

```

END

```

C SUBROUTINE DYNA (TQ,TCD,T)
C CALCULATES DYNAMOMETER TORQUE FROM TORQUE READOUT AND TORQUE CAPSULE
C CALIBRATION DATA.
C DIMENSION TCD(5)
DO 100 I=1,5
IF (TCD(I)-TQ) 100,100,101
100 CONTINUE
AI=100.*(I-1)
T=AI+100.*((TQ-TCD(I))/(TCD(I+1)-TCD(I)))
T=T/12.
RETURN
END

```

```

C SUBROUTINE TURB (RPM,CLNC)
C CALCULATES HEAD COEFFICIENT, LOSS COEFFICIENTS, EFFICIENCIES, AND FLOW
C ANGLES.
COMMON T4,T5,T2C,T21,T22,WVC,P1,PTO,PR1,PR2,PSR,DTIS,DHIS,CP,GAM,E
*XP,TNET,ROSP,T,ETA,ETAL,ACH1,PHI,V1,ALPH1,ZETAN,BETA1,PSI,PSIL,
*ZETR,ZETRL,TR,TNETR,ALF2,ALF2L,RPMR,WVCR,8FM,HEAD,DR
DTW=(TNET*ROSP)/(CP*WVC*778.16)
ETAL=CTH/DTIS
DTWNL=(T*RCSF)/(CP*WVC*778.16)
ETA=DTWNL/DTIS
CC=SQRT(2.*32.174*778.16*CP*DTIS)
D1=9.40
U1=3.14159*RFM*D1/720.
CC=CC/U1
HEAD=CC**2
DR=1.-(T5/DTIS)*(1.-(1./PR1)**EXP)

```



```

C THE LETTER U AT END OF VARIABLE NAME INDICATES DIVISION BY U1.

CALL PHIAL (CLAC)
V1U=V1/U1
X=ALPH1/57.29578
V1U=V1U*SIN(X)
W1U=V1U-1.
VM1U=V1U*CCS(X)
C W1U12=(W1/U1)**2
W1U12=VM1U**2+W1U**2
Y=W1U/V1U
BET=ATAN(Y)
BETA1=BET*57.29578
R1=4.7
R20=2.54
VU2U=(R1/R20)*((V1U-(ETA/2.)*HEAD)
C BET20=(R1/R20)*((V1U-(ETA/2.)*HEAD)
BET20=-69.85 DEGREES.
W20U=((V2U-R20/R1)/SIN(BET20)
W20UL=(V2UL-R20/R1)/SIN(BET20)
C W20TU=W20TH/U1
W20TU=V20U/W20TU
PS1=W20U/W20TU
PS1L=W20UL/W20TU
ZETRL=1.-PS1**2
ZETRL=1.-PS1L**2
VM2U=W20U*CCS(BET20)
VM2UL=W20UL*CCS(BET20)
ALF2=57.29578*ATAN(VU2U/VM2U)
ALF2L=57.29578*ATAN(VU2UL/VM2UL)
ETA=100.*ETA
ETAL=100.*ETAL
RETURN
END

```

```

C SUBROUTINE PHIAL (CLNC)
C CALCULATES VALUES OF PHI, ALPHA, V1, ZETAN, FROM RESULTS OF PROGRAM
  SCROLL.
  COMMON T4,T5,T20,T21,T22,WVC,P1,PTO,PR1,PR2,PSR,DTIS,CHIS,CP,GAM,E
  *XP,TNET,ROSP,T,ETA,ETAL,ACH1,PHI,V1,ALPH1,ZETAN,BETAI,PSI,PSIL,
  *ZETR,ZETRL,TR,TNETR,ALF2,ALF2L,RPMR,WVCR,BFM,HEAD,DR
  A=T5-.459.69
  GAMMA=1.4018-2.E-5*A
  EXP=(GAMMA-1.)/GAMMA
  CP5=.23943+3.4E-6*A+2.E-8*A**2
  G=2.*32.174*778.16*CP5
  B=T5*(1.-1./PR1**EXP)
  PHI=1.
  100 V1=PHI*.SQRT(G*B)
      T1=T5-(V1**2)/G
      ACH1A=V1/SQRT(32.174*GAMMA*53.3448*T1)
      PHIA=((.92473)*(1.01433-1.24601*CLNC+24.06839*CLNC**2-180.36258*CLN
      *C**3)*(0.53149+.18292*ACH1A-.09202*ACH1A**2)
      IF(ABS(PHI-PHIA)-.0001) 102,102,101
  101 PHI=PHI-.0001
      GO TO 100
  102 ACH1=ACH1A
      PHI=PHIA
      ALPH1=(81.762)*((.98267+.26958*CLNC-.65080*CLNC**2)*(.99624+.02223*
      *ACH1-.02940*ACH1**2)
      ZETAN=1.-PHI**2
      RETURN
      END

```

```

C SUBROUTINE REFER (RPM,THETA,GHG)
C COMPUTES SPEED, NET MOMENT, FLOW RATE, REDUCED TO STANDARD AIR IN
  ACCORDANCE WITH NASA METHOD.
  COMMON T4,T5,T20,T21,T22,WVC,P1,PTO,PR1,PR2,PSR,DTIS,CHIS,CP,GAM,E
  *XP,TNET,ROSP,T,ETA,ETAL,ACH1,PHI,V1,ALPH1,ZETAN,BETAI,PSI,PSIL,
  *ZETR,ZETRL,TR,TNETR,ALF2,ALF2L,RPMR,WVCR,BFM,HEAD,DR
  *REFERRED SPEED, T(THETA)
  RPMR=RPM/SQRT(T(THETA))
  DEL=(PTC*(GHG/13.54))/29.92
  X=(GAM+1.)/(2.*(GAM-1.))

```

```

C      EPS=(.81C/GAM)*((GAM+1.)/2.)**X
C      REFERRED FLCW RATE.
C      WVCR=WVC*(SQRT(THETA))*EPS/DEL
C      REFERRED MCMENT.
      TR=T*EPS/DEL
      TNETR=TNET*EPS/DEL
      RETURN
      END

```

/*

✻

1

7

16

COLUMN

72

TABLE B2

ADDITIONAL CONTROL CARDS REQUIRED FOR PROGRAM RADIAL

TABLE B3
TORQUE CALIBRATION DATA

SET	CLEARANCE (IN)	RUNS	APPLIED TORQUE (IN-LB)				
			0	100	200	300	400
1	0.081	1-4	5.	261.	518.	768.	1013.
		5-6, NOSPD 1	2.	255.	510.	762.	1009.
2	0.061	1-3	0.	255.	511.	760.	1007.
		4-6, NOSPD 2	3.	259.	514.	762.	1007.
3	0.041	1-3	0.	257.	511.	760.	1007.
		4-6, NOSPD 3	0.	257.	510.	759.	1004.
4	0.024	1-3	0.	256.	510.	760.	1006.
		4-6, NOSPD 4	1.	259.	513.	762.	1007.
5	0.015	1-4	0.	255.	511.	760.	1008.
		5-6, NOSPD 5	-2.	255.	510.	759.	1004.

PERFORMANCE EVALUATION OF ICP RADIAL TURPINE

TABLE B4

INPUT DATA

CLEARANCE = 0.081 IN

RUN/PT	RPM	TORQUE COUNTS	PUVC IN.HG	P5P IN.HG	H1 IN.H2O	DPVC IN.HG	PATM IN.HG	HREF1 IN.HG	V4 MM	V5 MM	V21 MM	V22 MM	TRM DEG F	TCJ DEG F
1	5650.	185.	9.06	5.85	23.25	3.246	30.07	0.0	1.340	1.245	0.0	0.0	77.8	32.3
1	7620.	149.	8.76	5.90	27.05	2.801	30.07	0.0	1.365	1.280	0.0	0.0	78.8	32.3
1	9670.	107.	8.27	5.50	35.51	1.883	30.07	0.0	1.380	1.305	0.0	0.0	79.2	32.3
1	11720.	65.	7.77	5.91	45.76	1.883	30.07	0.0	1.380	1.305	0.0	0.0	80.5	32.3
1	13330.	25.	7.30	5.56	55.79	1.366	30.07	0.0	1.380	1.320	0.0	0.0	81.5	32.3
2	7040.	272.	13.36	8.82	34.78	4.517	30.07	0.0	1.380	1.325	0.0	0.0	85.0	32.3
2	9090.	228.	12.97	9.83	40.31	4.208	30.07	0.0	1.390	1.335	0.0	0.0	85.0	32.3
2	11030.	181.	12.50	9.85	49.78	3.689	30.07	0.0	1.385	1.340	0.0	0.0	85.5	32.3
2	13050.	131.	11.98	8.50	62.08	3.113	30.07	0.0	1.390	1.340	0.0	0.0	85.5	32.3
2	15050.	170.	11.21	8.87	75.39	2.388	30.07	0.0	1.405	1.360	0.0	0.0	86.2	32.3
2	16220.	35.	10.81	8.91	85.26	1.932	30.07	0.0	1.405	1.360	0.0	0.0	86.2	32.3
3	8140.	356.	17.52	11.76	4.84	5.806	30.06	3.02	1.375	1.330	0.0	0.0	87.0	32.3
3	10140.	307.	16.10	11.75	10.35	5.391	30.06	3.02	1.375	1.335	0.0	0.0	87.4	32.3
3	12120.	251.	16.60	11.78	21.33	4.834	30.06	5.03	1.380	1.335	0.0	0.0	87.5	32.3
3	14120.	192.	16.00	11.80	29.33	4.219	30.06	5.05	1.390	1.335	0.0	0.0	87.7	32.3
3	16040.	135.	15.35	11.81	23.27	3.560	30.06	5.05	1.400	1.335	0.0	0.0	87.7	32.3
4	9320.	438.	21.62	14.67	11.33	6.981	30.06	3.40	1.310	1.255	0.0	0.0	84.1	32.3
4	11330.	380.	21.20	14.71	18.93	6.518	30.06	5.10	1.315	1.265	0.0	0.0	85.0	32.3
4	13310.	320.	20.64	14.74	8.02	5.964	30.06	5.10	1.325	1.265	0.0	0.0	85.0	32.3
4	15300.	255.	20.01	14.78	24.05	5.346	30.06	5.10	1.340	1.285	0.0	0.0	85.5	32.3
4	17200.	194.	19.43	14.81	39.14	4.575	30.06	5.10	1.340	1.290	0.0	0.0	85.5	32.3
5	10130.	509.	25.65	17.60	14.16	8.081	30.07	4.02	1.665	1.470	0.0	0.0	84.0	32.3
5	11480.	467.	25.37	17.60	19.03	7.782	30.07	4.03	1.585	1.390	0.0	0.0	85.3	32.3
5	12980.	417.	25.04	17.65	12.66	7.381	30.07	5.20	1.575	1.375	0.0	0.0	86.0	32.3
5	14450.	369.	24.61	17.66	8.02	6.919	30.07	6.42	1.565	1.365	0.0	0.0	86.0	32.3
5	16000.	313.	24.04	17.70	8.21	6.424	30.07	7.40	1.565	1.365	0.0	0.0	86.0	32.3
5	17350.	275.	23.76	17.83	17.66	6.079	30.07	7.40	1.560	1.340	0.0	0.0	86.0	32.3
6	10960.	590.	30.00	20.55	7.53	9.120	30.07	5.40	1.525	1.300	0.0	0.0	87.0	32.3
6	12500.	535.	29.34	20.57	14.58	8.766	30.07	5.38	1.525	1.295	0.0	0.0	87.0	32.3
6	14020.	482.	28.91	20.58	11.75	8.329	30.07	6.37	1.540	1.315	0.0	0.0	87.0	32.3
6	15550.	428.	28.40	20.61	12.32	7.853	30.07	7.31	1.560	1.340	0.0	0.0	87.0	32.3
6	17030.	369.	28.93	20.69	16.48	7.331	30.07	8.12	1.560	1.340	0.0	0.0	87.0	32.3
6	18070.	326.	28.53	20.66	12.88	6.923	30.07	9.11	1.560	1.320	0.0	0.0	87.0	32.3

PERFORMANCE EVALUATION OF ICP RADIAL TURBINE

TABLE B5

OUTPUT DATA

CLEARANCE = 0.001 IN.

REDUCED TO STANDARD AIR IN ACCORDANCE WITH NASA METHOD.
 TOTAL INLET PRESS. = 14.7 PSIA, TOTAL INLET TEMPERATURE
 = 518.7 DEG.R., GAMMA = 1.4, CP = 0.24 RTU/LRM-DEG.F.

RUN/PT	PRESS RATIO	REF. SPEED RPM	REF. FLOW LB/SEC	HEAD				DEG REACT	ANGLE ALPHA DEG	ANGLE BETA DEG	VEL COEFF GV	LOSS COEFF GV	NO BEARING LOSSES				MAXIMUM REAPING LOSSES												
				COEFF	REACT	ALPHA	BETA						ANGLE	VEL COEFF	LOSS COEFF	ROTNR	EFFIC- TENCY	REF MM FT.LR	ANGLE DEG	VEL COEFF	LOSS COEFF	ROTNR	EFFIC- TENCY	REF MM FT.LR	ANGLE DEG	VEL COEFF	LOSS COEFF	ROTNR	EFFIC- TENCY
1	1	200	5559.	0.911	6.076	0.299	81.92	72.31	0.891	0.206	0.437	0.751	32.22	4.87	-32.22	0.751	4.87	5.15	-44.35	0.02	0.437	63.43	5.15	4.87	5.15	-44.35	0.02	0.437	63.43
1	1	201	7488.	0.846	3.362	0.345	81.92	58.53	0.890	0.208	0.532	0.775	32.21	3.97	-32.21	0.775	3.97	4.30	-18.17	0.09	0.532	73.24	4.30	3.97	4.30	-18.17	0.09	0.532	73.24
1	1	200	9497.	0.692	1.416	0.451	81.80	-73.37	0.886	0.224	0.672	0.776	79.21	1.64	79.21	0.776	1.64	2.16	53.59	0.95	0.672	58.73	2.16	1.64	2.16	53.59	0.95	0.672	58.73
1	1	200	13083.	0.588	1.100	0.578	81.77	-81.74	0.876	0.233	0.775	0.775	87.80	0.57	87.80	0.775	0.57	1.10	73.12	0.74	0.775	26.73	1.10	0.57	1.10	73.12	0.74	0.775	26.73
2	1	301	6908.	1.048	5.616	0.303	81.80	71.55	0.909	0.192	0.544	0.675	-12.73	6.49	-12.73	0.675	6.49	6.84	-34.40	0.82	0.544	63.93	6.84	6.49	6.84	-34.40	0.82	0.544	63.93
2	1	300	8917.	0.999	3.368	0.350	81.81	58.93	0.897	0.195	0.482	0.720	-27.42	5.57	-27.42	0.720	5.57	5.09	-11.91	0.92	0.482	74.32	5.09	5.57	5.09	-11.91	0.92	0.482	74.32
2	1	301	10818.	0.857	1.637	0.429	81.82	4.51	0.894	0.207	0.535	0.682	56.66	4.47	56.66	0.682	4.47	4.87	20.35	0.93	0.535	76.40	4.87	4.47	4.87	20.35	0.93	0.535	76.40
2	1	299	14752.	0.875	1.225	0.529	81.81	-63.77	0.884	0.218	0.597	0.635	70.27	3.16	70.27	0.635	3.16	3.65	45.91	0.91	0.597	48.58	3.65	3.16	3.65	45.91	0.91	0.597	48.58
2	1	299	15899.	0.674	1.056	0.717	81.80	-82.52	0.880	0.225	0.934	0.256	86.29	0.77	86.29	0.256	0.77	1.27	76.79	0.65	0.934	27.31	1.27	0.77	1.27	76.79	0.65	0.934	27.31
3	1	401	7986.	1.136	5.329	0.306	81.77	70.94	0.904	0.183	0.478	0.723	-17.20	8.02	-17.20	0.723	8.02	8.39	-34.33	0.85	0.478	56.47	8.39	8.02	8.39	-34.33	0.85	0.478	56.47
3	1	400	9950.	1.094	3.426	0.342	81.78	60.43	0.903	0.185	0.525	0.689	-34.22	6.87	-34.22	0.689	6.87	7.29	-0.33	0.90	0.525	73.76	7.29	6.87	7.29	-0.33	0.90	0.525	73.76
3	1	399	11889.	0.964	2.400	0.411	81.79	21.09	0.900	0.197	0.503	0.704	53.07	5.71	53.07	0.704	5.71	6.16	24.35	0.92	0.503	77.42	6.16	5.71	6.16	24.35	0.92	0.503	77.42
3	1	399	13857.	0.884	1.765	0.506	81.82	-55.25	0.896	0.204	0.553	0.668	74.38	4.35	74.38	0.668	4.35	4.81	63.75	0.87	0.553	63.87	4.81	4.35	4.81	63.75	0.87	0.553	63.87
4	1	499	9165.	1.206	4.818	0.313	81.72	69.46	0.908	0.176	0.402	0.773	-17.78	9.31	-17.78	0.773	9.31	9.68	-32.59	0.89	0.402	70.11	9.68	9.31	9.68	-32.59	0.89	0.402	70.11
4	1	500	11140.	1.164	3.264	0.352	81.76	58.14	0.906	0.179	0.465	0.732	-28.75	8.02	-28.75	0.732	8.02	8.43	-0.74	0.87	0.465	75.03	8.43	8.02	8.43	-0.74	0.87	0.465	75.03
4	1	500	13085.	1.111	2.366	0.413	81.79	19.47	0.904	0.183	0.503	0.705	54.20	6.69	54.20	0.705	6.69	7.12	31.82	0.86	0.503	77.94	7.12	6.69	7.12	31.82	0.86	0.503	77.94
4	1	500	15032.	1.049	1.794	0.493	81.79	-50.68	0.901	0.189	0.482	0.720	62.92	5.41	62.92	0.720	5.41	5.84	46.15	0.85	0.482	76.58	5.84	5.41	5.84	46.15	0.85	0.482	76.58
4	1	500	16896.	0.980	1.419	0.566	81.81	-71.70	0.897	0.195	0.492	0.713	70.95	4.09	70.95	0.713	4.09	4.53	59.28	0.80	0.492	59.76	4.53	4.09	4.53	59.28	0.80	0.492	59.76
5	1	598	9894.	1.253	4.744	0.317	81.68	69.12	0.911	0.171	0.398	0.776	-18.03	10.37	-18.03	0.776	10.37	10.74	-31.31	0.87	0.398	70.60	10.74	10.37	10.74	-31.31	0.87	0.398	70.60
5	1	598	12411.	1.195	3.673	0.339	81.69	63.04	0.910	0.172	0.425	0.758	-36.80	9.51	-36.80	0.758	9.51	9.88	-11.50	0.85	0.425	75.03	9.88	9.51	9.88	-11.50	0.85	0.425	75.03
5	1	599	12716.	1.157	2.874	0.379	81.74	48.09	0.907	0.178	0.467	0.730	30.37	8.08	30.37	0.730	8.08	8.43	13.32	0.85	0.467	79.06	8.43	8.08	8.43	13.32	0.85	0.467	79.06
5	1	599	14167.	1.111	2.316	0.430	81.76	-42.91	0.904	0.182	0.450	0.706	48.50	7.49	48.50	0.706	7.49	7.84	28.57	0.84	0.450	76.97	7.84	7.49	7.84	28.57	0.84	0.450	76.97
5	1	603	15679.	1.078	1.890	0.487	81.78	-62.29	0.903	0.185	0.473	0.726	66.68	6.53	66.68	0.726	6.53	6.94	45.73	0.87	0.473	74.95	6.94	6.53	6.94	45.73	0.87	0.473	74.95
6	1	698	10762.	1.297	4.490	0.320	81.63	68.01	0.913	0.167	0.388	0.782	-15.61	11.27	-15.61	0.782	11.27	11.63	-28.29	0.87	0.388	72.05	11.63	11.27	11.63	-28.29	0.87	0.388	72.05
6	1	698	12276.	1.266	3.449	0.350	81.65	60.55	0.912	0.168	0.436	0.751	-16.98	10.18	-16.98	0.751	10.18	10.56	-3.51	0.85	0.436	76.06	10.56	10.18	10.56	-3.51	0.85	0.436	76.06
6	1	698	13769.	1.219	2.742	0.388	81.71	44.20	0.910	0.174	0.404	0.772	32.88	9.24	32.88	0.772	9.24	9.58	12.68	0.88	0.404	79.58	9.58	9.24	9.58	12.68	0.88	0.404	79.58
6	1	700	15717.	1.162	2.228	0.438	81.74	-44.73	0.907	0.178	0.448	0.729	45.02	8.19	45.02	0.729	8.19	8.53	28.48	0.84	0.448	77.12	8.53	8.19	8.53	28.48	0.84	0.448	77.12
6	1	698	17732.	1.130	1.654	0.490	81.76	-60.98	0.905	0.181	0.490	0.714	64.85	6.21	64.85	0.714	6.21	6.59	46.79	0.83	0.490	75.12	6.59	6.21	6.59	46.79	0.83	0.490	75.12

PERFORMANCE EVALUATION OF ICP RADIAL TURPINE

TABLE B6

CLEARANCE = 0.061 IN.

INPUT DATA

RUN/PT	RPM	TORQUE COUNTS	P5P IN. HG	H1 IN. H2O	DPVC IN. HG	PATM IN. HG	HREF1 IN. HG	V4 MV	V5 MV	V20 MV	V21 MV	V22 MV	TRM DEG. F	TCJ DEG. F
1	5710.	179.	5.84	9.88	3.241	30.03	1.01	1.780	1.665	1.180	1.260	1.345	80.5	32.0
1	7200.	151.	5.84	12.64	2.986	30.03	1.00	1.805	1.695	1.170	1.280	1.340	81.0	32.0
1	8970.	125.	5.86	12.09	2.680	30.03	1.37	1.800	1.685	1.165	1.325	1.380	82.5	32.0
1	10000.	97.	5.90	8.92	2.320	30.03	2.75	1.800	1.685	1.185	1.375	1.450	83.5	32.0
1	11810.	63.	5.91	9.12	1.866	30.03	2.75	1.795	1.675	1.185	1.440	1.680	84.0	32.0
1	13660.	17.	5.95	10.10	1.254	30.03	3.53	1.805	1.675	1.205	1.505	1.915	84.0	32.0
2	7080.	266.	8.78	16.65	4.573	30.03	1.35	1.845	1.750	1.195	1.265	1.345	84.0	32.0
2	9050.	223.	8.80	13.68	4.176	30.03	2.69	1.855	1.760	1.230	1.395	1.400	84.0	32.0
2	10600.	177.	8.81	12.79	3.729	30.03	3.59	1.855	1.775	1.230	1.505	1.595	84.5	32.0
2	13050.	128.	8.84	13.00	3.125	30.03	3.59	1.865	1.785	1.230	1.505	1.895	84.5	32.0
2	15100.	170.	8.85	9.11	2.453	30.03	4.93	1.865	1.780	1.230	1.605	2.040	85.0	32.0
2	16740.	18.	8.91	12.80	1.706	30.03	5.70	1.855	1.770	1.290	1.690	2.095	85.0	32.0
3	8270.	348.	11.72	8.85	5.825	30.03	2.80	1.870	1.795	1.295	1.320	1.425	85.0	32.0
3	10330.	299.	11.73	18.12	5.399	30.03	3.30	1.835	1.775	1.275	1.315	1.445	85.0	32.0
3	12320.	243.	11.73	19.19	4.873	30.03	3.31	1.830	1.755	1.255	1.365	1.775	85.0	32.0
3	14320.	187.	11.79	9.265	4.261	30.03	5.10	1.820	1.750	1.295	1.495	1.925	84.5	32.0
3	16260.	131.	11.83	8.35	3.578	30.03	6.25	1.810	1.740	1.295	1.605	1.980	84.0	32.0
3	17940.	165.	11.88	12.41	2.744	30.03	7.24	1.805	1.725	1.305	1.705	2.190	84.0	32.0
4	9150.	425.	14.66	11.57	6.945	30.14	3.42	1.674	1.615	1.130	1.172	1.283	68.2	32.0
4	10400.	374.	14.69	18.05	6.554	30.14	3.42	1.715	1.662	1.163	1.273	1.506	69.8	32.0
4	12800.	317.	14.70	4.15	6.034	30.14	5.30	1.731	1.684	1.166	1.385	1.935	69.8	32.0
4	15060.	247.	14.72	11.61	5.455	30.14	6.01	1.750	1.703	1.255	1.588	2.029	70.1	32.0
4	17040.	186.	14.76	12.92	4.679	30.14	7.15	1.762	1.709	1.316	1.857	2.204	71.0	32.0
5	10100.	512.	17.61	12.54	8.042	30.14	4.29	1.774	1.729	1.318	1.304	1.512	71.0	32.0
5	11800.	467.	17.61	17.78	7.337	30.14	4.21	1.782	1.739	1.302	1.270	1.602	72.0	32.0
5	13000.	418.	17.64	11.10	7.337	30.14	5.40	1.786	1.745	1.304	1.345	1.792	72.0	32.0
5	14540.	370.	17.65	6.30	6.813	30.14	6.60	1.774	1.745	1.326	1.594	1.987	72.0	32.0
5	16070.	312.	17.69	7.67	6.332	30.14	7.65	1.765	1.737	1.345	1.685	2.020	72.0	32.0
5	17500.	262.	17.70	6.04	5.811	30.14	8.67	1.772	1.736	1.385	1.685	2.143	73.0	32.0
6	11000.	589.	20.52	10.47	9.063	30.10	5.32	1.828	1.779	1.275	1.159	1.472	76.0	32.0
6	12480.	549.	20.59	11.27	8.733	30.10	5.72	1.831	1.753	1.297	1.276	1.722	78.0	32.0
6	13990.	489.	20.59	14.79	8.341	30.10	6.24	1.831	1.753	1.350	1.391	1.883	78.0	32.0
6	15460.	437.	20.62	8.78	7.844	30.10	7.60	1.810	1.738	1.361	1.529	1.981	78.0	32.0
6	16970.	371.	20.63	5.83	7.218	30.10	8.99	1.801	1.722	1.376	1.699	2.058	78.0	32.0
6	17950.	337.	20.66	15.42	6.933	30.10	9.00	1.784	1.718	1.376	1.707	2.140	78.0	32.0

PERFORMANCE EVALUATION OF ICP RADIAL TURBINE

TABLE B7

OUTPUT DATA

CLEARANCE = 0.061 IN.

REDUCED TO STANDARD AIR IN ACCORDANCE WITH NASA METHOD.
TOTAL INLET PRESS. = 14.7 PSIA; TOTAL INLET TEMPERATURE
= 518.7 DEG.R.; GAMMA = 1.4; CP = 0.24 BTU/LBM-DEG.F.

RUN/PT	PRESS RATIO	REF. SPEED RPM	REF. FLOW LBS/SEC	HEAD COEFF	DEG REACT	ANGLE ALPH1 DEG	ANGLE BETAI DEG	VEL COEFF GV	LOSS COEFF GV	NO BEARING LOSSES					MAXIMUM BEARING LOSSES				
										REF MOM FT.LB	ANGLE ALF20 DEG	VEL COEFF	LOSS ROTOR	EFFIC- IENCY	REF MOM FT.LB	ANGLE ALF20 DEG	VEL COEFF	LOSS ROTOR	EFFIC- IENCY
1	1.200	5544.	0.911	6.108	0.303	81.53	71.93	0.802	0.187	4.87	-27.34	0.716	0.499	63.25	5.14	-43.27	0.885	0.215	67.12
1	1.199	6984.	0.874	3.841	0.337	81.53	63.34	0.971	0.189	4.12	31.14	0.638	0.593	70.33	4.51	-18.65	0.843	0.209	67.92
1	1.199	8413.	0.827	2.649	0.353	81.53	37.25	0.899	0.192	3.41	58.11	0.617	0.620	74.15	3.83	7.62	0.843	0.179	76.86
1	1.200	9997.	0.769	1.921	0.478	81.52	-40.46	0.896	0.205	2.65	68.51	0.519	0.730	72.03	3.14	25.64	0.978	0.163	76.68
1	1.200	11463.	0.694	1.429	0.586	81.51	-72.52	0.892	0.207	1.73	77.27	0.519	0.730	61.42	2.26	46.93	0.978	0.163	76.68
1	1.200	13259.	0.563	1.070	0.724	81.48	-82.27	0.885	0.217	0.49	87.15	0.192	0.963	24.42	1.03	70.57	0.730	0.377	61.58
2	1.200	6856.	1.044	5.687	0.306	81.51	71.28	0.910	0.173	6.50	-11.79	0.658	0.567	64.00	6.85	-34.25	0.810	0.244	67.44
2	1.300	8761.	0.997	3.483	0.350	81.52	61.15	0.905	0.175	5.60	29.28	0.685	0.531	73.77	6.02	-11.15	0.890	0.208	70.25
2	1.299	10702.	0.941	2.331	0.427	81.53	12.84	0.905	0.180	4.25	59.93	0.643	0.586	75.99	4.92	24.22	0.893	0.182	84.05
2	1.299	12623.	0.859	1.676	0.529	81.53	-60.49	0.901	0.188	3.21	69.43	0.616	0.621	71.33	3.72	44.77	0.904	0.154	85.80
2	1.299	14608.	0.760	1.249	0.646	81.52	-77.96	0.895	0.199	1.78	80.44	0.462	0.786	51.33	2.28	60.12	0.804	0.154	85.80
2	1.299	16200.	0.633	1.017	0.756	81.50	-83.36	0.889	0.211	0.48	87.17	0.195	0.962	19.25	0.98	77.89	0.605	0.334	67.15
3	1.400	7997.	1.139	5.306	0.313	81.47	70.40	0.915	0.163	8.00	-11.60	0.681	0.537	66.30	8.37	-31.47	0.912	0.341	69.37
3	1.399	9898.	1.096	3.458	0.352	81.49	60.09	0.913	0.166	5.83	39.56	0.634	0.598	72.92	7.25	-5.35	0.799	0.362	70.46
3	1.399	11831.	1.040	2.418	0.424	81.50	21.69	0.913	0.171	5.67	56.61	0.645	0.585	76.37	6.43	28.93	0.833	0.306	81.64
3	1.399	13769.	0.970	1.788	0.512	81.52	-52.32	0.907	0.185	4.37	67.42	0.623	0.611	73.21	4.83	28.08	0.859	0.262	84.74
3	1.400	15749.	0.887	1.368	0.601	81.53	-73.90	0.893	0.196	3.06	74.07	0.618	0.618	64.28	3.53	60.30	0.859	0.262	84.74
3	1.400	17385.	0.774	1.123	0.704	81.52	-81.14	0.896	0.216	1.53	82.04	0.424	0.820	40.58	1.99	73.24	0.693	0.520	69.74
4	1.498	8897.	1.201	5.105	0.316	81.43	69.85	0.919	0.156	9.05	-0.07	0.646	0.593	66.56	9.42	-22.26	0.759	0.423	69.27
4	1.498	10719.	1.165	3.544	0.349	81.47	61.01	0.918	0.158	7.92	44.05	0.674	0.575	72.47	8.32	-16.20	0.727	0.423	70.25
4	1.498	12594.	1.117	2.591	0.408	81.47	33.55	0.915	0.162	6.65	62.85	0.674	0.575	74.66	7.08	16.96	0.727	0.423	70.25
4	1.497	14603.	0.980	1.891	0.456	81.52	-41.89	0.912	0.169	5.26	69.70	0.571	0.677	65.98	5.69	56.09	0.743	0.423	70.25
4	1.497	16520.	0.880	1.478	0.456	81.52	-69.87	0.908	0.176	3.94	74.55	0.568	0.677	65.98	4.37	64.43	0.743	0.423	70.25
5	1.597	9785.	1.255	4.844	0.326	81.39	68.90	0.931	0.151	10.31	-12.56	0.715	0.489	69.42	10.67	-27.92	0.815	0.337	70.88
5	1.597	11138.	1.226	3.736	0.349	81.40	62.91	0.931	0.152	9.37	21.43	0.677	0.489	73.37	9.77	-2.91	0.769	0.337	70.88
5	1.597	12590.	1.196	2.926	0.385	81.45	50.01	0.919	0.154	8.35	46.57	0.677	0.489	75.91	8.75	24.36	0.769	0.337	70.88
5	1.597	14080.	1.158	2.338	0.433	81.45	15.69	0.915	0.158	7.35	65.43	0.652	0.575	77.45	7.75	39.29	0.769	0.337	70.88
5	1.597	15566.	1.108	1.914	0.458	81.45	-40.47	0.915	0.163	6.14	65.43	0.652	0.575	77.45	6.54	52.64	0.769	0.337	70.88
5	1.597	16951.	1.061	1.613	0.548	81.49	-63.39	0.912	0.168	5.09	71.12	0.598	0.642	70.39	5.50	61.47	0.741	0.452	75.96
6	1.697	10641.	1.295	4.585	0.331	81.34	67.85	0.924	0.147	11.20	-10.79	0.727	0.471	71.31	11.56	-25.20	0.818	0.332	73.29
6	1.697	12074.	1.269	3.562	0.355	81.36	51.25	0.923	0.148	10.26	18.08	0.712	0.471	75.31	10.64	-22.79	0.818	0.332	73.29
6	1.698	13544.	1.200	2.833	0.394	81.38	39.04	0.922	0.151	9.27	38.04	0.705	0.501	78.31	9.63	17.98	0.818	0.332	73.29
6	1.698	14974.	1.154	2.321	0.439	81.41	13.46	0.920	0.154	8.25	49.77	0.657	0.568	79.38	8.63	33.12	0.818	0.332	73.29
6	1.697	16445.	1.125	1.921	0.456	81.45	-38.62	0.916	0.158	6.95	64.85	0.657	0.568	79.38	7.33	49.95	0.818	0.332	73.29
6	1.698	17396.	1.091	1.717	0.530	81.44	-56.71	0.916	0.161	6.28	64.84	0.656	0.557	74.45	6.56	54.50	0.818	0.332	73.29

PERFORMANCE EVALUATION OF ICP RADIAL TURBINE

TABLE B8

CLEARANCE = 0.041 IN.

INPUT DATA

RUN/PT	RPM	TORQUE COUNTS	P5P IN.HG	H1 IN.H2O	OPVC IN.HG	PATM IN.HG	HREF1 IN.HG	V4 MV	V5 MV	V20 MV	V21 MV	V22 MV	TRM DEG.F	ICJ DEG.F
1	1	171.	5.80	5.18	3.259	30.10	1.33	1.727	1.668	1.194	1.269	1.433	75.0	32.
1	2	144.	5.82	12.19	2.997	30.10	1.35	1.748	1.694	1.213	1.330	1.454	74.4	32.
1	3	120.	5.87	12.67	2.997	30.10	1.35	1.748	1.694	1.213	1.330	1.454	74.4	32.
1	4	90.	5.87	14.63	2.997	30.10	1.35	1.748	1.694	1.213	1.330	1.454	74.4	32.
1	5	63.	5.91	14.91	2.997	30.10	1.35	1.748	1.694	1.213	1.330	1.454	74.4	32.
1	6	12.	5.94	11.79	1.259	30.10	2.51	1.869	1.801	1.288	1.589	2.002	76.0	32.
2	1	261.	8.77	15.59	4.600	30.10	1.43	1.927	1.859	1.317	1.369	1.469	79.0	32.
2	2	231.	8.80	19.14	4.337	30.10	1.43	1.927	1.859	1.317	1.369	1.469	79.0	32.
2	3	198.	8.80	16.78	4.337	30.10	1.43	1.927	1.859	1.317	1.369	1.469	79.0	32.
2	4	163.	8.91	9.35	4.337	30.10	1.43	1.927	1.859	1.317	1.369	1.469	79.0	32.
2	5	127.	8.92	3.77	3.636	30.10	1.43	1.927	1.859	1.317	1.369	1.469	79.0	32.
2	6	88.	8.92	14.26	3.220	30.10	4.21	1.937	1.887	1.376	1.604	1.950	81.7	32.
2	7	40.	8.91	11.24	2.714	30.10	4.24	1.923	1.859	1.380	1.736	2.120	82.6	32.
3	1	350.	11.72	11.69	5.835	30.10	2.60	1.895	1.855	1.355	1.380	1.495	83.4	32.
3	2	311.	11.75	16.12	5.501	30.10	2.61	1.886	1.846	1.339	1.381	1.495	83.4	32.
3	3	261.	11.76	26.12	5.090	30.10	2.61	1.899	1.846	1.339	1.381	1.495	83.4	32.
3	4	197.	11.80	10.52	4.694	30.10	4.89	1.915	1.872	1.350	1.544	1.736	83.5	32.
3	5	137.	11.82	11.01	3.694	30.10	5.96	1.925	1.876	1.371	1.690	1.970	83.5	32.
3	6	68.	11.87	6.19	2.821	30.10	5.99	1.927	1.877	1.385	1.804	2.229	83.5	32.
4	1	433.	14.65	12.80	7.005	30.02	3.41	1.827	1.757	1.258	1.301	1.428	74.6	32.
4	2	386.	14.66	13.34	6.627	30.02	3.80	1.834	1.772	1.275	1.356	1.562	74.6	32.
4	3	344.	14.66	15.55	6.237	30.02	4.27	1.857	1.795	1.275	1.447	1.870	75.0	32.
4	4	292.	14.72	11.96	5.780	30.02	5.32	1.861	1.799	1.356	1.541	2.013	75.0	32.
4	5	243.	14.75	11.90	5.252	30.02	5.32	1.866	1.815	1.411	1.753	2.048	75.0	32.
4	6	197.	14.75	13.21	4.712	30.02	7.09	1.879	1.824	1.429	1.823	2.220	75.0	32.
4	7	169.	14.80	18.63	4.393	30.02	7.09	1.879	1.824	1.429	1.823	2.220	75.0	32.
5	1	510.	17.60	7.49	8.079	30.02	4.70	2.003	1.929	1.370	1.334	1.508	75.0	32.
5	2	475.	17.63	11.97	7.793	30.02	4.70	2.012	1.936	1.373	1.355	1.624	75.0	32.
5	3	430.	17.66	18.33	7.434	30.02	5.00	2.015	1.936	1.373	1.355	1.624	75.0	32.
5	4	380.	17.66	13.56	6.984	30.02	5.00	2.019	1.936	1.412	1.542	1.834	75.0	32.
5	5	328.	17.68	19.49	6.485	30.02	7.29	2.023	1.946	1.436	1.640	2.054	75.0	32.
5	6	272.	17.69	15.26	5.917	30.02	7.29	2.023	1.946	1.471	1.782	2.182	75.0	32.
6	1	595.	20.52	8.14	9.097	30.02	5.50	2.037	1.920	1.421	1.322	1.617	75.0	32.
6	2	548.	20.54	12.55	8.755	30.02	5.56	2.030	1.920	1.416	1.358	1.744	75.0	32.
6	3	498.	20.56	19.60	8.383	30.02	6.56	2.026	1.919	1.417	1.462	1.869	75.0	32.
6	4	439.	20.60	10.46	7.911	30.02	7.80	2.029	1.919	1.447	1.554	2.044	75.0	32.
6	5	381.	20.61	7.38	7.358	30.02	8.56	2.024	1.919	1.447	1.554	2.044	75.0	32.
6	6	340.	20.63	8.94	6.897	30.02	9.56	2.022	1.919	1.447	1.554	2.044	75.0	32.

PERFORMANCE EVALUATION OF ICP RADIAL TURBINE

TABLE B9

OUTPUT DATA

CLEARANCE = 0.041 IN.

REDUCED TO STANDARD AIR IN ACCORDANCE WITH NASA METHOD.
 TOTAL INLET PRESS. = 14.7 PSIA, TOTAL INLET TEMPERATURE
 = 518.7 DEG. R., GAMMA = 1.4, CP = 0.24 BTU/LBM-DEG. F.

RUN/PT	PRESS RATIO	REF. SPEED RPM	REF. FLOW LB/SEC	HEAD COEFF	DEG REACT	ANGLE ALPHA DEG	ANGLE BETA DEG	VEL COEFF GV	LOSS COEFF GV	NO BEARING LOSSES					MAXIMUM BEARING LOSSES				
										REF MOM FT.LB	ANGLE ALF20 DEG	VEL COEFF	LOSS COEFF ROTOR	EFFIC- ENCY	REF MOM FT.LB	ANGLE ALF20 DEG	VEL COEFF	LOSS COEFF ROTOR	EFFIC- ENCY
1	1.198	5602.	0.925	5.935	0.301	81.19	71.08	0.906	0.179	4.57	24.82	0.508	0.742	59.53	4.87	-19.07	0.691	0.537	63.26
1	1.198	7043.	0.876	3.765	0.341	81.20	61.87	0.905	0.181	3.94	62.57	0.459	0.790	66.18	4.22	15.66	0.710	0.496	72.85
1	1.199	8393.	0.835	2.681	0.356	81.19	-36.82	0.903	0.185	3.18	74.37	0.418	0.825	68.45	3.86	41.06	0.730	0.464	77.97
1	1.199	9849.	0.776	1.927	0.474	81.18	-70.88	0.896	0.197	2.37	81.27	0.378	0.891	64.52	2.86	58.76	0.730	0.464	77.97
1	1.199	11420.	0.704	1.438	0.577	81.18	-77.35	0.896	0.197	1.63	82.15	0.378	0.857	56.38	2.15	60.63	0.730	0.464	77.97
1	1.199	13304.	0.563	1.059	0.579	81.18	-77.35	0.896	0.197	0.24	-84.64	2.023	0.891	12.38	0.70	89.43	0.154	0.076	29.68
2	1.295	6910.	1.045	5.582	0.306	81.18	70.45	0.914	0.167	5.36	6.45	0.590	0.652	63.17	6.71	-25.29	0.743	0.478	66.62
2	1.299	8252.	1.015	3.921	0.336	81.18	63.63	0.913	0.170	5.73	37.45	0.597	0.689	68.20	6.35	-4.57	0.788	0.478	66.62
2	1.299	9654.	0.977	2.860	0.383	81.19	46.56	0.911	0.174	4.90	60.67	0.558	0.744	72.18	5.35	25.95	0.783	0.387	78.47
2	1.302	11200.	0.926	1.717	0.441	81.19	-33.67	0.906	0.179	4.01	72.33	0.506	0.782	71.81	4.49	49.14	0.751	0.415	77.24
2	1.302	12507.	0.871	1.341	0.518	81.19	-55.80	0.901	0.188	3.11	77.25	0.467	0.788	66.60	3.51	59.77	0.745	0.382	77.24
2	1.299	14101.	0.800	1.106	0.610	81.18	-74.33	0.896	0.197	2.14	80.03	0.461	0.944	56.60	2.64	65.70	0.745	0.382	77.24
2	1.299	15539.	0.697	1.106	0.706	81.18	-81.02	0.896	0.197	0.93	86.28	0.237	0.944	31.10	1.43	76.94	0.611	0.327	47.87
3	1.399	8050.	1.140	5.227	0.314	81.14	69.57	0.919	0.156	8.03	-11.87	0.687	0.527	67.05	8.40	-31.56	0.819	0.320	70.16
3	1.399	9664.	1.105	3.634	0.348	81.15	61.19	0.918	0.162	7.51	-28.22	0.664	0.555	73.31	7.51	-5.27	0.768	0.340	70.16
3	1.399	11339.	1.062	2.674	0.406	81.17	36.75	0.916	0.169	5.91	59.22	0.588	0.655	74.58	6.39	32.76	0.790	0.340	70.16
3	1.399	13448.	0.987	1.897	0.501	81.19	-43.72	0.917	0.177	4.53	75.38	0.576	0.655	72.00	4.90	42.59	0.812	0.340	70.16
3	1.399	15548.	0.901	1.327	0.566	81.19	-75.36	0.909	0.175	3.12	-89.32	0.112	0.987	39.62	1.98	86.60	0.469	0.340	51.61
4	1.499	8955.	1.208	5.084	0.321	81.10	68.96	0.923	0.148	9.36	-16.16	0.716	0.487	68.69	9.74	-31.83	0.829	0.313	71.42
4	1.499	10624.	1.175	3.589	0.356	81.13	60.37	0.922	0.150	8.32	22.96	0.690	0.524	74.52	8.73	-4.91	0.823	0.320	71.42
4	1.499	12352.	1.140	2.713	0.399	81.15	43.30	0.920	0.153	7.81	43.40	0.618	0.539	77.36	7.81	16.34	0.824	0.320	71.42
4	1.499	14997.	1.094	2.001	0.474	81.17	-49.31	0.915	0.162	6.23	61.80	0.635	0.597	74.59	6.67	50.20	0.835	0.320	71.42
4	1.499	17520.	0.985	1.365	0.513	81.18	-78.89	0.912	0.168	4.23	74.57	0.608	0.570	64.71	4.66	64.65	0.835	0.320	71.42
5	1.600	9851.	1.258	4.752	0.328	81.05	68.03	0.926	0.143	10.30	-8.95	0.697	0.515	69.47	10.57	-25.64	0.797	0.366	71.96
5	1.600	11072.	1.234	3.293	0.378	81.06	62.29	0.925	0.146	9.04	10.04	0.703	0.506	77.78	9.04	-12.76	0.825	0.366	71.96
5	1.600	13494.	1.166	2.373	0.430	81.11	51.73	0.922	0.154	7.67	36.50	0.708	0.540	79.36	7.67	12.76	0.835	0.366	71.96
5	1.600	15356.	1.122	1.972	0.486	81.13	-30.74	0.920	0.159	6.54	49.50	0.653	0.540	77.41	6.54	29.61	0.811	0.371	71.96
5	1.600	16818.	1.071	1.643	0.543	81.16	-60.48	0.917	0.159	5.42	67.02	0.653	0.573	73.41	5.83	43.83	0.793	0.371	71.96
6	1.699	10711.	1.296	4.534	0.332	81.00	66.99	0.928	0.139	11.46	-16.81	0.765	0.415	72.50	11.76	-29.20	0.855	0.269	74.80
6	1.699	13069.	1.242	3.271	0.359	81.02	60.54	0.926	0.143	10.46	28.91	0.744	0.446	78.01	10.46	-8.46	0.860	0.269	74.80
6	1.699	14993.	1.205	2.315	0.439	81.08	47.04	0.924	0.146	8.97	47.09	0.755	0.473	80.28	8.97	8.46	0.860	0.269	74.80
6	1.699	16369.	1.160	1.941	0.493	81.11	-34.24	0.922	0.154	7.63	56.60	0.706	0.501	78.17	7.63	29.87	0.819	0.269	74.80
6	1.698	17437.	1.122	1.711	0.534	81.13	-56.17	0.920	0.154	6.44	60.00	0.719	0.493	77.07	6.44	48.03	0.835	0.269	74.80

PERFORMANCE EVALUATION OF ICP RADIAL TURBINE

TABLE B10

INPUT DATA
CLEARANCE = 0.024 IN.

RUN/PT	RPM	TORQUE COUNTS	P5P IN.HG	H1 IN.H2O	DPVC IN.HG	PATM IN.HG	HREF1 IN.HG	V4 MV	V5 MV	V20 MV	V21 MV	V22 MV	TRM DEG.F	TCJ DEG.F
1	5770.	175.	9.10	23.48	3.306	30.11	0.0	1.809	1.739	1.234	1.287	1.462	80.0	32.0
1	7010.	152.	8.90	25.71	3.071	30.11	0.0	1.837	1.766	1.249	1.332	1.496	80.9	32.0
1	8510.	126.	8.62	25.34	2.797	30.11	0.0	1.838	1.768	1.262	1.393	1.492	81.0	32.0
1	10040.	94.	8.24	37.44	2.413	30.11	0.0	1.824	1.754	1.278	1.443	1.593	81.0	32.0
1	11600.	65.	5.88	45.66	2.008	30.11	0.0	1.836	1.763	1.301	1.510	1.783	81.0	32.0
1	13730.	14.	5.93	59.93	1.239	30.11	0.0	1.812	1.739	1.310	1.571	1.980	80.	32.0
2	7170.	265.	13.38	35.06	4.641	30.11	0.0	1.862	1.796	1.300	1.345	1.419	79.9	32.0
2	8500.	236.	13.12	38.55	4.377	30.11	0.0	1.869	1.801	1.304	1.379	1.442	80.0	32.0
2	10000.	202.	12.15	44.76	4.056	30.11	0.0	1.876	1.796	1.309	1.408	1.527	80.0	32.0
2	11450.	166.	12.45	52.56	3.691	30.11	0.0	1.876	1.806	1.339	1.482	1.772	80.0	32.0
2	13000.	128.	12.01	62.11	3.238	30.11	0.0	1.889	1.821	1.377	1.574	1.971	80.0	32.0
2	14630.	94.	11.54	72.67	2.726	30.11	0.0	1.908	1.833	1.399	1.650	2.066	80.0	32.0
2	16520.	28.	10.67	89.40	1.805	30.11	0.0	1.937	1.848	1.411	1.764	2.160	80.	32.0
3	8370.	353.	17.59	46.95	5.899	30.11	0.0	1.970	1.888	1.399	1.426	1.515	80.5	32.0
3	9950.	314.	17.67	52.75	5.483	30.11	0.0	1.986	1.909	1.388	1.431	1.515	80.5	32.0
3	11520.	272.	17.28	14.42	5.155	30.11	0.0	1.996	1.934	1.405	1.452	1.554	80.5	32.0
3	12510.	244.	17.05	21.20	4.887	30.11	0.0	2.001	1.946	1.415	1.500	1.584	80.5	32.0
3	13990.	202.	16.52	32.20	4.438	30.11	0.0	2.013	1.956	1.440	1.595	1.944	80.5	32.0
3	15340.	160.	16.02	42.55	3.929	30.11	0.0	2.008	1.960	1.455	1.680	2.065	80.5	32.0
3	17030.	110.	15.84	19.71	3.297	30.11	0.0	2.012	1.959	1.475	1.794	2.233	79.9	32.0
3	18250.	162.	14.68	33.07	2.649	30.11	0.0	2.015	1.952	1.488	1.884	2.306	79.8	32.0
4	9310.	437.	21.82	13.06	7.047	30.10	3.40	1.745	1.651	1.191	1.262	1.366	80.7	32.0
4	10810.	398.	21.42	11.38	6.763	30.10	3.89	1.872	1.777	1.252	1.346	1.528	80.5	32.0
4	12310.	354.	21.12	16.86	6.393	30.10	4.84	1.903	1.812	1.286	1.392	1.688	79.9	32.0
4	13840.	307.	20.60	11.65	5.941	30.10	5.28	1.936	1.851	1.354	1.459	1.787	79.8	32.0
4	15310.	258.	20.30	19.59	5.431	30.10	6.30	1.957	1.865	1.637	1.387	1.915	80.0	32.0
4	16800.	212.	19.62	11.59	4.875	30.10	7.03	1.959	1.874	1.427	1.752	2.218	79.9	32.0
4	18380.	155.	19.02	10.43	4.202	30.10	8.21	1.963	1.874	1.446	1.857	2.297	79.9	32.0
5	10350.	525.	25.80	8.70	8.170	30.10	4.60	1.982	1.887	1.386	1.367	1.528	79.1	32.0
5	12070.	470.	25.48	7.82	7.777	30.10	5.16	1.977	1.886	1.397	1.392	1.690	79.0	32.0
5	13500.	424.	25.10	9.65	7.393	30.10	5.80	1.975	1.880	1.420	1.487	1.886	79.0	32.0
5	15030.	368.	24.60	6.71	6.892	30.10	6.95	1.971	1.889	1.450	1.599	1.987	79.0	32.0
5	16510.	314.	24.10	6.58	6.327	30.10	7.92	1.971	1.891	1.477	1.699	2.152	78.1	32.0
5	18090.	260.	23.51	7.56	5.716	30.10	8.85	1.970	1.899	1.477	1.818	2.240	78.1	32.0
6	12200.	605.	29.80	10.44	9.214	30.04	5.30	1.968	1.902	1.437	1.370	1.655	76.0	32.0
6	14000.	559.	29.50	19.76	8.884	30.04	5.80	1.971	1.902	1.426	1.396	1.707	76.3	32.0
6	15550.	509.	29.10	19.16	8.490	30.04	6.32	1.966	1.896	1.435	1.456	1.819	76.3	32.0
6	17000.	448.	28.61	12.20	7.971	30.04	7.45	1.970	1.890	1.446	1.557	1.953	77.0	32.0
6	18030.	389.	28.02	16.59	7.391	30.04	8.85	1.970	1.887	1.471	1.673	2.053	77.0	32.0
6	18030.	349.	27.62	10.80	6.986	30.04	9.40	1.960	1.883	1.471	1.739	2.149	77.1	32.0

PERFORMANCE EVALUATION OF ICP RADIAL TURBINE

TABLE B11

OUTPUT DATA

CLEARANCE = 0.024 IN.

REDUCED TO STANDARD AIR IN ACCORDANCE WITH NASA METHOD:
 TOTAL INLET PRESS. = 14.7 PSIA, TOTAL INLET TEMPERATURE
 = 518.7 DEG.R., $G_{A,STD} = 1.4$, $C_p = 0.24$ BTU/LBM-DEG.F.

RUN/PT	PRESS	REF. SPEED RPM	REF. FLOW LB/SEC	HEAD COEFF	DEG REACT	ANGLE ALPHA DEG	ANGLE BETA DEG	VEL COEFF GV	LOSS COEFF GV	NO BEARING LOSSES					MAXIMUM BEARING LOSSES				
										REF MOM FT.LB	ANGLE ALF20 DEG	VEL COEFF	LOSS ROTOR	EFFIC- IENCY	REF MOM FT.LB	ANGLE ALF20 DEG	VEL COEFF	LOSS ROTOR	EFFIC- IENCY
1	1	199	0.920	5.997	0.302	80.88	70.62	0.910	0.171	4.71	2.27	0.578	0.665	61.15	5.00	-30.67	0.750	0.437	64.97
1	1	200	0.886	4.075	0.329	80.88	63.81	0.910	0.173	4.08	51.91	0.510	0.740	66.73	4.46	0.08	0.749	0.439	72.85
1	1	199	0.845	2.760	0.376	80.87	48.91	0.904	0.182	3.38	78.50	0.398	0.834	70.39	3.82	52.88	0.784	0.416	78.56
1	1	199	0.784	1.982	0.476	80.87	-31.91	0.904	0.182	2.50	81.36	0.382	0.854	66.42	3.99	51.59	0.763	0.417	78.56
1	1	199	0.715	1.485	0.577	80.86	-68.99	0.900	0.189	1.72	81.36	0.382	0.854	57.60	2.23	58.65	0.814	0.337	75.17
1	1	199	0.560	1.058	0.749	80.82	-82.38	0.891	0.205	0.33	81.36	0.102	0.990	16.60	0.87	74.67	0.671	0.550	44.17
2	2	6933	1.051	5.540	0.307	80.86	69.78	0.918	0.157	6.51	-5.21	0.636	0.595	64.60	6.86	-30.98	0.789	0.378	68.18
2	2	6933	1.020	3.949	0.336	80.86	63.17	0.915	0.162	5.88	25.62	0.640	0.591	71.17	5.47	-12.98	0.823	0.316	76.18
2	2	6933	0.980	2.853	0.388	80.87	45.31	0.913	0.167	5.02	25.62	0.602	0.609	74.40	5.47	-16.25	0.823	0.316	76.18
2	2	6933	0.934	2.176	0.453	80.88	-67.19	0.909	0.173	4.17	69.90	0.555	0.679	73.37	4.50	40.03	0.806	0.352	81.86
2	2	6933	0.874	1.686	0.533	80.88	-57.81	0.909	0.173	3.17	75.90	0.530	0.719	68.13	4.50	40.03	0.806	0.352	81.86
2	2	6933	0.800	1.335	0.617	80.88	-74.41	0.909	0.181	2.31	81.36	0.530	0.666	61.30	2.81	56.20	0.897	0.347	74.61
2	2	6933	0.650	1.047	0.750	80.85	-82.41	0.897	0.195	0.65	81.36	0.259	0.933	24.13	1.11	75.53	0.645	0.585	42.61
3	3	8071	1.148	5.192	0.314	80.82	68.90	0.923	0.147	8.14	-15.30	0.707	0.501	67.95	8.51	-33.31	0.838	0.298	71.68
3	3	8071	1.107	3.749	0.352	80.85	62.86	0.922	0.150	7.21	20.95	0.682	0.535	73.83	7.62	-13.70	0.837	0.299	76.50
3	3	8071	1.073	2.682	0.392	80.86	42.91	0.921	0.153	6.21	20.95	0.628	0.587	70.03	6.13	-20.46	0.829	0.312	81.32
3	3	8071	1.045	2.036	0.436	80.87	13.91	0.916	0.161	5.65	51.20	0.626	0.609	74.88	5.45	30.56	0.852	0.313	82.78
3	3	8071	0.993	1.868	0.458	80.88	-41.50	0.913	0.167	4.69	69.90	0.631	0.677	69.86	4.15	54.63	0.852	0.313	82.78
3	3	8071	0.933	1.517	0.567	80.88	-66.63	0.908	0.175	3.62	76.38	0.568	0.677	57.34	2.98	54.63	0.852	0.313	82.78
3	3	8071	0.853	1.260	0.648	80.87	-76.63	0.908	0.184	2.52	81.76	0.568	0.677	38.11	1.86	72.77	0.852	0.313	82.78
3	3	8071	0.761	1.100	0.726	80.87	-81.22	0.903	0.184	1.40	81.76	0.427	0.918	24.13	1.86	72.77	0.852	0.313	82.78
4	4	9042	1.211	4.954	0.321	80.78	68.12	0.927	0.140	9.37	-12.73	0.707	0.500	69.19	9.74	-29.70	0.820	0.327	71.95
4	4	9042	1.184	3.704	0.347	80.79	61.37	0.926	0.145	8.50	20.95	0.687	0.528	74.26	8.91	-14.30	0.818	0.332	77.80
4	4	9042	1.151	2.854	0.390	80.83	46.46	0.925	0.149	7.53	44.69	0.663	0.560	77.51	8.79	-18.30	0.818	0.332	77.80
4	4	9042	1.109	2.264	0.445	80.85	27.31	0.923	0.154	6.54	51.20	0.646	0.569	76.25	6.95	30.56	0.818	0.332	77.80
4	4	9042	1.058	1.853	0.503	80.86	-42.75	0.920	0.159	5.51	69.90	0.656	0.569	72.25	5.94	46.27	0.818	0.332	77.80
4	4	9042	1.000	1.541	0.560	80.86	-64.75	0.917	0.166	4.42	81.76	0.665	0.558	61.83	4.69	55.27	0.818	0.332	77.80
4	4	9042	0.927	1.287	0.631	80.88	-75.26	0.913	0.166	3.27	81.76	0.665	0.558	42.61	3.69	64.27	0.818	0.332	77.80
5	5	9975	1.263	4.671	0.327	80.73	67.07	0.930	0.135	10.53	-15.90	0.749	0.439	71.66	10.90	-29.88	0.850	0.285	74.18
5	5	9975	1.230	3.474	0.355	80.75	60.66	0.928	0.140	9.47	18.27	0.730	0.467	76.97	9.86	-12.93	0.845	0.285	74.18
5	5	9975	1.200	2.746	0.400	80.77	42.91	0.925	0.144	8.51	44.69	0.663	0.477	79.38	8.91	-14.30	0.845	0.285	74.18
5	5	9975	1.157	2.135	0.454	80.80	27.31	0.923	0.148	7.53	51.20	0.646	0.516	77.08	8.79	-18.30	0.845	0.285	74.18
5	5	9975	1.107	1.853	0.508	80.83	-42.75	0.920	0.153	6.54	69.90	0.656	0.516	72.25	6.95	30.56	0.845	0.285	74.18
5	5	9975	1.051	1.541	0.565	80.85	-65.26	0.920	0.153	5.51	81.76	0.665	0.516	42.61	5.50	55.27	0.845	0.285	74.18
6	6	10813	1.306	4.450	0.330	80.69	66.11	0.932	0.131	11.53	-16.00	0.773	0.403	73.46	11.89	-28.51	0.864	0.254	75.77
6	6	10813	1.282	3.569	0.358	80.72	60.05	0.932	0.132	10.61	10.07	0.746	0.443	76.96	10.90	-12.93	0.864	0.254	75.77
6	6	10813	1.251	2.859	0.388	80.76	43.70	0.931	0.138	9.69	28.56	0.757	0.427	80.97	10.90	-12.93	0.864	0.254	75.77
6	6	10813	1.211	2.316	0.442	80.81	27.31	0.928	0.142	8.50	51.20	0.646	0.461	79.59	9.86	-12.93	0.864	0.254	75.77
6	6	10813	1.163	1.937	0.493	80.85	-42.75	0.926	0.145	7.53	69.90	0.656	0.461	72.25	8.91	30.56	0.864	0.254	75.77
6	6	10813	1.130	1.721	0.533	80.81	-53.92	0.924	0.145	6.56	81.76	0.665	0.461	42.61	8.91	30.56	0.864	0.254	75.77

PERFORMANCE EVALUATION OF ICP RADIAL TURBINE

CLEARANCE = 0.015 IN.

TABLE B12

INPUT DATA

RUN/PT	RPM	TORQUE COUNTS	PUVC IN.HG	P5P IN.HG	H1 IN.H2O	DPVC IN.HG	PATM IN.HG	HREF1 IN.HG	V4 MV	V5 MV	V20 MV	V21 MV	V22 MV	IPM DEG. F	ICJ DEG. F
1	5790.	178.	9.10	5.83	23.53	3.295	30.16	0.0	1.841	1.759	1.163	1.250	1.422	79.0	32.0
1	7480.	147.	8.82	5.86	27.09	2.970	30.16	0.0	1.851	1.767	1.180	1.311	1.417	79.1	32.0
1	9030.	118.	8.50	5.89	33.01	2.659	30.16	0.0	1.848	1.772	1.199	1.378	1.457	79.2	32.0
1	10490.	84.	8.16	5.90	39.93	2.283	30.16	0.0	1.857	1.783	1.227	1.444	1.411	79.8	32.0
1	12050.	54.	7.73	5.91	47.79	1.869	30.16	0.0	1.869	1.788	1.243	1.496	1.820	79.8	32.0
1	13700.	11.	7.15	5.94	60.55	1.201	30.16	0.0	1.865	1.775	1.247	1.534	1.957	79.7	32.0
2	7190.	266.	13.43	8.79	35.28	4.671	30.16	0.0	1.896	1.836	1.264	1.326	1.390	78.0	32.0
2	8960.	227.	13.07	8.80	40.36	4.285	30.16	0.0	1.900	1.840	1.268	1.369	1.455	78.0	32.0
2	10500.	190.	12.65	8.81	47.34	3.940	30.16	0.0	1.908	1.840	1.283	1.421	1.571	77.9	32.0
2	11200.	153.	12.32	8.82	56.00	3.533	30.16	0.0	1.909	1.839	1.295	1.471	1.790	78.0	32.0
2	13440.	119.	11.91	8.83	12.60	3.103	30.16	3.81	1.911	1.840	1.310	1.544	1.948	78.0	32.0
2	14960.	77.	11.36	8.86	24.19	2.523	30.16	3.81	1.913	1.838	1.319	1.620	2.083	78.1	32.0
2	16720.	15.	10.54	8.91	21.19	1.612	30.16	3.81	1.914	1.835	1.333	1.733	2.210	78.1	32.0
3	8370.	356.	17.64	11.72	7.79	5.929	30.16	2.90	1.928	1.862	1.335	1.391	1.446	78.5	32.0
3	10490.	300.	17.17	11.73	15.54	5.444	30.16	2.90	1.929	1.864	1.319	1.397	1.551	78.6	32.0
3	12490.	243.	16.66	11.76	27.28	4.931	30.16	2.90	1.929	1.868	1.320	1.459	1.817	79.0	32.0
3	14600.	182.	16.03	11.80	22.21	4.230	30.16	4.32	1.908	1.861	1.329	1.552	2.017	79.0	32.0
3	16050.	128.	15.31	11.82	22.69	3.517	30.16	5.34	1.889	1.838	1.355	1.673	2.168	79.0	32.0
3	18050.	60.	14.49	11.89	20.46	2.637	30.16	6.92	1.864	1.817	1.358	1.762	2.272	78.5	32.0
4	9410.	442.	21.85	14.70	17.76	7.131	30.13	3.02	1.871	1.836	1.330	1.343	1.482	78.1	32.0
4	1090.	392.	21.54	14.74	12.93	6.765	30.13	3.83	1.864	1.838	1.321	1.322	1.619	78.0	32.0
4	13010.	336.	21.00	14.77	12.72	6.290	30.13	5.81	1.851	1.820	1.315	1.371	1.838	78.0	32.0
4	15000.	272.	20.40	14.79	14.93	5.589	30.13	5.70	1.838	1.796	1.331	1.529	1.984	78.5	32.0
4	17000.	209.	19.61	14.83	15.07	4.817	30.13	6.97	1.837	1.793	1.347	1.632	2.044	77.5	32.0
4	18100.	165.	19.11	14.87	10.86	4.277	30.13	8.08	1.836	1.793	1.360	1.702	2.174	77.2	32.0
5	10320.	534.	26.04	17.72	13.79	8.310	30.21	4.20	1.938	1.834	1.238	1.277	1.463	69.1	32.0
5	12040.	477.	25.63	17.75	10.23	7.902	30.21	5.00	1.972	1.873	1.285	1.354	1.652	71.0	32.0
5	13520.	428.	25.28	17.77	8.49	7.506	30.21	5.88	1.986	1.886	1.327	1.460	1.893	72.5	32.0
5	15060.	372.	24.77	17.80	10.91	6.957	30.21	6.63	1.980	1.891	1.357	1.570	2.011	73.5	32.0
5	16500.	317.	24.20	17.82	11.91	6.398	30.21	7.53	1.989	1.896	1.372	1.641	2.049	73.1	32.0
5	17980.	266.	23.70	17.83	11.45	5.839	30.21	8.75	1.986	1.895	1.400	1.779	2.256	73.0	32.0
6	12390.	611.	30.08	20.69	7.64	9.376	30.21	5.49	2.145	2.048	1.347	1.345	1.532	70.8	32.0
6	14020.	571.	29.80	20.72	8.89	8.094	30.21	5.87	2.145	2.054	1.355	1.357	1.701	70.0	32.0
6	15530.	455.	28.90	20.74	8.16	8.665	30.21	6.56	2.145	2.056	1.373	1.450	1.883	69.5	32.0
6	16980.	396.	28.29	20.78	8.28	8.133	30.21	7.62	2.136	2.052	1.393	1.550	2.010	69.0	32.0
6	18150.	351.	27.80	20.81	11.95	7.105	30.21	9.35	2.134	2.050	1.414	1.733	2.213	69.5	32.0

CLEARANCE = 0.015 IN.

[illegible]

APPENDIX C

PROGRAM NOSPD

Program NOSPD calculates the referred moments and referred flow rates for the stopped-rotor tests and is in essence a much simplified version of program RADIAL. The computational techniques used are the same in both programs and will not be repeated. Program NOSPD is listed in Table C1, and the input and output data are given in Table C2. Table B3 lists the torque calibration data used for each run. The items of input data defined in the preceding section apply to this program, except as noted below.

<u>Card No.</u>	<u>FORTRAN</u>	<u>Description</u>
1	NRUNS	Number of runs (clearances) to be processed
2	CLNC	
3	TCD	
4	NPTS	
5	V4, V5, TCJ, PATM, P5P, DPVC, TQ, TRM	

TABLE C1
LISTING OF PROGRAM NOSPD

```

C PROGRAM NOSPD.
C CALCULATES REFERRED MOMENTS AND REFERRED FLOW RATES FOR
C STOPPED-ROTOR TESTS.
C
C DIMENSION V4(10),V5(10),TCJ(10),PATM(10),P5P(10),DPVC(10),PUVC(10)
C *,TO(10),TRM(10),TCD(50)
C WRITE HEADING FOR OUTPUT.
C WRITE(6,1)
C 1 FORMAT(1H1,///,T38,'PERFORMANCE EVALUATION OF ICP RADIAL TURBINE',
C *///,T56,'TABLE',///,T47,'RESULTS OF ZERO-SPEED TESTS',///,T40,'INPUT
C * DATA',T97,'OUTPUT DATA',///,T99,'REF.',T109,'REF.',T115,'V4',T23,
C *,'V5',T31,'TCJ',PATM,P5P,DPVC,PUVC,TORQUE,TRM,T90
C *,'PRESS.',MOMENT,IN.HG,IN.HG,COUNTS,DEG.F
C *,'IN.HG',IN.HG,IN.HG,IN.HG,RATIO,FT.LB
C *,'LBM/SEC',/)
C WRITE(6,103)
C 103 FORMAT(12,'-----')
C *
C READ INPUT DATA.
C READ(5,2) NRUNS
C 2 FORMAT(14)
C DO 3 N=1,NRUNS
C READ(5,4) CLNC
C 4 FORMAT(5.3)
C READ(5,5) (TCD(I),I=1,5)
C 5 FORMAT(5F7.1)
C WRITE HEADING FOR RUN.
C WRITE(6,6) CLNC
C 6 FORMAT(//,T40,'RUN',T61,'CLEARANCE = ',F5.3,/)
C READ(5,2) NPTS
C DO 7 K=1,NPTS
C READ(5,8) V4(K),V5(K),TCJ(K),PATM(K),P5P(K),DPVC(K),PUVC(K),TO(K),
C *TRM(K)
C 8 FORMAT(9F8.4)
C PROCESS DATA POINT.
C GHG=13.639C5-1.363030E-3*TRM(K)
C CF1=7C.438824*GHG/13.54
C CALL TEMP (V4(K),V5(K),TCJ(K),T4,T5)
C CALL FLOW (DPVC(K),PUVC(K),GHG,T4,WVC)
C CALL PRESS(T5,PATM(K),P5P(K),GHG,CF1,WVC,PR2,PTO)
C CALL EDC (T5,PR2,GAM,EXP,CP,THETA)
C CALL TORQ (TCD,TQ(K),TNET)
C CALL REFER (PTO,GHG,GAM,THETA,TNET,WVC,WVCR,TNETR)
C WRITE INPUT DATA AND RESULTS FOR THE DATA POINT.
C WRITE(6,10) K,V4(K),V5(K),TCJ(K),PATM(K),P5P(K),DPVC(K),PUVC(K),TO

```

```

*(K),TRM(K),PR2,INEIR,WVCR
10 FORMAT(2X,I4,4X,2F8.3,3F8.2,F9.3,F8.2,F7.0,F7.1,6X,F7.3,F8.2,F10.3
*)
7 CONTINUE
IF(N.EQ.NRUNS) GO TO 100
GO TO 3
100 WRITE(6,101)
101 FORMAT(1H1)
103 CONTINUE
RETURN
END

```

```

SUBROUTINE TEMP (V4,V5,ICJ,T4,T5)
V=V4
J=1
100 T=ICJ+0.144+35.77*V-0.4518*V**2
IF(T-100.1102,102,101)
101 T=ICJ+1.252+34.86*V-0.1855*V**2
102 T=T+459.69
103 IF(J-1) 103,103,104
J=2
T4=T
V=V5
GO TO 100
104 T5=T
RETURN
END

```

```

SUBROUTINE FLOW(DPVC, FUV, PATM, GHG, T4, WVC)
DVC=DPVC*GHG/13.54
PVC=(PUVC+PATM)*GHG/13.54
A=1.+1.85E-5*(T4-532.)
Z=1.9+2.4E-3*(T4-560.)
Y=1.-.351*DVC/PVC
WVC=2.2854*A*Y*SQR(T(PVC*DVC/T4))
X=WVC*.8131/Z
WVC=(1.+CC1275/X)*WVC
RETURN
END

```

```

100 SUBROUTINE PRESS (T5, PATM, P5P, GHG, CF1, WVC, PR2, PTC)
A=T5-459.69
CP=.23943+3.4E-6*A+2.E-8*A**2
PS5=(PATM+P5P)*GHG/13.54
TT=T5
RHO=PS5*CF1/(TT*53.3448)
VO=WVC/(RHO*3.14159*6.25/144.)
TO=T5-(VO**2)/(2.*32.174*778.16*CP)
DTT=TT-TO
TT=TO
IF(ABS(DTT)-.01)>101, GO1, 100
PTO=PS5+RHO*(VO**2)/(2.*32.174*CF1)
PR2=PTO/(PATM*GHG/13.54)
RETURN
END
101

```

```

SUBROUTINE EDC (T5,PR2,GAM,EXP,CP,THETA)
A=T5-459.69
GA=1.4018-2.E-5*A
EX=(GA-1.)/GA
DT=T5*(1.-1./PR2**EX)
AA=T5-459.69-DT/2.
AAA=ABS(AA-A)
IF(AAA-1.) 107,107,106
105 A=AA
GO TO 105
107 GAM=GA
EXP=EX
CP=23943+3.4E-6*AA+2.E-8*AA**2
IF(GAM*T5)2050,2050,2051
2050 WRITE(6,2052) K,GAM,T5
2052 FORMAT(/,6X,I4,2F8.3)
2051 CONTINUE
THETA=(GAM/1.4)*(T5/518.7)
RETURN
END

```

```

SUBROUTINE TORQ (TCD,TQ,TNET)
DIMENSION TCD(5)
BFM=0.0
DO 100 I=1,5
IF(TCD(I)-TQ) 100,100,101
CONTINUE
100 IF(I.LT.5) GO TO 102
T=100.*(I-2)+100.*((TQ-TCD(I-1))/(TCD(I)-TCD(I-1)))
GO TO 103
102 AI=100.*(I-1)
T=AI+100.*((TQ-TCD(I))/(TCD(I+1)-TCD(I)))
103 TNET=T+BFM
RETURN
END

```



```

SUBROUTINE REFER (PTO,GHG,GAM,THETA,TNET,WVC,WVCR,TNETR)
DEL=(PTO*(.4891585*GHG/13.54)}/14.7
X=(GAM+1.)/(2.*(GAM-1.))
EPS=(.810/GAM)*((GAM+1.)/2.)**X
WVCR=WVC*(SQRT(THETA))*EPS/DEL
TNETR=TNET*EPS/DEL
RETURN
END

```

PERFORMANCE EVALUATION OF ICP RADIAL TURBINE

TABLE C2

RESULTS OF ZERO-SPEED TESTS

PT	INPUT DATA						OUTPUT DATA					
	V4 MV	V5 MV	ICJ DEG.F.	PATM IN.HG	P5P IN.HG	DPVC IN.HG	PUVC IN.HG	TORQUE COUNTS	TRM DEG.F	PRESS. RATIO	REF. MOMENT FT.LB	REF. FLOW RATE LBM/SEC
CLEARANCE = 0.081												
RUN 1												
1	1.640	1.355	32.00	30.07	2.90	2.066	4.93	125.	87.8	1.100	3.72	0.757
2	1.640	1.400	32.00	30.07	5.87	3.926	9.75	249.	87.9	1.201	6.79	1.004
3	1.635	1.395	32.00	30.07	8.76	5.452	14.20	367.	87.5	1.400	9.20	1.142
4	1.635	1.380	32.00	30.07	11.70	6.891	18.54	488.	87.5	1.500	11.20	1.209
5	1.620	1.375	32.00	30.07	14.64	8.184	22.83	605.	87.1	1.599	13.15	1.358
6	1.620	1.375	32.00	30.07	17.56	9.364	26.94	718.	87.1	1.699	14.13	1.397
7	1.620	1.375	32.00	30.07	20.51	10.502	31.00	829.	87.0		16.07	
CLEARANCE = 0.061												
RUN 2												
1	1.719	1.626	32.00	30.10	2.91	2.043	4.94	126.	76.0	1.100	3.62	0.756
2	1.762	1.679	32.00	30.10	5.82	3.348	9.63	250.	75.2	1.199	6.70	0.936
3	1.816	1.738	32.00	30.10	8.81	5.429	14.23	374.	75.0	1.302	9.18	1.143
4	1.823	1.759	32.00	30.10	11.70	6.830	18.64	492.	75.0	1.401	11.35	1.240
5	1.834	1.774	32.00	30.10	14.70	8.083	22.85	608.	75.0	1.502	13.14	1.306
6	1.847	1.784	32.00	30.10	17.60	9.265	26.91	724.	75.0	1.600	14.79	1.357
7	1.851	1.783	32.00	30.10	20.53	10.371	30.95	835.	75.0	1.699	16.14	1.394
CLEARANCE = 0.041												
RUN 3												
1	1.984	1.885	32.00	30.02	2.90	2.076	5.00	127.	73.6	1.100	3.69	0.763
2	2.000	1.910	32.00	30.02	5.81	3.873	9.69	247.	73.5	1.200	6.68	1.003
3	2.026	1.970	32.00	30.02	8.73	5.410	14.14	369.	73.9	1.300	9.20	1.143
4	2.064	1.987	32.00	30.02	11.67	6.809	18.50	487.	74.0	1.400	11.35	1.240
5	2.076	2.010	32.00	30.02	14.61	8.031	22.79	602.	73.8	1.500	13.12	1.305
6	2.076	2.013	32.00	30.02	17.52	9.237	26.82	718.	73.5	1.599	14.77	1.357
7			32.00	30.02	20.47	10.032	30.84	827.	73.5	1.699	16.09	1.376
CLEARANCE = 0.024												
RUN 4												
1	1.973	1.853	32.00	30.04	2.90	2.063	4.96	129.	77.2	1.100	3.70	0.760
2	1.985	1.884	32.00	30.04	5.91	3.876	9.66	253.	77.9	1.203	6.77	1.000
3	1.996	1.899	32.00	30.04	8.72	5.448	14.19	372.	77.3	1.398	9.21	1.147
4	2.005	1.910	32.00	30.04	11.63	6.844	18.50	486.	77.3	1.500	13.14	1.213
5	2.005	1.920	32.00	30.04	14.61	8.041	22.82	606.	77.0	1.599	14.75	1.362
6	2.005	1.921	32.00	30.04	17.53	9.235	26.90	720.	76.6	1.697	16.08	1.400
7			32.00	30.04	20.43	10.045	30.96	829.				
CLEARANCE = 0.015												
RUN 5												
1	2.005	1.879	32.00	30.21	2.92	2.110	5.00	127.	72.0	1.100	3.75	0.766
2	2.013	1.923	32.00	30.21	5.84	3.916	9.75	251.	72.5	1.200	6.90	1.005
3	2.010	1.931	32.00	30.21	8.70	5.458	14.26	371.	72.5	1.300	9.19	1.143
4	2.005	1.932	32.00	30.21	11.70	6.863	18.63	492.	72.5	1.401	13.14	1.210
5	1.953	1.908	32.00	30.21	14.68	8.148	22.95	607.	72.2	1.500	14.85	1.359
6	1.953	1.908	32.00	30.21	17.68	9.344	27.06	727.	72.0	1.601	16.15	1.395
7	1.944	1.885	32.00	30.21	20.61	10.419	31.09	836.				

INITIAL DISTRIBUTION LIST

	No. Copies
1. Defense Documentation Center Cameron Station Alexandria, Virginia 22314	20
2. Library Naval Postgraduate School Monterey, California 93940	2
3. Commander, Naval Air Systems Command Navy Department Washington, D. C. 20360	1
4. Mr. I. Silver Propulsion Administrator (Code 330) Research and Technology Naval Air Systems Command Navy Department Washington, D. C. 20360	1
5. Dr. F. I. Tanczos Technical Director (Code 033) Research and Technology Naval Air Systems Command Navy Department Washington, D. C. 20360	1
6. Commander, Naval Ship Systems Command Navy Department Washington, D. C. 20360	1
7. Office of Naval Research (Power Branch) Attn: Mr. J. K. Patton, Jr. Navy Department Washington, D. C. 20360	1
8. Superintendent Naval Academy Annapolis, Maryland 21402	1
9. Chairman Department of Engineering Naval Academy Annapolis, Maryland 21402	1
10. Chairman, Department of Aeronautics Naval Postgraduate School Monterey, California 93940	2

	No. Copies
11. Professor R. D. Zucker Department of Aeronautics Naval Postgraduate School Monterey, California 93940	3
12. Professor M. H. Vavra Department of Aeronautics Naval Postgraduate School Monterey, California 93940	2
13. LT David D. Williams, USN 1637 77th Avenue, N. E. Bellevue, Washington, 98004	3
14. Dr. Allen E. Fuhs Chief Scientist (Code APX) AeroPropulsion Laboratory (AFSC) Wright Patterson Air Force Base, Ohio 45433	1
15. Dr. D. M. Dix Chief Engineer Northern Research and Engineering Corp. 219 Vassar St., Cambridge, Mass. 02139	1

Unclassified

Security Classification

DOCUMENT CONTROL DATA - R & D

Security classification of title, body of abstract and indexing annotation must be entered when the overall report is classified)

1 ORIGINATING ACTIVITY (Corporate author) Naval Postgraduate School Monterey, California 93940		2a. REPORT SECURITY CLASSIFICATION Unclassified	
		2b. GROUP None	
3 REPORT TITLE Determination of Performance Parameters of a Dual Discharge Radial Turbine			
4 DESCRIPTIVE NOTES (Type of report and, inclusive dates) None			
5 AUTHOR(S) (First name, middle initial, last name) David Daniel Williams			
6 REPORT DATE December 1968		7a. TOTAL NO. OF PAGES 158	7b. NO. OF REFS 12
8a. CONTRACT OR GRANT NO. b. PROJECT NO N/A c. d.		9a. ORIGINATOR'S REPORT NUMBER(S) N/A 9b. OTHER REPORT NO(S) (Any other numbers that may be assigned this report)	
10 DISTRIBUTION STATEMENT Distribution of this document is unlimited.			
11. SUPPLEMENTARY NOTES None		12 SPONSORING MILITARY ACTIVITY Naval Postgraduate School Monterey, California 93940	

13 ABSTRACT

This study was conducted to establish the performance parameters of a radial inflow, dual discharge turbine and to determine the effect of variations in axial clearance on these parameters. The representative stream surface is taken at the outer discharge radius instead of at a computed mass-average discharge radius, as was done previously. This technique results in considerably simplified computations and in better correlation of the rotor loss parameters.

Tests were conducted at axial clearances from 0.015 to 0.081 inches and at total-to-static pressure ratios from 1.2 to 1.7 for each clearance. The test installation is located at the Turbo-Propulsion Laboratory of the Naval Postgraduate School, Monterey, California.

14

KEY WORDS

LINK A

LINK B

LINK C

ROLE

WT

ROLE

WT

ROLE

WT

RADIAL TURBINE

AXIAL CLEARANCE

PERFORMANCE PARAMETERS

DUDLEY KNOX LIBRARY
NAVAL POSTGRADUATE SCHOOL
MONTEREY CA 93943-5101

DUDLEY KNOX LIBRARY



3 2768 00305694 6